Phase Transformation in Helical Structures: Theory and Application

A DISSERTATION
SUBMITTED TO THE FACULTY OF THE GRADUATE SCHOOL
OF THE UNIVERSITY OF MINNESOTA
BY

Fan Feng

IN PARTIAL FULFILLMENT OF THE REQUIREMENTS
FOR THE DEGREE OF
DOCTOR OF PHILOSOPHY

Richard D. James

September, 2018

Acknowledgements

It has been six years since the first time I came to Minnesota. I still remember the first "infinitely long" winter I experienced here had already shocked me a lot. Minnesota in winter is just like a father: severe, deep and persistent. But Minnesota in summer is like a mother: warm, comfortable and tender. That's how parents usually play different roles in a family of China. After six years, Minnesota has been my second hometown, with many unforgettable people I should thank.

First and foremost, I would like to thank my Ph.D advisor, Professor Richard D. James, not only for his professional guidance, tremendous patience and continuous support on my study, but also for the extraordinary influence of his personality on myself. My research has a hard and slow start here. I still remember that when I was struggling with my project, besides inspired suggestions, Dick talked to me frankly and ruthlessly, "Fan, you are talented. Think about your talent and do not waste it." Dick's voices were ringing continuously in my ears on my way of pursuing Ph.D degree. I feel quite comfortable and enjoyable with my research now. Without my advisor, I can never have such a joyful journey and feel the beauty of nature in my life.

Second, I would like to thank my collaborator, Dr. Paul Plucinsky, for his effort, help and inspiration on both of the objective structure and origami work. I also want to thank my wonderful committees, Prof. Ryan Elliott, Prof. Brad Holschuh, and Prof. Ellad Tadmor, for their help on my final defense. They also gave me many constructive suggestions on my thesis and career. I should thank many professors that have given amazing courses I have taken or sit in. I have taken many wonderful mechanics courses from Dick, Ryan, Ellad, Prof. Ellen Longmire and Prof. Roger Fosdick in AEM department. I also enjoyed many math courses from Prof. Bernardo Cockburn, Prof. Nicolai Krylov, Prof. Tyler Lawson, Prof. Svitlana Mayboroda, Prof. Peter Polacik and Prof.

Mikhail Safonov in MATH department, even though I got some low scores on exams.

Next, I would like to thank all the members and visitors from Dick's group, including Saurav Aryan, Amartya Banerjee, Ashely Bucsek, Xian Chen, Vivekanand Dabade, Hanlin Gu, Paul Plucinsky, Hanuš Seiner, Yintao Song and Frank Yu, for their helpful discussions and inspirations. Of course, I also want to thank the friends I have met in Minnesota, including Jiadi Fan, Lin Lin, Yixuan Li, Hao Xu, Mingjian Wen, Shu Wang, Kuan Zhang, Junfeng Zhu and more. My life becomes more colorful because of them. Besides my Minnesota friends, I also keep communicating with my college friends, including Wenbo Fu, Yingfei Gu, Junru Li, Chenghui Yu, Wang Yang and more. Most of them are working on theoretical or experimental physics. Even I am away from their areas now, their spirits are always motivating me to chase my own dream harder and harder.

Last but not least, I have to owe my deepest gratitude to my family: my dad Renyue Feng, my mom Xiangfen Xing, my sister Jian Feng, her husband Zhiqiang Tong and their cute daughter Duoduo, for their limitless patience and selfless support. Finally, I want to thank myself for the persistence.

The Ph.D journey is done and I am looking forward to the future. A marathoner never stops his steps!

Dedication

To my family.

Abstract

A *helical structure* is a collection of molecules at positions given by the orbit of a helical group acting on the position vectors of the atoms of a single molecule. In this thesis, we systematically study phase transformations from one helical structure to another and search for potential applications. Motivated in part by recent work that relates the presence of compatible interfaces with properties such as the hysteresis and reversibility of a phase transformation, we give necessary and sufficient conditions on the structural parameters of two helical phases such that they are compatible. We show that, locally, four types of compatible interfaces are possible: vertical, horizontal, helical and elliptical. Furthermore, we discuss more complex microstructures in transforming helical structures that mix different types of these interfaces. Similar to crystal case, we conjecture that compatible helical transformations with low hysteresis and fatigue resistance would exhibit an unusual shape memory effect involving both twist and extension.

The example we give for the application side is the phase-transforming helical Miura origami (HMO). An HMO is the origami structure generated by applying a helical group on a unit cell. The unit cell here is a partially folded four-fold Miura parallelogram. Here we demonstrate the methodology to construct a closed HMO and study its phase transformation properties. To do this, firstly, we conduct a rigorous analysis of the kinematics of the unit cell. We show that, by choosing discrete Abelian group generators and satisfying special discrete conditions, the HMO is generated to close itself at some isolated folding angle, which also means the structure is rigid. Furthermore, inspired by compatible interfaces we have in helical structures, we show that compatible horizontal and helical interfaces occur between two variants − the two different ways of folding for the same unit cell. By transforming one variant to the other, finally, we achieve overall twist and extension actuations, which can be used to develop novel actuators and artificial muscles.

Contents

List of Tables

List of Figures

Chapter 1

Introduction

1.1 Background

Phase transformation is the concept that usually describes the transformation between solid, liquid, and gaseous states of matter. Phase transformations are everywhere in our daily life. A typical example in Minnesota winter is that people usually make the road safer in the snow and ice by spreading salt − lowering the transformation temperature from ice to liquid water by changing its composition. The first formal study of phase transformation can be traced back to 1822 when Charles Caignard de la Tour measured the temperature, pressure, and volume change to characterize the transformation between gas and liquid phases in alcohol [1].

There are tremendous types of phase transformations in a wide range of matters. The first classification of general types of phase transformation is given by Paul Ehrenfest in 1933. In his classification, the first-order phase transformations exhibit some discontinuity in the first derivative of the free energy with respect to some thermodynamic parameters. The second-order phase transformations are continuous in the first derivative, but exhibit discontinuity in the second derivative. Since this classification is not able to describe phase transformation that has a divergence in the derivative, a modern classification is given as follows: A first-order phase transformation (discontinuous phase transformation) exhibits discontinuous change in entropy at a fixed temperature and therefore leads to some latent heat, while a second-order phase transformations (continuous phase transformation) involves no latent heat at a fixed temperature. A

phenomenological theory for the second-order phase transformation is given by Lev Landau [2] .

Martensitic phase transformation of a crystal is a first-order (in both classifications), solid-solid, diffusionless transformation[1]. It is commonly observed in nature and extensively studied in theories as well as applications [4, 5, 6, 7, 8, 9]. Usually, the crystal has a high-symmetry *austenite* phase at high temperatures and a low-symmetry *martesite* phase at low temperatures. Here physical symmetry plays a significant role in the study of crystalline solids with three-dimensional translation symmetry. Crystallography is the science of determining the structure of crystal as well as its symmetry. A widely used experimental technique is X-ray diffraction crystallography [10, 11, 12]. However, a lot of solids in nature that people are particularly interested in are not crystalline solids, such as carbon nanotube, C_{60}, black phosphorus and so on. Thus, a more general terminology to describe the symmetry of these materials is necessary. The concept of *objective structures* is developed to fulfill those demands.

As defined by James in [13], an *objective atomic structure* is a collection of atoms that each atom sees the same "environment" up to orthogonal transformations and translations. An *objective molecular structure* is a collection of molecules such that the corresponding atoms in different molecules see the same environment up to orthogonal transformations and translations. The physical meaning of this concept is intrinsically related to the symmetry of the system. A variety of material properties under the objective framework has been investigated. Falk and James [2006] have developed elastic theory for the tail sheath of the virus bacteriophage T4 [14]. [2007, 2010, 2012] have extended molecular dynamics method in the objective structure regime to *objective molecular dynamics* [15, 16] and design a new viscometer using this method [17]. Objective structures also involve physical governing equations associated with the same symmetry. Under this trace, X-ray diffraction has been extended to twisted X-ray diffraction for the determination of structures with helical symmetry [18, 19]. Banerjee and his collaborators have published a series of work regarding *objective density functional theory* as an extended theory of DFT in the objective structure framework [20, 21, 22, 23].

[1]Diffusionless transformation means no long-range diffusion of atoms occurs during the transformation. An example of solid-solid phase transformation with diffusion is precipitation [3].

The aim of this thesis is to develop a martensitic phase transformation theory in objective structures, more precisely, in helical structures. Indeed, many structures with helical symmetry in nature exhibit change of phases in some sense. For instance, bacterial flagella can adopt different helical shapes to accommodate different kinds of environments [24]. Bacteriophage T4 can eject its viral DNA by contracting its spring-like sheath [25]. Besides biological examples, many mechanical structures are helical and also have phase transformation phenomena. Taking the advantage of shape change during helical transformation, researchers have developed new artificial muscles with better performance [26], reconfigurable helical antenna based on origami [27] and so on. However, a martensitic phase transformation theory for helical structures is absent.

Inspired by martensitic phase transformation theory in crystal, we can naturally ask a series of questions associated with helical structures as follows. What are the compatibility conditions for interfaces between different helical structures and how to satisfy them? Is there a concept analogous to Cauchy-Born rule? During the phase transformation, are there any variants of helical structures and what is the symmetry relation between them? Is it possible to have microstructures and how to classify them? Are there any new possible applications of helical phase transformation?

The thesis answers these questions to some extend. The thesis consists of theory and application part. For the theory part, we firstly demonstrate the similar rank-one compatibility condition for helical structures. By using nearest neighbor generators, we formulate the local compatibility problem under some mild hypotheses. Then we solve the local compatibility problem rigorously and come up with four types of elastic free interfaces − horizontal, vertical, helical and elliptical interfaces. Then we discuss the symmetry of helical structures and possible variants. Similar to fruitful microstructures found in lattices, we show some examples of microstructures in helical structures at the end of the theory part. For the application part, we give an interesting and promising example − helical Miura origami. Amazingly, the theory is applicable to origami design, basically because of the fact that the deformations that construct helical structure and helical origami are both from $\mathbb{R}^2$ to $\mathbb{R}^3$. Phase transformation in helical Miura origami also gives us some actuation phenomena that are useful in actuator design and artificial muscles.

1.2 Martensitic phase transformation in crystalline lattice

Here we give a brief introduction of Martensitic phase transformation in crystalline lattices as well as some important concepts such as Cauchy-Born rule, energy wells, variants and so on.

1.2.1 Free energy functional and continuous compatibility condition

Let Ω be an undistorted continuum solid, which is usually chosen as the reference domain. Suppose the deformation $\mathbf{y} : \Omega \to \mathbb{R}^3$ describes the distortion of Ω during transformation as shown in Figure 1.1. We are interested in the continuum theory

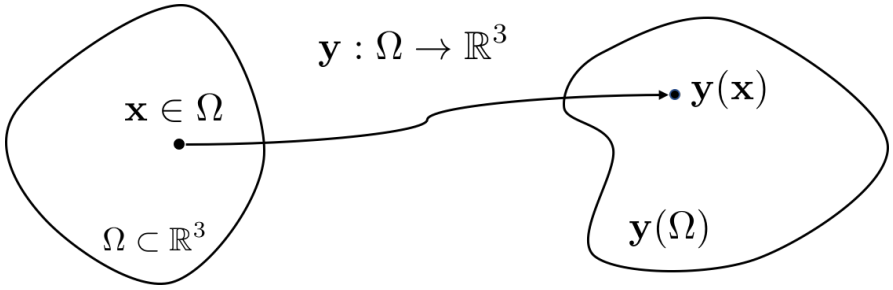

Figure 1.1: Deformation of a continuum solid.

for martensitic phase transformation. In thermodynamics, the free energy functional yields the spontaneous changing state of a system by the second law of thermodynamics. Suppose the free energy density is a functional of deformation gradient and temperature, say, $\varphi(\nabla \mathbf{y}, \theta)$, where θ is temperature. The total free energy of a specimen within the deformed region Ω is given by

$$\int_{\Omega} \varphi(\nabla \mathbf{y}, \theta) d\mathbf{x}. \tag{1.1}$$

Consider two different deformations $\mathbf{y}_1$ and $\mathbf{y}_2$ shown in Figure 1.1. The reference bodies Ω_1 and Ω_2 undergo different deformations $\mathbf{y}_1$ and $\mathbf{y}_2$ respectively. Suppose the whole deformed body remains continuous, and also, the interface between these two domains is undistorted, which also means the interface is stress-free. Then the deformation gradients have to satisfy the *continuous compatibility condition.*

Theorem 1.2.1 (Continuous compatibility condition)**.** *There exists a continuous piecewise affine function* $\mathbf{y}$ *as shown in Figure 1.2 such that*

$$\mathbf{y} = \begin{cases} \mathbf{F}_1\mathbf{x} + \mathbf{c}_1 & \mathbf{x} \in \Omega_1 \\ \mathbf{F}_2\mathbf{x} + \mathbf{c}_2 & \mathbf{x} \in \Omega_2 \end{cases} \tag{1.2}$$

if and only if

$$\mathbf{F}_1 - \mathbf{F}_2 = \mathbf{a} \otimes \hat{\mathbf{n}} \tag{1.3}$$

for some $\mathbf{a}, \hat{\mathbf{n}} \in \mathbb{R}^3$.

The condition is also called *Hadamard jump condition* or *rank-one compatibility condition.*

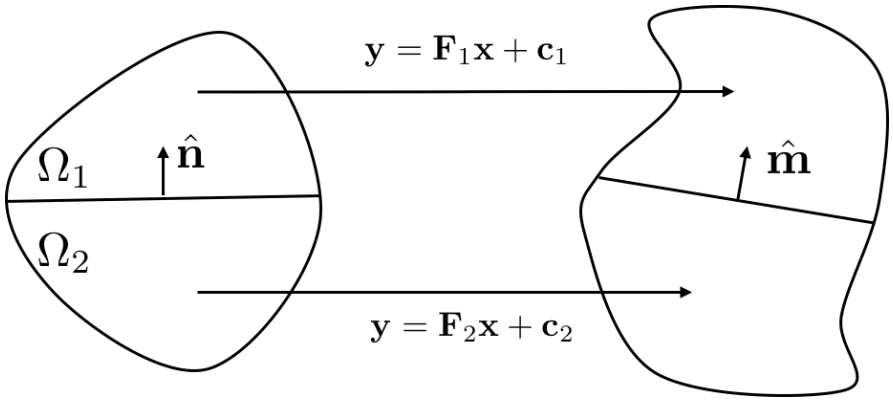

Figure 1.2: Continuous compatibility condition.

1.2.2 Cauchy-Born rule, material symmetry and variants

A *Bravais lattice* $\mathcal{L}(\mathbf{e}_i, \mathbf{o})$ is an infinite set of points in three-dimensional space generated by the translation of a single point $\mathbf{o}$ throught three linearly independent lattice vectors $\mathbf{e}_1, \mathbf{e}_2, \mathbf{e}_3$, i.e.,

$$\mathcal{L}(\mathbf{e}_i, \mathbf{o}) = \{\mathbf{x} : \mathbf{x} = \mu^i \mathbf{e}_i + \mathbf{o} \text{ where } \mu^1, \mu^2, \mu^3 \text{ are integers}\}. \tag{1.4}$$

From a generalized view of point, a Bravais lattice is the orbit of a discrete translation group T applied on $\mathbf{o} \in \mathbb{R}^3$, say,

$$\mathcal{L}(\mathbf{e}_i, \mathbf{o}) = T(\mathbf{o}) \tag{1.5}$$

where

$$T = \{g_1^{\mu^1} g_2^{\mu^2} g_3^{\mu^3} : g_i = (\mathbf{I}|\mathbf{e}_i),\ \mu_i \in \mathbb{Z}\}. \tag{1.6}$$

This description of Bravais lattice opens a new window to understand other types of atomic structures. That is, as the orbit of different discrete groups, we could have different atomic structures.

In the discrete sense, the free energy functional is a function of lattice parameters and temperature. Let $\{\mathbf{E}_i\}$ be the lattice parameters in reference configuration and $\{\mathbf{e}_i\}$ be lattice parameters in deformed configuration. Then $\mathbf{e}_i = \mathbf{F}_i^j \mathbf{E}_j$ and $\mathbf{F}$ is the deformation matrix. We restrict $\mathbf{F}$ in *Erickson-Pitteri neighborhood* for the reason that the deformation should be reasonably small and not be too large shears or plasticity [28, 29, 30]. Then there exists another free energy functional $\hat{\varphi}(\mathbf{F}, \theta)$ which should be consistent with continuous description $\varphi(\nabla \mathbf{y}, \theta)$. The connection between continuum and discreteness is *Cauchy-Born rule* which states that macroscopic and atomic movement are the same as well as the free energy functionals, saying $\nabla \mathbf{y} = \mathbf{F}$ and $\varphi(\nabla \mathbf{y}, \theta) = \hat{\varphi}(\mathbf{F}, \theta)$. Cauchy-Born rule is also studied in [31, 32, 33, 34, 35].

Those linear transformations transform a lattice back to itself are defined as the *symmetry group* of the lattice. The *point group* of a lattice is the set of rotations that map a lattice back to itself. Let $\mathscr{P}_a$ be the point group of austenite phase (higher symmetry) and $\mathscr{P}_m$ be the point group of martensite phase (lower symmetry). The concepts of variants and energy wells, which are important in the following discussion of microstructures, come from group-subgroup relation between point groups of austenite and martensite in the following argument. The frame indifference of free energy density $\varphi(\mathbf{F}, \theta) = \varphi(\mathbf{RF}, \theta)$ suggests us the free energy density $\varphi(\mathbf{U}, \theta)$ as a function of stretch matrix $\mathbf{U}$. We firstly define

$$\mathscr{A} = \{\mathbf{F} : \mathbf{F} = \mathbf{R} \text{ for some rotation } \mathbf{R}\} \tag{1.7}$$

as the energy well of austenite. Define

$$\mathscr{M}_1 = \{\mathbf{F} : \mathbf{F} = \mathbf{R}\mathbf{U}_1 \text{ for some rotation } \mathbf{R}\} \tag{1.8}$$

as the first energy well of martensite, similarily for $\mathscr{M}_2, \ldots, \mathscr{M}_N$. In energy well $\mathscr{M}_i$, $\mathbf{U}_i = \mathbf{Q}^{\mathrm{T}}\mathbf{U}_1\mathbf{Q}$ for some $\mathbf{Q}$ in $\mathscr{P}_a$ but not in $\mathscr{P}_m$. Then the number of variants is

$$\frac{\text{order of } \mathscr{P}_a}{\text{order of } \mathscr{P}_m}. \tag{1.9}$$

Figure 1.3 shows the energy wells in austenite and martensite[36].

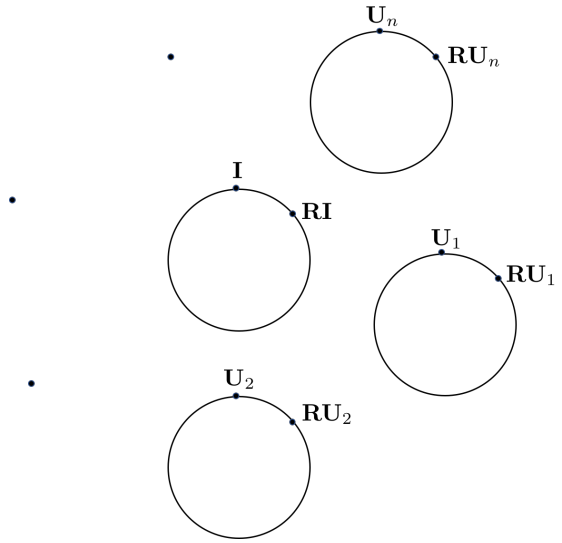

Figure 1.3: Schematic of the energy wells of lattice.

Suppose there is an undistorted interface between austenite and martensite. By rank-one compatibility condition, the deformation gradient $\mathbf{I}$ of austenite is rank-one connected with the deformation gradient $\mathbf{R}\mathbf{U}_i$ of martensite. The following theorem gives the condition on $\mathbf{U}_i$.

Theorem 1.2.2 (Austenite-martensite interface)**.** *The compatibility equation*

$$\mathbf{R}\mathbf{U}_i - \mathbf{I} = \mathbf{a} \otimes \hat{\mathbf{n}} \tag{1.10}$$

between austenite and martensite holds for some $\mathbf{R} \in SO(3)$, $\mathbf{a}, \hat{\mathbf{n}} \in \mathbb{R}^3$ *if and only if the middle eigenvalue* λ_2 *of* $\mathbf{U}_i$ *equals one, say,*

$$\lambda_1 \leq 1,\ \lambda_2 = 1,\ \lambda_3 \geq 1, \tag{1.11}$$

where $\lambda_1, \lambda_2, \lambda_3$ *are eigenvalues of* $\mathbf{U}_i$.

1.3 Objective structures

Here we give a brief introduction to objective structures. Most of the results are collected from [13] and unpublished notes [37].

As defined by James in [13], an objective atomic structure is a collection of atoms for which every atom sees the same environment, up to orthogonal transformations and rotations. If the positions of a collection of atoms are presented by $\mathscr{O} = \{\mathbf{x}_1, \mathbf{x}_2, \ldots, \mathbf{x}_N\}$, with N finite or infinite, then this collection is an objective structure if there exits a collection of corresponding rotation matrices $\{\mathbf{R}_1, \mathbf{R}_2, \ldots, \mathbf{R}_N\}$ such that

$$\mathscr{O} = \{\mathbf{x}_i + \mathbf{R}_i(\mathbf{x}_j - \mathbf{x}_1) : j = 1, \ldots, N\} \tag{1.12}$$

for every fixed $i \in \{1, \ldots, N\}$. More explaination, the set of relative vectors $\{\mathbf{x}_j - \mathbf{x}_1 : j = 1, \ldots, N\}$ is invariant up to rotation if we look from different atoms $\mathbf{x}_i$. Examples of objective structures are carbon nanotubes, C_{60}, black phosphorus and many structures in biology such as bacteriophage T4 tail.

We study objective structures based on discrete isometry groups. Here we present some important concepts, notations and theorems regrading isometry groups. An isometry is an affine transformation $g : \mathbb{R}^3 \to \mathbb{R}^3$ with the form $g = (\mathbf{Q}|\mathbf{c}), \mathbf{Q} \in \mathrm{O}(3), \mathbf{c} \in \mathbb{R}^3$ such that $\mathbf{x} \in \mathbb{R}^3$ is mapped to $\mathbf{Q}\mathbf{x} + \mathbf{c}$, say, $g(\mathbf{x}) = \mathbf{Q}\mathbf{x} + \mathbf{c}$. "Isometry" means the map preserves distances, which is, for any $\mathbf{x}_1, \mathbf{x}_2 \in \mathbb{R}^3$, $|g(\mathbf{x}_1) - g(\mathbf{x}_2)| = |\mathbf{x}_1 - \mathbf{x}_2|$. Define the product of two isometries $g_1 = (\mathbf{Q}_1|\mathbf{c}_1)$ and $g_2 = (\mathbf{Q}_2|\mathbf{c}_2)$ as $g_1 g_2(\mathbf{x}) = g_1(g_2(\mathbf{x}))$, which means $g_1 g_2 = (\mathbf{Q}_1\mathbf{Q}_2|\mathbf{c}_1 + \mathbf{Q}_1\mathbf{c}_2)$. Then we have the definition of isometry group as follows.

Definition 1.3.1. *An isometry group* $\mathcal{I}$ *is the set of isometries satisfying the group axioms:*

1. *Closure. If* $g_1, g_2 \in \mathcal{I}$, $g_1 g_2 \in \mathcal{I}$.

2. *Associativity. For all* $g_1, g_2, g_3 \in \mathcal{I}$, $(g_1 g_2) g_3 = g_1 (g_2 g_3)$. *This is obvious by substituting the definition of product.*

3. *Identity. The identity is* $(\mathbf{I}|\mathbf{0})$.

4. *Inverse. If* $g = (\mathbf{Q}|\mathbf{c}) \in \mathcal{I}$, *then the inverse* $g^{-1} = (\mathbf{Q}^T| - \mathbf{Q}^T\mathbf{c})$ *is also in* $\mathcal{I}$.

Definition 1.3.2. *A discrete isometry group is an isometry group with no accumulation points in its orbit.*

Theorem 1.3.1 (Dayal, Elliot and James)**.** *If one allows for intersecting images, every objective structure is the orbit of a discrete group of isometries on a finite set of points in* $\mathbb{R}^3$.

Theorem 1.3.1 allows us to study the corresponding isometry groups instead of objective structures themselves, so we can benefit from group properties such as commutativity, group representations, etc. Then it is useful to classify all possible isometry groups as follows.

Theorem 1.3.2 (Dayal, Elliot and James)**.** *Every discrete group of isometries is either a space group, a net group, a rod group, a helical group or a discrete group of rotations.*

Here a space group is a discrete isometry group containing three linearly independent translation isometries. A net group is a discrete isometry group containing two linearly independent translation isometries. A rod group is a discrete isometry group containing one translation isometry. A helical group is a discrete isometry group containing no translation and not consisting of entire rotations as its elements. Figure 1.4 shows some examples of objective structures generated by different isometry groups applied on a point in $\mathbb{R}^3$. To develop a general phase transformation theory for all possible isometry groups is too ambitious Thus, we concentrate mainly on helical groups (also some rod groups). The details are discussed in the next chapter.

1.4 Outline of the thesis

The main content of the thesis is outlined as follows. In Chapter 2, we develop the phase transformation theory for helical structures generated by helical groups. As shown

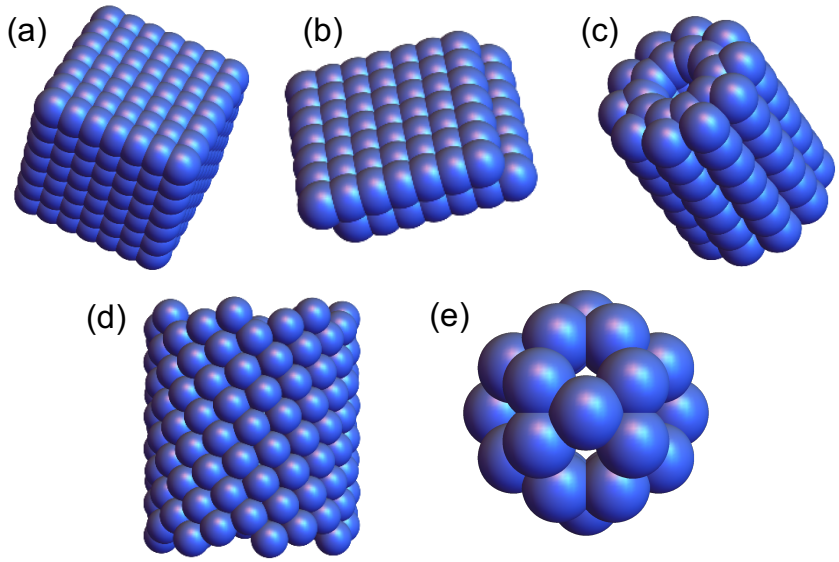

Figure 1.4: Examples of objective structures generated by a (a) space group, (b) net group, (c) rod group, (d) helical group, and (e) group of rotations.

by [37] , helical groups can be expressed in four different forms. Among them, we choose the largest Abelian helical group[2]. The original expression of this group has the problem that the nearest neighbors in the helical structure are not the nearest neighbors in the domain of power of group generators. Then a reparameterization of the group is necessary. We show that, under some very mild conditions, there exist nearest neighbor generators that generate the same helical group and satisfy the corresponding nearest neighbor condition. Under this reparameterization, it is convenient to describe interfaces on the reference domain − the domain of powers of generators. We also give a precise description of this domain. Then we formulate the compatibility problem of the interface between two different helical structures, similar to the rank-one condition in lattices. The proposed compatibility problem is solved rigorously, depending on the curvatures of the interface on reference domain. We give the full solutions of compatible interfaces − horizontal, vertical, helical, elliptical interfaces − as well as the conditions on parameters. At the end of this chapter, we give some examples of microstructures.

[2]The reason here is that the helical structure generated by a non-Abelian group can be treated as a structure generated by an Abelian group on a different set of points.

Chapter 3 gives an example of the application of the theory − phase-transforming helical Miura origami (HMO). In this chapter, we start with the basic kinematics of Miura four-fold node. We realize that, except for some special cases, the folding process of a four-fold node has one free parameter, and also, two branches of the solution for folding are observed. By applying helical group generators on the Miura four-fold parallelogram as the unit cell and satisfying some global closing conditions, we can construct a closed HMO. The full domain of parameters of the Miura four-fold parallelogram is given, up to scaling. Thus, theoretically, we can compute all possible closed HMO. Even though the rigidity of all HMO is still unknown, some HMO are proved to be rigid in our computational domain due to our numerical results. Inspired by our phase transformation theory of helical structures, we can transform one variant (one branch of solution in HMO) to the other (the other branch of the solution in HMO) to have a deployable structure. The mechanism of this transformation could be some low-energy bending and buckling path, which is not investigated yet.

Chapter 4 provides a brief summary and some potential future work.

Chapter 2

Phase transformation in helical structures

In this chapter, we develop martensitic phase transformation theory for helical structures. First, we generate the helical structure by the original helical groups. Second, nearest neighbor generators and the corresponding domain of their powers are derived to generate the same group. Then we propose the local compatibility problem by applying the rank-one condition. Finally, we solve the proposed local compatibility problem rigorously in helical structures. The results show that there are four types of compatible interfaces − horizontal, vertical, helical and elliptical interfaces − depending on group parameters and reference interface curves. This is an exact analogue to $\lambda_2 = 1$ in lattice case. The material in this chapter is directly adopted from [38] and [39].

2.1 Introduction

A *helical structure* is a molecular structure obtained by taking the orbit of a single molecule under a so-called *helical group*. The helical groups are the discrete groups of isometries (i.e., orthogonal transformations and translations) that do not contain any pure translations and do not fix a point. Helical structures are special cases of the more general concept of *objective structures* [13]. An objective structure is a discrete collection of atoms where corresponding atoms in each molecule "see the same environment". For reasons that are not understood and are related to the celebrated and far-from-solved

"crystallization problem", objective structures are surprisingly well-represented among scientifically and technologically important nanostructures.

Helical structures, in particular, are ubiquitous. Single-walled carbon nanotubes of any chirality as well as many biological molecules are helical. They are especially common in non-animal viruses. An example of a helical structure that undergoes a phase transformation of the type discussed here is the tail sheath of bacteriophage T4 [40, 41]. This highly effective transformation is employed by the T4 virus to drive the stiff tail tube through the cell wall of the host, and the viral DNA then enters the host through the tail tube. It can be seen that, aside from being helical, this transformation has many features in common with martensitic phase transformations in crystals as first noticed by Olson and Hartman [42], such as being diffusionless, and exhibiting a large coordinated shape change. The transformation also exhibits a latent heat [43], and the transformation can be accurately modeled by a free energy of the type used in studies of phase transformations [14]. The forms of the helical generators of both phases of this tail tube are special cases of those studied in this paper [14], but the phases of bacteriophage T4 do not precisely satisfy the strong conditions of compatibility found here. This is possibly related to the fitness requirement of T4 to have sufficiently large hysteresis so that the transformation does not occur spontaneously. In fact, T4 has a trigger involving its tail fibers and baseplate which induces the transformation only after it has attached itself to its host. Another typical example is the phase transformation of bacterial flagella, which are mechanically induced by the bacterium's molecular motor [44, 45, 46]. The bacterium can enter into "swimming" mode to move toward a favorable chemical and thermal environment, or a "tumbling" mode to alter its direction, by switching chirality of the flagellum. The thermodynamics of such phenomena was explained by minimizing Gibbs free energy, including chemical and mechanical parts, and thermomechanical phase diagrams are given in [47]. Other widely studied nanotubes are BCN [48], GaN [49], MoS_2 and WS_2 [50, 51].

A recent development that may make the of tuning of lattice parameters suggested here possible is an implementation of density functional theory that fully incorporates helical symmetry, so that typical total energy calculations on nanotubes with no axial periodicity can be carried out with a few atom calculation (2 atoms for arbitrarily

twisted C nanotubes) [21, 22, 52]. With these tools many different twisted and extended nanotubes can be evaluated and phase transformations can be identified. Twist and extension are not only valuable parameters to seek novel phase transformations, but they can also be used to seek special conditions of compatibility identified here. Phase transformations having a change in magnetoelectric or transport properties are particularly interesting in an engineering context due to the rod-like geometry of nanotubes, together with the fact that their lengths can be macroscopic.

In this chapter we develop a theory of diffusionless phase transformations in helical structures with a focus on low energy interfaces. The main guideline behind this study is to systematically replace the translation group by the helical group, but to otherwise exploit the patterns of thought used in atomistic and continuum theories of phase transformations [53, 5, 54, 55, 56, 30]. We show that familiar concepts from phase transformations in crystals such as *variants*, *twins*, *compatible interfaces* and *habit planes* have analogs in the helical case, though the analogy is not perfect.

To develop a phase transformation theory for helical structures, we consider structures generated by the the largest Abelian discrete helical group acting on a finite set of points in $\mathbb{R}^3$, as described in Section 2.2. This assumption includes structures generated by all the helical groups as long as we choose the generating molecule appropriately, as we explain below. We then focus on compatible interfaces. Compatibility is fundamentally a metric property, i.e., it concerns conditions under which atoms that are close together before transformation remain close together after transformation. However, closeness of powers of group generators does not generally imply closeness of molecules. Therefore, we are led to develop a reparameterization of the group by *nearest neighbor generators*, as well as a suitable domain—analogous to a reference configuration of continuum mechanics—of powers of the generators that imply a 1–1 relation between powers and molecules with convenient metric properties. The reparameterization of the groups in terms of nearest neighbor generators and the characterization of their domains is presented as a series of rigorously derived algorithms in Sections 2.3.

The powers of generators are integers, but we notice that the resulting formulas for molecular positions make sense for non-integer values of the powers and still the metric properties hold: closeness of powers (whether integer or not) implies closeness of molecules. Using this observation, we then define compatibility in continuum mechanics

terms (cf., [57]) in Section 2.4. Further, we work out all local solutions for compatible interfaces for all values of the group parameters (under mild restrictions) in this section. The conditions group parameters for compatible interfaces that we find are strictly analogous to the condition $\lambda_2 = 1$ in theories of phase transformations in crystals. We conjecture that the dramatic reduction of the sizes of hysteresis loops observed in transforming crystals when λ_2 is tuned to the value 1 by compositional changes will also occur in helical structures.

The local interfaces we find can all be extended to form loops or infinite lines (Section 2.4), except for elliptical interface. By introducing left and right helical variants, we can have slip and mechanical twinning in Section 2.6. Moreover, one can combine various compatible interfaces to form nanostructures that are analogous to austenite/martensite interface and supercompatible interfaces in crystals [58, 59].

Finally, it should be noted that interfaces of the type identified here in atomic structures are also seen in macroscopic hollow tubes made of NiTi shape memory material [60]. See also [39].

2.2 Isometry groups and helical structures

As noted in the introduction, a helical structure is the orbit of a molecule under a helical group. To define this precisely, note that a molecule can be specified by a finite number of position vectors (and corresponding species) of its atoms, $\mathbf{p}_1, \ldots, \mathbf{p}_M$. Further, a helical group can be represented schematically[1] by $\{g_0, g_1, g_2, \ldots\}$ with say $g_0 = \textit{identity}$. Consequently, a helical structure is given by $\{g_0(\mathbf{p}_1), \ldots, g_0(\mathbf{p}_M)\} \cup \{g_1(\mathbf{p}_1), \ldots, g_1(\mathbf{p}_M)\} \cup \{g_2(\mathbf{p}_1), \ldots, g_2(\mathbf{p}_M)\} \cup \ldots$.

A helical group is a discrete group consisting of *isometries* that do not fix a point and which does not contain any pure translations. That is, each $g_i,\ i = 0, 1, 2, \ldots$, is an isometry of the form $(\mathbf{Q}_i|\mathbf{c}_i)$ in conventional notation, where $\mathbf{Q}_i$ is an orthogonal transformation on $\mathbb{R}^3$ and $\mathbf{c}_i \in \mathbb{R}^3$. Each g_i is restricted to satisfy $(\mathbf{Q}_i|\mathbf{c}_i) \neq (\mathbf{I}|\mathbf{c})$ for any $\mathbf{c} \neq 0$, as the latter describes a pure translation, and there is no $\mathbf{x}_0 \in \mathbb{R}^3$ such that $(\mathbf{Q}_i - \mathbf{I})\mathbf{x}_0$ is the same for every i. (If they are the same, the resulting group is a

[1] where the elements g_i are defined subsequently. These are restricted to be isometries, and none of them can be a pure translation.

point group.) The group product is $g_i g_j = (\mathbf{Q}_i\mathbf{Q}_j|\mathbf{Q}_i\mathbf{c}_j + \mathbf{c}_i)$, the identity is $g_0 = (\mathbf{I}|0)$, and the inverses are $g_i^{-1} = (\mathbf{Q}_i^T| - \mathbf{Q}_i^T\mathbf{c}_i)$. Further, the action of g_i on $\mathbf{p} \in \mathbb{R}^3$, as indicated above, is simply $g_i(\mathbf{p}) = \mathbf{Q}_i\mathbf{p} + \mathbf{c}_i$. Finally, the *orbit* of $\mathbf{p}$ is the collection $g_0(\mathbf{p}), g_1(\mathbf{p}), g_2(\mathbf{p}), \ldots$

Volume E of the International Tables of Crystallography (IT) contains a listing of *subperiodic groups*, i.e., the discrete isometry groups not containing a full set of 3 linearly independent translations. By definition, helical groups are discrete isometry groups containing no translations, and so they would appear to fall under the umbrella of this classification. However, as is known to crystallographers, Volume E of IT does not contain the helical groups. The is due to an unfortunate feature of the scheme by which IT is organized. That is, in IT two isometry groups G_1 and G_2 are considered the same if they are related by an affine transformation, $G_2 = aG_1a^{-1}$ where $a = (\mathbf{A}|\mathbf{c})$, $\det \mathbf{A} \neq 0$ (or, for some parts of IT, $\det \mathbf{A} > 0$). Here the product rule is the same as the one given above[2]. By this classification, there are infinitely many helical groups and a listing according to the scheme of IT is impossible. For example, by this classification scheme, the simple helical group specified in (2.1) below is actually an infinite number of different groups, one for each distinct choice of the angle θ[3].

For the purpose of this chapter, and, one could argue, for many other purposes in science and engineering, the affine equivalence is not relevant, as one would often like to know "what are all the groups". Indeed, for the purpose of exploring conditions of compatibility, we need explicit formulas for the groups with all the free parameters displayed[4]. We have rigorously derived the formulas for all the helical groups in this way [37]. From this, every helical group is given by one of four formulas:

$$\{h^m : m \in \mathbb{Z}\}, \tag{2.1}$$

$$\{h^m f^s : m \in \mathbb{Z},\ s = 1, 2\}, \tag{2.2}$$

$$\{h^m g^n : m \in \mathbb{Z},\ n = 1, \ldots, i\}, \tag{2.3}$$

$$\{h^m g^n f^s : m \in \mathbb{Z},\ n = 1, \ldots, i,\ s = 1, 2\}, \tag{2.4}$$

[2]For $\mathbf{Q}_i^T$ substitute $\mathbf{A}^{-1}$

[3]that is, there is no affine map which relates $\{h^m : m \in \mathbb{Z}\}, \{\tilde{h}^m : m \in \mathbb{Z}\}$ for $\theta \neq \tilde{\theta}$.

[4]Abstract groups (multiplication tables) are not so useful, and for the applications in this paper it does not matter if the abstract group suddenly gets bigger at a particular set of values of the parameters.

where

1. $h = (\mathbf{R}_\theta|\tau\mathbf{e} + (\mathbf{R}_\theta - \mathbf{I})\mathbf{p}_0\}$, $\mathbf{R}_\theta\mathbf{e} = \mathbf{e}$, $|\mathbf{e}| = 1$, $\mathbf{p}_0 \in \mathbb{R}^3$, $\mathbf{p}_0 \cdot \mathbf{e} = 0, \tau \in \mathbb{R} \setminus \{0\}$, is a screw displacement with an angle θ that is an irrational multiple of 2π.

2. $g = (\mathbf{R}_\psi|(\mathbf{R}_\psi - \mathbf{I})\mathbf{p}_0)$, $\mathbf{R}_\psi\mathbf{e} = \mathbf{e}$, is a proper rotation with angle $\psi = 2\pi/i$, $i \in \mathbb{Z}$, $i \neq 0$.

3. $f = (\mathbf{R}|\,(\mathbf{R} - \mathbf{I})\mathbf{p}_1)$, $\mathbf{R} = -\mathbf{I} + 2\mathbf{e}_1 \otimes \mathbf{e}_1$, $|\mathbf{e}_1| = 1, \mathbf{e} \cdot \mathbf{e}_1 = 0$ is a 180° rotation with axis perpendicular to $\mathbf{e}$. Here, $\mathbf{p}_1 = \mathbf{p}_0 + \xi\mathbf{e}$, for some $\xi \in \mathbb{R}$.

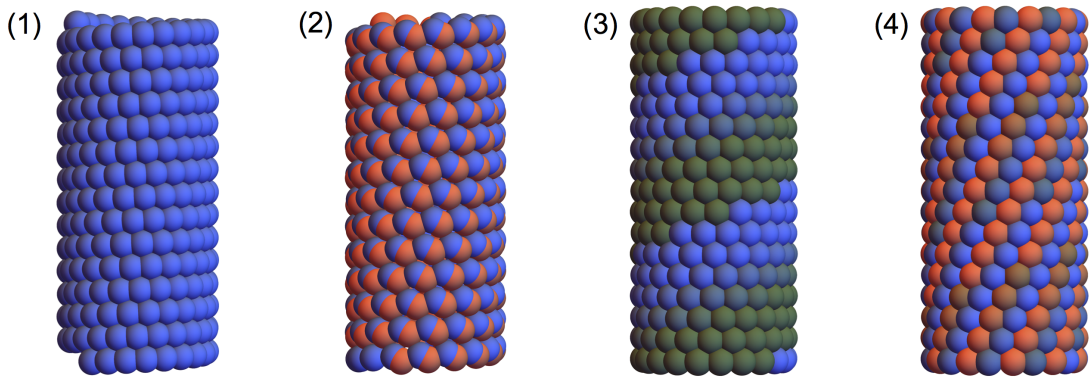

Figure 2.1: Helical groups corresponding to (2.1), (2.2), (2.3), (2.4), respectively. Each picture is the orbit of a single ball under the corresponding group and the coloring is according to the powers s or n.

Groups (2.1) and (2.3) are Abelian (the elements commute) and clearly (2.1) is a subgroup of (2.3). Groups (2.2) and (2.4) are not Abelian because the element f does not commute with g or h. However, note that $f^2 = identity$. Thus, the action of f on a molecule produces a copy of the molecule slightly tilted away from the opposite end of the cylinder. Then, to get the full structure in the orbit of (2.4), we operate the group (2.3) on this pair of molecules. If the structure is reasonably dense with molecules, we can always consider a pair close together, since there will be some molecule close to the axis through $\mathbf{e}_1$. (Note that $\mathbf{e}_1$ is perpendicular to the axis of the cylinder on which the structure lies.) But, if this pair is close together, then we can reasonably discuss compatibility in terms of the group (2.3). We therefore focus on the largest Abelian helical group (2.3) below.

Another reason for this focus is based on discrete notions studied in [14] which suggest that compatibility is related fundamentally to Abelian groups. This concerns the interpretation of compatibility as relating to the process of returning to the same atom position by going around a loop in the space $\mathbb{Z}^2$ of powers of the group elements.

We note that incidentally our assumptions also include several rod groups. (Rod groups have periodicity along the axis through $\mathbf{e}$.) This is because we do not use the assumption that θ is an irrational multiple of 2π in any of the results below.

Consider the two phases a and b each described as orbits of a molecule under the general Abelian helical group (2.3). Assign group parameters $\theta_{a,b} \in \mathbb{R}$, $\alpha_{a,b} = 2\pi/i_{a,b}$, $i_{a,b} \in \mathbb{Z} \setminus \{0\}$, $\tau_{a,b} \in \mathbb{R}$, $\mathbf{z}_{a,b} \in \mathbb{R}^3$ and $\mathbf{e}_{a,b} \in \mathbb{R}^3$, $|\mathbf{e}_{a,b}| = 1$. Define $\mathbf{Q}_\xi^{a,b} \in \mathrm{SO}(3)$ having axis $\mathbf{e}_{a,b}$ and angle ξ, i.e.,

$$\mathbf{Q}_\xi^{a,b} = \sin\xi \mathbf{W}^{a,b} + \cos\xi(\mathbf{I} - \mathbf{e}_{a,b} \otimes \mathbf{e}_{a,b}) + \mathbf{e}_{a,b} \otimes \mathbf{e}_{a,b}, \tag{2.5}$$

respectively, where $\mathbf{W}^{a,b} = -\mathbf{W}^{a,b\ T} = -\mathbf{e}_1^{a,b} \otimes \mathbf{e}_2^{a,b} + \mathbf{e}_2^{a,b} \otimes \mathbf{e}_1^{a,b}$, where $\mathbf{e}_1^{a,b}, \mathbf{e}_2^{a,b}, \mathbf{e}_{a,b}$ is a right- orthonormal basis. From this hypothesis—in particular that $\mathbf{e}_a, \mathbf{e}_b$ do not depend on ξ—we also have that

$$\frac{d}{d\xi}\mathbf{Q}_\xi^a = \mathbf{Q}_\xi^a \mathbf{W}^a, \quad \frac{d}{d\xi}\mathbf{Q}_\xi^b = \mathbf{Q}_\xi^b \mathbf{W}^b. \tag{2.6}$$

Note that $\mathbf{Q}_\xi^{a,b}\mathbf{W}^{a,b} = \mathbf{W}^{a,b}\mathbf{Q}_\xi^{a,b}$, respectively. The two elements h^m and g^n can be combined and the group (2.3) can be written as

$$\begin{aligned} G_a &= \left\{ \left(\mathbf{Q}^a_{m\theta_a + n\alpha_a} \,\middle|\, m\tau_a \mathbf{e}_a + (\mathbf{I} - \mathbf{Q}^a_{m\theta_a+n\alpha_a})\mathbf{z}_a \right) : m \in \mathbb{Z},\ n = 1, \ldots, i_a \right\}, \\ G_b &= \left\{ \left(\mathbf{Q}^b_{m\theta_b + n\alpha_b} \,\middle|\, m\tau_b \mathbf{e}_b + (\mathbf{I} - \mathbf{Q}^b_{m\theta_b+n\alpha_b})\mathbf{z}_b \right) : m \in \mathbb{Z},\ n = 1, \ldots, i_b \right\}, \end{aligned} \tag{2.7}$$

with sub/superscripts a and b denoting the two phases. It can be seen from the formulas in (2.7) that $G_{a,b}$ are groups under the product rule for isometries given in the

introduction, e.g.,

$$\left(\mathbf{Q}^a_{m\theta_a+n\alpha_a}\middle|\, m\tau_a\mathbf{e}_a+(\mathbf{I}-\mathbf{Q}^a_{m\theta_a+n\alpha_a})\mathbf{z}_a\right)\left(\mathbf{Q}^a_{m'\theta_a+n'\alpha_a}\middle|\, m'\tau_a\mathbf{e}_a+(\mathbf{I}-\mathbf{Q}^a_{m'\theta_a+n'\alpha_a})\mathbf{z}_a\right)$$
$$=\left(\mathbf{Q}^a_{(m+m')\theta_a+(n+n')\alpha_a}\middle|\,(m+m')\tau_a\mathbf{e}_a+(\mathbf{I}-\mathbf{Q}^a_{(m+m')\theta_a+(n+n')\alpha_a})\mathbf{z}_a\right). \tag{2.8}$$

Note that if $(n+n')>i_a$, then $(n+n')$ in (2.8) can be replaced by $(n+n')\mathrm{mod}\ i_a$.

The two groups G_a and G_b have different parameters. Our main task is to determine all choices of these parameters that give compatible interfaces.

These groups act on position vectors of atoms in one molecule as described above. For the purpose of studying compatibility we picture the molecule as reasonably compact and we discuss conditions of compatibility in terms of its center of mass. The precise statement of this assumption is that a typical diameter of the molecule is on the order of, or less than, the nearest neighbor distance between molecules defined in Section **??**. The examples of helical structures given in the introduction (including the tail sheath of bacteriophage T4) have this property.

The helical structures a and b consist of atomic positions given by the corresponding groups each acting on its respective center-of-mass position $\mathbf{p}_{a,b}$. Therefore, the center-of-mass positions of the helical structures are given by

$$\begin{aligned}\mathbf{y}_a(n,m) &= \mathbf{Q}^a_{m\theta_a+n\alpha_a}(\mathbf{p}_a-\mathbf{z}_a)+m\tau_a\mathbf{e}_a+\mathbf{z}_a,\ m\in\mathbb{Z},\ n=1,\ldots,i_a,\\ \mathbf{y}_b(n,m) &= \mathbf{Q}^b_{m\theta_b+n\alpha_b}(\mathbf{p}_b-\mathbf{z}_b)+m\tau_b\mathbf{e}_b+\mathbf{z}_b,\ m\in\mathbb{Z},\ n=1,\ldots,i_b.\end{aligned} \tag{2.9}$$

In the language of objective structures the structure a as viewed from the center of mass position $\mathbf{y}_a(m,n)$ is exactly the same as the structure viewed from $\mathbf{y}_a(m',n')$, for any choices of the integers m,n,m',n' (even though there may be no atoms at these centers of mass).

2.3 Helical structure generated by nearest-neighbor generators

2.3.1 Nearest-neighbor reparameterization of the groups

In this section, we drop the superscripts a, b and consider a single helical group G defined as above by

$$G = \{g(n,m) : m \in \mathbb{Z},\ n = 1, \ldots, i\}, \quad g(n,m) = \left(\mathbf{Q}_{m\theta+n\alpha} \middle| \ m\tau\mathbf{e} + (\mathbf{I} - \mathbf{Q}_{m\theta+n\alpha})\mathbf{z}\right). \tag{2.10}$$

As before, let the atomic positions be given by $\mathbf{y}(n,m) = g(n,m)(\mathbf{p})$. We assume without loss of generality that, $\mathbf{p} - \mathbf{z} \neq 0$, $(\mathbf{p} - \mathbf{z}) \cdot \mathbf{e} = 0$, $\tau \neq 0$ to avoid degenerate structures (lines, rings). Note that $g(0,0) = id$, so that $\mathbf{y}(0,0) = \mathbf{p}$.

Conditions of compatibility between phases ensure that nearby atoms before transformation remain near each other after transformation. Thus, distances are important. However, the standard parameterization of the groups given above in terms of n and m does not in general have the property that if $\mathbf{y}(n,m)$ is near $\mathbf{y}(n',m')$ in $\mathbb{R}^3$, then (n,m) is near (n',m') in $\mathbb{Z}^2$. Therefore, it is desirable to reparameterize the groups so that nearest and next-to-nearest neighbors of any point $\tilde{\mathbf{y}}(n,m)$ are $\tilde{\mathbf{y}}(n+1,m)$, $\tilde{\mathbf{y}}(n,m+1)$. Because G is an isometry group (i.e., preserves distances), we then have at least four nearest and next-to-nearest neighbors with positions $\tilde{\mathbf{y}}(n+1,m)$, $\tilde{\mathbf{y}}(n-1,m)$, $\tilde{\mathbf{y}}(n,m+1)$, $\tilde{\mathbf{y}}(n,m-1)$. (Of course, there may be additional nearest, or next-to-nearest, neighbors such as the case when $\tilde{\mathbf{y}}(n,m)$ is surrounded by six nearest neighbors.) As we show below, under mild assumptions on the group parameters, it is always possible to find such nearest neighbor generators.

A nearest neighbor reparameterization implies that nearest (and next to nearest) neighbors of the reparameterized structure correspond to nearest neighbors of (n,m) in the 2D lattice $\mathbb{Z}^2$. Thus,

$$\begin{aligned} dist^2(n,m) = |\mathbf{y}(n,m) - \mathbf{y}(0,0)|^2 &= |(\mathbf{Q}_{m\theta+n\alpha} - \mathbf{I})(\mathbf{p} - \mathbf{z}) + m\tau\mathbf{e}|^2 \\ &= 4r^2 \sin^2\left(\frac{m\theta + n\alpha}{2}\right) + m^2\tau^2, \end{aligned} \tag{2.11}$$

where $r = |\mathbf{p} - \mathbf{z}|$ (and subject to appropriate constraints). The minimizers always exist.

Indeed, as in continuum mechanics, we can use $\mathbb{Z}^2$ as a reference configuration.

Nearest and second nearest neighbors are obtained by minimizing[5] $dist^2(n,m)$ over integers m, n with $n \in \{1,\dots,i\}$. Let m_0 be the smallest integer greater than $2r^2/\tau^2 - 1/2$. No minimizer of (2.11) can have $|m| > m_0$, because, otherwise, decreasing $|m|$ by one decreases $dist$. Thus, since $n \in \{1,\dots,i\}$, the minimization of $dist^2(n,m)$ is a finite integer minimization problem, and both first and second nearest neighbors can always be found. However, we have non-uniqueness because $dist^2(n,m) = dist^2(-n,-m)$, and there may be additional degeneracy as mentioned above.

Since we have the existence of minimizers, we can suppose a minimizer of $dist^2(m,n)$ is given by $(n_1, m_1),\ n_1 \in \{1,\dots,i\}$. Further, we can consider the auxiliary minimization problem

$$\min_{m,n}\{dist^2(n,m)\colon m_1 n \neq n_1 m\}, \tag{2.12}$$

and suppose $(n_2, m_2),\ n_2 \in \{1,\dots,i\}$ is a minimizer to this problem. Hence, we study the group elements $g_1 = g(n_1,m_1)$ and $g_2 = g(n_2,m_2)$. Here, we call g_1 the *nearest neighbor generator* and g_2 is the *second nearest neighbor generator*[6]. The meaning of the constraint $m_1 n_2 \neq m_2 n_1$ is explained in detail below, but clearly it serves to rule out $n_2 = -n_1, m_2 = -m_1$ and other behavior such as $g_1^2 = g_2$ which would be problematic for a concept of compatibility.

We will show that the group G is generated by the nearest neighbor generators g_1 and g_2. Let

$$G' = \{g_1^p g_2^q : (p,q) \in \mathbb{Z}^2\}, \quad \text{(omit repeated elements)}. \tag{2.13}$$

Since g_1 and g_2 are both elements of the group G (as well as their products), G' is a subgroup of G. To show that $G' = G$, we will argue by contradiction. The basic idea is to define a unit cell[7] based on g_1 and g_2. Since these are nearest neighbor generators,

[5] In this formula, we have chosen the reference atom $\mathbf{y}(0,0)$ simply for convenience. Notice that the distance from the reference atom to its nearest and next nearest neighbors is independent of the particular choice of reference atom. For this reason, we are free to make this choice.

[6] It is possible for $dist(n_1,m_1) = dist(n_2,m_2)$, in which case the second nearest neighbor is actually the also the nearest neighbor, (i.e., if $\mathbf{y}(0,0)$ has six nearest neighbors, rather than just two).

[7] A *unit cell* in this case is the direct analog of that for the translation group, i.e., the images of the unit cell under the group cover the cylinder $\mathcal{C}$ defined just after (2.14), and images corresponding to distinct group elements are distinct.

this unit cell contains a single atom at one of the vertices. However, in supposing that $G' \neq G$, we will argue that there must be another atom inside this unit cell. This is the desired contradiction.

To define the unit cell, we first note that the formula $g_1^p g_2^q$ also makes sense when p and q are real numbers. The two vectors

$$\frac{d}{d\xi} g_1^\xi(\mathbf{p})|_{\xi=0}, \quad \frac{d}{d\eta} g_2^\eta(\mathbf{p})|_{\eta=0}, \tag{2.14}$$

define tangent vectors on the cylindrical surface $\mathcal{C} = \{\mathbf{z} + r(\cos\omega\,\mathbf{e}_1 + \sin\omega\,\mathbf{e}_2) + \zeta\mathbf{e} : 0 < \omega \leq 2\pi,\ \zeta \in \mathbb{R}\}$ where $\mathbf{e}_1, \mathbf{e}_2, \mathbf{e}$ are orthonormal. These two tangents are not parallel since by construction $m_1 n_2 \neq m_2 n_1$. We call this condition the *non-degeneracy condition*[8]. Hence,

$$\mathcal{U} = \{(g_1^\xi(\mathbf{p}), g_2^\eta(\mathbf{p})) : 0 \leq \xi < 1,\ 0 \leq \eta < 1\} \subset \mathcal{C} \tag{2.15}$$

is a unit cell for G' and has positive area.

To show $G' = G$, we argue by contradiction. We suppose that there are integers $\tilde{n}, \tilde{m}$ such that the isometry $\tilde{g} = g(\tilde{n}, \tilde{m}) \in G$ but $\tilde{g} \notin G'$. Let $\xi, \eta \in \mathbb{R}$ satisfy

$$\tilde{m} = \xi m_1 + \eta m_2 \quad \tilde{n} = \xi n_1 + \eta n_2. \tag{2.16}$$

Note that (2.16) is solvable for $(\xi, \eta) \in \mathbb{R}^2$ because we have assumed $m_1 n_2 \neq n_1 m_2$. Since $\tilde{g} \notin G'$, $(\tilde{m}, \tilde{n})$ are not both zero and at least one of ξ and η is not an integer. By subtracting suitable integers from $\tilde{m}$ and $\tilde{n}$, we can assume without loss of generality that $\xi, \eta \in [-1/2, 1/2]$ and ξ, η are not both zero.

We make the standing assumption on θ and α that $-\pi/2 \leq m_1\theta + n_1\alpha \leq \pi/2$ and $-\pi/2 \leq m_2\theta + n_2\alpha \leq \pi/2$. These reasonable assumptions imply that the unit cell $\mathcal{U}$ does not extend more than halfway around the cylinder $\mathcal{C}$. We also note that $\sin^2(\delta/2)$ is a strictly convex, even function of δ on the interval $-\pi/2 \leq \delta \leq \pi/2$. Then, using the

[8] If $m_1 n_2 = m_2 n_1$, then the two functions $g_1^\xi(\mathbf{p}), g_2^\eta(\mathbf{p})$ parameterize the same curve on the cylinder. In this case, g_1 and g_2 cannot be used to define a unit cell of the cylinder.

distance formula in (2.11), we have that

$$|g_1^{\xi} g_2^{\eta}(\mathbf{p}) - \mathbf{p}|^2 = 4r^2 \sin^2\left(\frac{\xi(m_1\theta + n_1\alpha) + \eta(m_2\theta + n_2\alpha)}{2}\right) + (\xi m_1 + \eta m_2)^2\tau^2. \quad (2.17)$$

By changing g_1 or g_2 to its inverse, if necessary (which does not change the distances $|g_{1,2}(\mathbf{p}) - \mathbf{p}|$), we can assume that $m_1 \geq 0, m_2 \geq 0$.

Using the evenness of $\sin^2$ (i.e., $\sin^2(\delta/2) = \sin^2(|\delta|/2)$) and its monotonicity on on the interval $(0, \pi/2)$, we observe that

$$\begin{aligned}\sin^2\left(\frac{\xi(m_1\theta + n_1\alpha) + \eta(m_2\theta + n_2\alpha)}{2}\right) &= \sin^2\left(\frac{|\xi(m_1\theta + n_1\alpha) + \eta(m_2\theta + n_2\alpha)|}{2}\right) \\ &\leq \sin^2\left(\frac{\frac{1}{2}|(m_1\theta + n_1\alpha)| + \frac{1}{2}|(m_2\theta + n_2\alpha)|}{2}\right) \\ &\leq \frac{1}{2}\sin^2\left(\frac{m_1\theta + n_1\alpha}{2}\right) + \frac{1}{2}\sin^2\left(\frac{m_2\theta + n_2\alpha}{2}\right). \end{aligned} \quad (2.18)$$

since $\xi, \eta \in [-1/2, 1/2]$. Here, the last step follows from the convexity of $\sin^2(\delta/2)$ on $[-\pi/2, \pi/2]$. This calculation, together with the observation $(\xi m_1 + \eta m_2)^2 \leq (1/4)(m_1 + m_2)^2$, shows that

$$\begin{aligned}|g_1^{\xi} g_2^{\eta}(\mathbf{p}) - \mathbf{p}|^2 &\leq \frac{1}{2}|g_1(\mathbf{p}) - \mathbf{p}|^2 - (\tau^2/2)m_1^2 + \frac{1}{2}|g_2(\mathbf{p}) - \mathbf{p}|^2 \\ &\quad - (\tau^2/2)m_2^2 + (\tau^2/4)(m_1 + m_2)^2 \\ &\leq |g_2(\mathbf{p}) - \mathbf{p}|^2 - (\tau^2/4)(m_2 - m_1)^2 \\ &\leq |g_2(\mathbf{p}) - \mathbf{p}|^2. \end{aligned} \quad (2.19)$$

Here we have used that $g_2(\mathbf{p})$ is a *second* nearest neighbor of $\mathbf{p} \in \mathcal{C}$. Following back through the inequalities, we see that equality holds in (2.19) only if $g_1 = g_2$ which is forbidden by our hypothesis $m_1 n_2 \neq m_2 n_1$. And also $g_1^{\xi} g_2^{\eta} \neq g_1$ by this hypothesis. Thus we reach the conclusion that $|g_1^{\xi} g_2^{\eta}(\mathbf{p}) - \mathbf{p}| < |g_2(\mathbf{p}) - \mathbf{p}|$ which contradicts that $g_2(\mathbf{p})$ is a second nearest neighbor of $\mathbf{p}$. Hence, $G' = G$.

We collect these results in the form of an algorithm below:

Algorithm: nearest neighbor generators. Let G be given by (2.10) with group parameters $\tau \neq 0, \alpha = 2\pi/i,\ i \in \mathbb{N}$, and let $r = |\mathbf{p} - \mathbf{z}| > 0$, $(\mathbf{p} - \mathbf{z}) \cdot \mathbf{e} = 0$, the unit

vector $\mathbf{e}$ being on the axis of $\mathbf{Q}_{(\cdot)}$. Let (n_1, m_1) be a minimizer of the finite-dimensional minimization problem,

$$\min_{\substack{n \in \{1,\ldots,i\} \\ m \in \mathbb{Z} \cap [-h,h]}} 4r^2 \sin^2\left(\frac{m\theta + n\alpha}{2}\right) + m^2\tau^2, \tag{2.20}$$

and let (n_2, m_2) be a minimizer of (2.20) subject to the constraint $m_1 n \neq m n_1$. Here, h is the smallest integer greater than $2r^2/\tau^2 - 1/2$. Assume that $-\pi/2 \leq m_1\theta + n_1\alpha \leq \pi/2$ and $-\pi/2 \leq m_2\theta + n_2\alpha \leq \pi/2$. Then nearest neighbor generators of G are given by

$$g_1 = g(n_1, m_1), \quad g_2 = g(n_2, m_2). \tag{2.21}$$

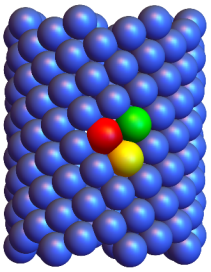

Figure 2.2: Illustration of nearest neighbor generators found by the algorithm (see text). Red is mapped to yellow by g_1 and red is mapped to green by g_2.

2.3.2 Domain of powers of the nearest neighbor generators

The parameterization above of G consists of powers of the two nearest neighbor generators. A group for generating a helical structure should not have repeated elements[9] since we want one an only one atom at each point in the orbit. However, arbitrary powers of g_1, g_2 will give repeated elements. In this section, we give a general procedure for finding a suitable domain of these powers that specifies the group G completely and has no repeated elements.

Let nearest neighbor generators $g_1 = g(n_1, m_1)$ and $g_2 = g(n_2, m_2)$ be given as

[9] In general, the theorems of group theory assume an indexing with no repeated elements.

above so that $m_1 n_2 \neq m_2 n_1$ with $n_1, n_2 \in \{1, \ldots, i\}$, where $i \in \mathbb{N}$ is given. Note that m_1 and m_2 cannot both be zero, so first we assume $m_1 \neq 0$. There are always values $(p, q) \neq (0, 0)$ such that $g_1^p g_2^q = id$. Under our hypotheses, these are those $(p, q) \in \mathbb{Z}^2$ satisfying

$$pn_1 + qn_2 = ni, \quad pm_1 + qm_2 = 0. \tag{2.22}$$

Since $n_1 m_2 - n_2 m_1 \neq 0$, the solutions of this system are pairs of integers (p, q) satisfying

$$p = n\, i \left(\frac{m_2}{n_1 m_2 - n_2 m_1}\right), \quad q = n\, i \left(\frac{-m_1}{n_1 m_2 - n_2 m_1}\right). \tag{2.23}$$

From these solutions and the assumption $m_1 \neq 0$, there is a unique solution $(p^\star, q^\star)$ of $(p, q) \neq (0, 0)$ of $g_1^p g_2^q = id$ that contains the smallest positive value of q. $\mathcal{D} = \mathbb{Z} \times \{1, \ldots, q^\star\}$ serves as a domain for the powers (p, q) with the property that there are no repeated elements.

To see this, note first that any $q \in \mathbb{Z}$ is expressible in the form $q = jq^\star + q'$ where $j \in \mathbb{Z}$ and $q' \in \{1, \ldots, q^\star\}$. Thus, $g_1^p g_2^q = g_1^{p' + jp^\star} g_2^{q' + jq^\star} = g_1^{p'} g_2^{q'}$, so the powers (p, q) of any group element can be assumed to lie in $\mathcal{D}$.

Thus we only need to show that two distinct pairs of powers $(p, q) \in \mathcal{D}$ and $(p', q') \in \mathcal{D}$ do not give the same group element. To see this, assume that $g_1^p g_2^q = g_1^{p'} g_2^{q'}$ for $q, q' \in \{1, \ldots, q^\star\}$ and, without loss of generality, $q \geq q'$. Then

$$g_1^{p - p'} g_2^{q - q'} = id. \tag{2.24}$$

By the minimality property of $q^\star$, this implies that $q = q'$, and (2.24) is reduced to $g_1^{p - p'} = id$. The latter is possible under the condition $m_1 \neq 0$ and the assumptions on the group parameters $\tau, \mathbf{z}$ if and only if $p = p'$. We have shown that each point $(p, q) \in \mathcal{D}$ (using nearest-neighbor generators g_1, g_2) corresponds to one and only one element of G.

In this argument, we made the additional hypothesis that $m_1 \neq 0$. This is without loss of generality. Note that the condition $n_1 m_2 - n_2 m_1 \neq 0$ forbids m_1 and m_2 to vanish simultaneously. Thus if $m_1 = 0$, then $m_2 \neq 0$. Consequently, we can simply replace g_1 with g_2 and g_2 with g_1 if this is the case. This generates the same structure but with $m_1 \neq 0$.

In total so far, we have deduced that $G = \{g_1^p g_2^q \colon (p,q) \in \mathcal{D}\}$ (with $m_1 \neq 0$), and this description has no repeated elements. In fact, we can relax the description of the unit domain to include integer translations of the domain $\mathcal{D}$, i.e., $\mathcal{D}_{q_0} = \mathbb{Z}\times\{q_0+1,\ldots,q_0+q^\star\}$ for any $q_0 \in \mathbb{Z}$. Specifically, we claim $G_{q_0} = \{g_1^{\tilde{p}} g_2^{\tilde{q}} \colon (\tilde{p},\tilde{q}) \in \mathcal{D}_{q_0}\}$ satisfies $G_{q_0} = G$ for any $q_0 \in \mathbb{Z}$, and G_{q_0} has no repeated elements. To prove this, we consider an arbitrary $q_0 \in \mathbb{Z}$. For the latter, we suppose $g_1^{\tilde{p}} g_2^{\tilde{q}}, g_1^{\bar{p}} g_2^{\bar{q}} \in G_{q_0}$ such that $g_1^{\tilde{p}} g_2^{\tilde{q}} = g_1^{\bar{p}} g_2^{\bar{q}}$. It follows that $g_1^{\tilde{p}} g_2^{\tilde{q}-q_0} = g_1^{\bar{p}} g_2^{\bar{q}-q_0} \in G$, and since G has no repeated elements, we obtain $\tilde{p} = \bar{p}$ and $\tilde{q} = \bar{q}$ as desired. For the former, we notice first that $G_{q_0} \subset G$ is trivial since G generates the entire helical structure. Thus, we need only to prove $G \subset G_{q_0}$. In this direction, let $(p,q) \in \mathcal{D}$. Recall that $g_1^{p^\star} g_2^{q^\star} = id$ and note that q_0 is expressible as $q_0 = jq^\star + q'$ for some $j \in \mathbb{Z}$ and $q' \in \{0,\ldots,q^\star - 1\}$. Thus, $g_1^p g_2^q \in G$ satisfies

$$g_1^p g_2^q = g_1^{p+jp^\star} g_2^{q+jq^\star} = \begin{cases} g_1^{p+jp^\star} g_2^{q-q'+q_0} \\ g_1^{p+(j+1)p^\star} g_2^{q-q'+q^\star+q_0}. \end{cases} \tag{2.25}$$

If $q - q' > 0$, then $q - q' + q_0 \in \{q_0+1,\ldots,q_0+q^\star\}$. Consequently, $g_1^{p+jp^\star} g_2^{q-q'+q_0} \in G_{q_0}$. Otherwise, $q - q' \leq 0$, and so $q - q' + q^\star + q_0 \in \{q_0+2,\ldots,q_0+q_\star\}$. Consequently, $g_1^{p+(j+1)p^\star} g_2^{q-q'+q^\star+q_0} \in G_{q_0}$. In either case, given (2.25), we see that there is a $(\tilde{p},\tilde{q}) \in \mathcal{D}_{q_0}$ such that $g_1^p g_2^q = g_1^{\tilde{p}} g_2^{\tilde{q}} \in G_{q_0}$. Hence, $G \subset G_{q_0}$ as desired.

To summarize these results:

Algorithm: domain of powers of the generators. Assume the conditions on parameters listed above for the derivation of nearest neighbor generators, and choose the labeling of the generators g_1 and g_2 so that $m_1 \neq 0$. Let $\hat{q}(n) = -n\,i\,m_1/(n_1m_2 - n_2m_1)$ and define

$$q^\star = \min_{\substack{n \in \mathbb{Z}\setminus\{0\} \\ \hat{q}(n) > 0 \\ \hat{q}(n) \in \mathbb{Z}}} \hat{q}(n). \tag{2.26}$$

Then for any $q_0 \in \mathbb{Z}$, $\mathcal{D}_{q_0} = \mathbb{Z} \times \{q_0+1,\ldots,q_0+q^\star\}$ has the property that $G = \{g_1^p g_2^q : (p,q) \in \mathcal{D}_{q_0}\}$, and this description has no repeated elements.

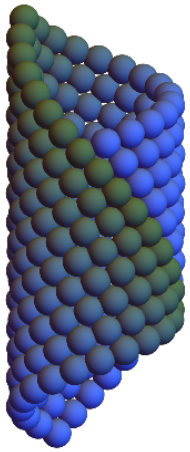

Figure 2.3: Illustration of the calculation of the domain $\mathcal{D}$. In this case $q^\star = 14$ and the shading is according to the value of q.

2.4 Compatibility condition in helical structures

2.4.1 Discrete vs. continuum concepts of compatibility

Compatibility in discrete structures is fundamentally connected with Abelian groups. It concerns the fact that a product of group elements that corresponds to a loop in the space of powers $\mathbb{Z}^n$ of the n generators gives the identity. When the group is the infinitesimal translation group operating on $\mathbb{R}^n$ and the action of the group on vector fields $\mathbf{v}(\mathbf{p}), \mathbf{p} \in \mathbb{R}^n$ is arranged appropriately, this gives the usual notion of calculus, i.e., conditions under which $\mathbf{v} = \nabla\varphi$. Another example is given in [14] in which molecules interact according to their positions and orientations.

As far as we are aware, there is no theory of compatibility for interfaces between discrete structures having different sets of structural parameters. This would involve the formulation of appropriate definitions that say that one can set up a correspondence of neighboring molecules, such that corresponding molecules before transformation remain close after partial transformation, when separated by a phase boundary.

On the other hand, there is a straightforward and simple notion of compatibility at interfaces for discrete structures that is directly inherited from continuum ideas. In the present case it is the following. After passing to nearest neighbor parameterization

as above, we consider the formulas $\mathbf{y}_{a,b}(p,q)$ defined above. The functions $\mathbf{y}_a(p,q)$ and $\mathbf{y}_b(p,q)$ are defined on different discrete domains, but they make perfect sense if they are extended to a strip in $\mathbb{R}^2$. We wish to use continuity of these functions to impose compatibility, and for this purpose we will extend their domains to all values of $(p,q) \in \mathbb{R} \times (0, q^\star_{a,b}] \subset \mathbb{R}^2$. Restrict the structure a to be locally on one side of an interface $(p,q) = (\hat{p}(s), \hat{q}(s)),\ s_1 < s < s_2$ and b to be on the other side. Then, under suitable smoothness assumptions, the standard continuum notion of compatibility is

$$\nabla_{p,q}\mathbf{y}_a(\hat{p}(s),\hat{q}(s)) - \nabla_{p,q}\mathbf{y}_b(\hat{p}(s),\hat{q}(s)) = \mathbf{a}(s) \otimes \mathbf{n}(s), \quad \mathbf{n}(s) = (-\hat{q}'(s), \hat{p}'(s)); \quad (2.27)$$

that is, equivalently,

$$\Big(\partial_p \mathbf{y}_a(\hat{p}(s),\hat{q}(s)) - \partial_p \mathbf{y}_b(\hat{p}(s),\hat{q}(s))\Big)\hat{p}'(s) + \Big(\partial_q \mathbf{y}_a(\hat{p}(s),\hat{q}(s)) - \partial_q \mathbf{y}_b(\hat{p}(s),\hat{q}(s))\Big)\hat{q}'(s) = 0. \quad (2.28)$$

Note that there is a lot of freedom here. Even with this canonical interpolation, note that we have complete freedom on where to place the interface $(\hat{p}(s), \hat{q}(s))$ between the discrete positions. In this chapter we define compatibility by using (2.28).

Note that we use the same interface $(\hat{p}(s), \hat{q}(s))$ in the reference domain for both structures in $\mathbb{R}^2$. This also does not seem to be restrictive, since we allow the group parameters as well as the $(0,0)$ positions to be assignable. However, the interface has to respect the two (potentially different) periods $q^\star_a$ and $q^\star_b$. If, say, $q^\star_a < q^\star_b$ and the interface extends into the region $q^\star_a < q < q^\star_b$ then $\mathbf{y}_a$ is undefined on this region: there are no molecules from structure a that can be matched with those of b across this part of the interface. Thus we assume $0 < \hat{q}(s) \leq min\{q^\star_a, q^\star_b\}$. Moreover, we solve rigorously the local problem: under mild hypotheses we find necessary and sufficient conditions that (2.28) is satisfied in a sufficiently small neighborhood $s_1 < s < s_2$ on which $0 < \hat{q}(s) \leq min\{q^\star_a, q^\star_b\}$. Then we show that some of these solutions can be extended to larger intervals.

2.4.2 Local compatibility

Hypotheses on the groups. Let $G_a \neq G_b$ be the two helical groups

$$\begin{aligned} G_a = & \left\{ \left(\mathbf{Q}^a_{m\theta_a+n\alpha_a} \,\middle|\, m\tau_a \mathbf{e}_a + (\mathbf{I} - \mathbf{Q}^a_{m\theta_a+n\alpha_a})\mathbf{z}_a \right) : m \in \mathbb{Z},\ n = 1, \ldots, i_a \right\}, \\ G_b = & \left\{ \left(\mathbf{Q}^b_{m\theta_b+n\alpha_b} \,\middle|\, m\tau_b \mathbf{e}_b + (\mathbf{I} - \mathbf{Q}^b_{m\theta_b+n\alpha_b})\mathbf{z}_b \right) : m \in \mathbb{Z},\ n = 1, \ldots, i_b \right\}, \end{aligned} \quad (2.29)$$

where $\mathbf{z}_{a,b}, \mathbf{e}_{a,b} \in \mathbb{R}^3$, the unit vector $\mathbf{e}_{a,b}$ being on the axis of $\mathbf{Q}^{a,b}_{(.)} \in \mathrm{SO}(3)$, and $\tau_{a,b} \neq 0, \theta_{a,b} \in \mathbb{R}, \alpha_{a,b} = 2\pi/i_{a,b}, i_{a,b} \in \mathbb{N}$. The helical structures are generated by applying these groups on $\mathbf{p}_{a,b} \in \mathbb{R}^3$ with $r_{a,b} = |\mathbf{p}_{a,b} - \mathbf{z}_{a,b}| > 0$, $(\mathbf{p}_{a,b} - \mathbf{z}_{a,b}) \cdot \mathbf{e}_{a,b} = 0$. Nearest neighbor generators given by (2.20) and (2.26) generate the re-parameterized groups

$$\begin{aligned} G_a = & \left\{ \left(\mathbf{Q}^a_{p\psi_a+q\beta_a} \,\middle|\, (pm^a_1 + qm^a_2)\tau_a \mathbf{e}_a + (\mathbf{I} - \mathbf{Q}^a_{p\psi_a+q\beta_a})\mathbf{z}_a \right) : p \in \mathbb{Z},\ q = 1, \ldots, q^\star_a \right\}, \\ G_b = & \left\{ \left(\mathbf{Q}^b_{p\psi_b+q\beta_b} \,\middle|\, (pm^b_1 + qm^b_2)\tau_b \mathbf{e}_b + (\mathbf{I} - \mathbf{Q}^b_{p\psi_b+q\beta_b})\mathbf{z}_b \right) : p \in \mathbb{Z},\ q = 1, \ldots, q^\star_b \right\} \end{aligned} \quad (2.30)$$

with no repeated elements. Here $\psi_{a,b} = m^{a,b}_1\theta_{a,b} + n^{a,b}_1\alpha_{a,b}, \beta_{a,b} = m^{a,b}_2\theta_{a,b} + n^{a,b}_2\alpha_{a,b}$, and, to satisfy the algorithms for construction of the nearest neighbor generators, the integers $m^{a,b}_1$ and $m^{a,b}_2$ satisfy the condition $m^{a,b}_1 n^{a,b}_2 \neq m^{a,b}_2 n^{a,b}_1$. The latter is equivalent to $m^{a,b}_2\psi_{a,b} \neq m^{a,b}_1\beta_{a,b}$ and $\pi/2 \leq \psi_{a,b}, \beta_{a,b} \leq \pi/2$.

Hypotheses on the interface and compatibility. The two helical structures generated by (2.30) are

$$\begin{aligned} \mathbf{y}_a(p,q) &= \mathbf{Q}^a_{p\psi_a+q\beta_a}\mathbf{r}_a + (pm^a_1 + qm^a_2)\tau_a\mathbf{e}_a + \mathbf{z}_a,\ p \in \mathbb{Z},\ q = 1, \ldots, q^\star_a, \\ \mathbf{y}_b(p,q) &= \mathbf{Q}^b_{p\psi_b+q\beta_b}\mathbf{r}_b + (pm^b_1 + qm^b_2)\tau_b\mathbf{e}_b + \mathbf{z}_b, \quad p \in \mathbb{Z},\ q = 1, \ldots, q^\star_b, \end{aligned} \quad (2.31)$$

where $\mathbf{r}_{a,b} = \mathbf{p}_{a,b} - \mathbf{z}_{a,b}$, $\mathbf{r}_{a,b} \cdot \mathbf{e}_{a,b} = 0$. Following the previous discussion, we extend the domain of $\mathbf{y}_{a,b}(p,q)$ to a suitable subset of $\mathbb{R}^2$, and we seek an arclength parameterized continuously differentiable curve $(\hat{p}(s), \hat{q}(s)) \in \mathbb{R}^2$ defined on $s_1 < s < s_2$ and satisfying $0 \leq \hat{q}(s) \leq min\{q^\star_a, q^\star_b\}$, $\hat{p}'(s)^2 + \hat{q}'(s)^2 = 1$. The condition that the interface can be

parameterized by arclength is without loss of generality, since the condition (2.28) is linear in $\hat{p}', \hat{q}'$. The *local compatibility condition* is then given by

$$\begin{aligned}\hat{p}'(s)\Big(\mathbf{Q}^a_{\hat{p}(s)\psi_a+\hat{q}(s)\beta_a}(\psi_a\mathbf{W}^a\mathbf{r}_a + m_1^a\tau_a\mathbf{e}_a) - \mathbf{Q}^b_{\hat{p}(s)\psi_b+\hat{q}(s)\beta_b}(\psi_b\mathbf{W}^b\mathbf{r}_b + m_1^b\tau_b\mathbf{e}_b)\Big)\\ = -\hat{q}'(s)\Big(\mathbf{Q}^a_{\hat{p}(s)\psi_a+\hat{q}(s)\beta_a}(\beta_a\mathbf{W}^a\mathbf{r}_a + m_2^a\tau_a\mathbf{e}_a) - \mathbf{Q}^b_{\hat{p}(s)\psi_b+\hat{q}(s)\beta_b}(\beta_b\mathbf{W}^b\mathbf{r}_b + m_2^b\tau_b\mathbf{e}_b)\Big),\end{aligned} \tag{2.32}$$

for $s \in (s_1, s_2)$ and with the hypotheses on the parameters given above. We obtained this formula simply by substituting (2.31) into (2.28).

Below, we identify necessary and sufficient conditions on structural parameters $\{\psi_{a,b}, \beta_{a,b}, \tau_{a,b} \in \mathbb{R}; \mathbf{r}_{a,b}, \mathbf{z}_{a,b}, \mathbf{e}_{a,b} \in \mathbb{R}^3, |\mathbf{e}_{a,b}| = 1; m_1^{a,b}, m_2^{a,b} \in \mathbb{Z}\}$ satisfying the restrictions given above that allow for the existence of such curves. Note that we allow the full set of parameters to vary, so that the two helical phases can lie on different cylinders of arbitrary positive radius, with arbitrary orientation, and lying on arbitrary axes. Further, the structural parameters defining pitch and other characteristics are subject to only very mild restrictions.

Simplification of the local compatibility condition. The compatibility condition (2.32) can be simplified. To do this, we first consolidate some of the notation.

We set $\mathbf{x}(s) = (\hat{p}(s), \hat{q}(s))$ for the arc-length parameterized curves defined above. Thus, we have $|\mathbf{x}'(s)| = 1$ for all $s \in (s_1, s_2)$, and so we define

$$\mathbf{t}(s) = \mathbf{x}'(s), \quad \mathbf{n}(s) = -(\mathbf{t}(s)\cdot\mathbf{e}_2)\mathbf{e}_1 + (\mathbf{t}(s)\cdot\mathbf{e}_1)\mathbf{e}_2. \tag{2.33}$$

It follows that $\mathbf{t}(s)$ is *tangent* to the interface and $\mathbf{n}(s)$ is *normal* to the interface at each point $\mathbf{x}(s)$. Further, the set $\{\mathbf{t}(s), \mathbf{n}(s)\}$ forms an orthonormal basis for all $s \in (s_1, s_2)$. Finally, we can write

$$\mathbf{t}'(s) = \kappa(s)\mathbf{n}(s), \quad s_1 < s < s_2, \tag{2.34}$$

where $\kappa(s) \in \mathbb{R}$ gives the *curvature* of the interface at each $\mathbf{x}(s)$. In addition to this

notation describing the interface, we introduce the vectors

$$\mathbf{f}_{a,b} = \begin{pmatrix} \psi_{a,b} \\ \beta_{a,b} \end{pmatrix}, \quad \mathbf{g}_{a,b} = \tau_{a,b} \begin{pmatrix} m_1^{a,b} \\ m_2^{a,b} \end{pmatrix} \tag{2.35}$$

in order to consolidate the parameters. Then the non-degeneracy condition can be rewritten as

$$\mathbf{f}_{a,b} \cdot \mathbf{g}_{a,b}^{\perp} \neq 0 \tag{2.36}$$

where $\mathbf{g}_{a,b}^{\perp} = -(\mathbf{g}_{a,b} \cdot \mathbf{e}_2)\mathbf{e}_1 + (\mathbf{g}_{a,b} \cdot \mathbf{e}_1)\mathbf{e}_2$ (recall the hypotheses on the groups above).

The local compatibility equation can now be written as a total derivative,

$$\Big(\mathbf{Q}^a(\mathbf{x}(s) \cdot \mathbf{f}_a)\mathbf{r}_a + (\mathbf{x}(s) \cdot \mathbf{g}_a)\mathbf{e}_a\Big)' = \Big(\mathbf{Q}^b(\mathbf{x}(s) \cdot \mathbf{f}_b)\mathbf{r}_b - (\mathbf{x}(s) \cdot \mathbf{g}_b)\mathbf{e}_b\Big)' \tag{2.37}$$

for $s \in (s_1, s_2)$, where we have set $\mathbf{Q}^{a,b}(\mathbf{x}(s) \cdot \mathbf{f}_{a,b}) = \mathbf{Q}^{a,b}_{\hat{p}(s)\psi_{a,b}+\hat{q}(s)\beta_{a,b}}$.

Cases based on curvature. We can succinctly catalogue all possible ways of obtaining a locally compatible interface based on properties of the parameterized interface $\mathbf{x}(s)$ (see (2.33) and (2.34)). First note that either $\mathbf{t}(s) = \mathbf{t} = const.$ on (s_1, s_2) or there is a point $s^* \in (s_1, s_2)$ where the curvature is nonzero. In the latter case, since we are solving the local problem, we shrink the interval (s_1, s_2), $s_1 < s^* < s_2$ so that $\kappa(s) \neq 0$ on (s_1, s_2). Thus, for the *locally compatible interface* there are two cases to consider:

1. $\mathbf{t}(s) = \mathbf{t} = const.$ for all $s \in (s_1, s_2)$.

2. The curvature $\kappa(s) \neq 0$ for all $s \in (s_1, s_2)$.

In the remainder of this section, we develop a complete characterization of local compatibility. We state this characterization in the form of theorems for each of the two cases above. These results are then summarized and discussed in the next section.

2.4.3 Implications of interface reference curvature

Lemma 2.4.1. *The curvature $\kappa(s) = 0$ for all $s \in (s_1, s_2)$ if and only if $(\mathbf{e}_a \times \mathbf{e}_b) = 0$.*

Proof. ($\Leftarrow$). Without loss of generality, we can assume $\mathbf{e}_a = \mathbf{e}_b = \mathbf{e}$ since the case $\mathbf{e}_a = -\mathbf{e}_b$ has an identical structure (after replacing $\mathbf{f}_a$ with $-\mathbf{f}_a$ and $\mathbf{g}_a$ with $-\mathbf{g}_a$). By

explicit differentiation and some rearranging of terms, the compatibility condition in (2.37) has the form

$$(\mathbf{t}(s)\cdot\mathbf{f}_a)\mathbf{Q}(\mathbf{x}(s)\cdot\mathbf{f}_a)\mathbf{W}\mathbf{r}_a-(\mathbf{t}(s)\cdot\mathbf{f}_b)\mathbf{Q}(\mathbf{x}(s)\cdot\mathbf{f}_b)\mathbf{W}\mathbf{r}_b=\Big((\mathbf{g}_b-\mathbf{g}_a)\cdot\mathbf{t}(s)\Big)\mathbf{e} \tag{2.38}$$

for $s\in(s_1,s_2)$ in this case. Here, $\mathbf{Q}(\cdot)=\mathbf{Q}^a(\cdot)=\mathbf{Q}^b(\cdot)$ and $\mathbf{W}=\mathbf{W}^a=\mathbf{W}^b$ since $\mathbf{e}_{a,b}=\mathbf{e}$ (recall (2.5)). Both $\mathbf{Q}(\mathbf{x}(s)\cdot\mathbf{f}_b)\mathbf{W}\mathbf{r}_b$ and $\mathbf{Q}(\mathbf{x}(s)\cdot\mathbf{f}_a)\mathbf{W}\mathbf{r}_a$ are perpendicular to $\mathbf{e}=\mathbf{e}_{a,b}$. Thus, equality holds if and only if both sides vanish. For the right-hand side, this means $(\mathbf{g}_b-\mathbf{g}_a)\cdot\mathbf{t}(s)=0$. By differentiating this identity, we also require $\kappa(s)(\mathbf{g}_b-\mathbf{g}_a)\cdot\mathbf{n}(s)=0$. Finally, since $\mathbf{n}(s)$ is perpendicular to $\mathbf{t}(s)$, we conclude $\kappa(s)=0$ for all $s\in(s_1,s_2)$ or $\mathbf{g}_a=\mathbf{g}_b$. Notice that if the latter condition *does not* hold, then we are done as we have proved $\kappa(s)$ vanishes in this case. Hence, we assume $\mathbf{g}_a=\mathbf{g}_b$.

Substituting $\mathbf{g}_a=\mathbf{g}_b$ back into (2.38), the left-hand side vanishes. There are then two distinct cases to consider:

(a) The vectors $\mathbf{Q}(\mathbf{x}(s)\cdot\mathbf{f}_b)\mathbf{W}\mathbf{r}_b$ and $\mathbf{Q}(\mathbf{x}(s)\cdot\mathbf{f}_a)\mathbf{W}\mathbf{r}_a$ are parallel for all $s\in(s_1,s_2)$.

(b) These vectors are linearly independent on some interval[10] $(\tilde{s}_1,\tilde{s}_2)\subset(s_1,s_2)$.

We suppose (a). Then, we can write $\mathbf{Q}(\mathbf{x}(s)\cdot\mathbf{f}_a)\mathbf{W}\mathbf{r}_a=\pm(|\mathbf{r}_a|/|\mathbf{r}_b|)\mathbf{Q}(\mathbf{x}(s)\cdot\mathbf{f}_b)\mathbf{W}\mathbf{r}_b$, where the $\pm$ is fixed for all s (given the smoothness hypothesis). This implies $\mathbf{W}\mathbf{r}_a=\pm(|\mathbf{r}_a|/|\mathbf{r}_b|)\mathbf{Q}(\mathbf{x}(s)\cdot(\mathbf{f}_b-\mathbf{f}_a))\mathbf{W}\mathbf{r}_b$ since $\mathbf{e}_{a,b}=\mathbf{e}$. By differentiating this quantity, we deduce the identity $\mathbf{t}(s)\cdot(\mathbf{f}_b-\mathbf{f}_a)=0$. By differentiating this, we deduce that either $\kappa(s)=0$ on for all s or $\mathbf{f}_b=\mathbf{f}_a$. We assume the latter, as the former is desired. Actually though, in substituting this back into (2.38) (using that $\mathbf{g}_a=\mathbf{g}_b$ and $\mathbf{f}_a=\mathbf{f}_b\neq 0$), we conclude $\mathbf{r}_a=\mathbf{r}_b$ since $\mathbf{Q}(\mathbf{x}(s)\cdot(\mathbf{f}_b-\mathbf{f}_a))=\mathbf{I}$. But then, since $\mathbf{g}_a=\mathbf{g}_b$, $\mathbf{f}_a=\mathbf{f}_b$ and $\mathbf{r}_a=\mathbf{r}_b$, violating the hypothesis $G_a\neq G_b$.

We suppose (b). Then, $\mathbf{Q}(\mathbf{x}(s)\cdot\mathbf{f}_b)\mathbf{W}\mathbf{r}_b$ and $\mathbf{Q}(\mathbf{x}(s)\cdot\mathbf{f}_a)\mathbf{W}\mathbf{r}_a$ are linearly independent for all $s\in(\tilde{s}_1,\tilde{s}_2)$. Consequently, the left-hand side of (2.38) vanishes on this interval if and only if $\mathbf{t}(s)\cdot\mathbf{f}_b=\mathbf{t}(s)\cdot\mathbf{f}_a=0$ for all $s\in(\tilde{s}_1,\tilde{s}_2)$. By differentiating these identities (as we did above), we conclude that either $\kappa(s)=0$ for $s\in(\tilde{s}_1,\tilde{s}_2)$ or $\mathbf{f}_a=\mathbf{f}_b=0$. The latter contradicts the hypotheses on the group parameters stated at the start of this section. So the former must be true in this case.

[10] If they are linearly independent at a single point, then, by continuity, they must be linearly independent on some interval.

Consequently, we always have vanishing curvature in this case. That is, we have determined that $(\mathbf{e}_a \times \mathbf{e}_b) = 0$ implies $\kappa(s) = 0$ for all s, as desired.

($\Rightarrow$). Suppose, for the sake of a contradiction, that $\kappa(s) = 0$ for all $s \in (s_1, s_2)$ but $(\mathbf{e}_a \times \mathbf{e}_b) \neq 0$. By explicitly differentiating the compatibility condition in (2.37), we obtain

$$(\mathbf{t}\cdot\mathbf{f}_b)\mathbf{Q}^b(\mathbf{x}(s)\cdot\mathbf{f}_b)\mathbf{W}^b\mathbf{r}_b - (\mathbf{t}\cdot\mathbf{f}_a)\mathbf{Q}^a(\mathbf{x}(s)\cdot\mathbf{f}_a)\mathbf{W}^a\mathbf{r}_a = (\mathbf{g}_a\cdot\mathbf{t})\mathbf{e}_a - (\mathbf{g}_b\cdot\mathbf{t})\mathbf{e}_b \tag{2.39}$$

for all $s \in (s_1, s_2)$. Notice that the tangent $\mathbf{t}(s) = \mathbf{t} = const$ in this case. Thus, by differentiating twice more, we obtain two additional equations

$$\begin{aligned}(\mathbf{t}\cdot\mathbf{f}_b)^2\mathbf{Q}^b(\mathbf{x}(s)\cdot\mathbf{f}_b)\mathbf{r}_b &= (\mathbf{t}\cdot\mathbf{f}_a)^2\mathbf{Q}^a(\mathbf{x}(s)\cdot\mathbf{f}_a)\mathbf{r}_a,\\ (\mathbf{t}\cdot\mathbf{f}_b)^3\mathbf{Q}^b(\mathbf{x}(s)\cdot\mathbf{f}_b)\mathbf{W}^b\mathbf{r}_b &= (\mathbf{t}\cdot\mathbf{f}_a)^3\mathbf{Q}^a(\mathbf{x}(s)\cdot\mathbf{f}_a)\mathbf{W}^a\mathbf{r}_a,\end{aligned} \tag{2.40}$$

which must hold for all $s \in (s_1, s_2)$. We dot both of these equations with $\mathbf{e}_b$ so that the left-hand sides vanish. Then, we must have $\mathbf{t}\cdot\mathbf{f}_a = 0$ or $\mathbf{e}_b\cdot\mathbf{Q}^a(\mathbf{x}(s)\cdot\mathbf{f}_a)\mathbf{W}^a\mathbf{r}_a = \mathbf{e}_b\cdot\mathbf{Q}^a(\mathbf{x}(s)\cdot\mathbf{f}_a)\mathbf{r}_a = 0$. However, the latter implies that $\mathbf{e}_b$ is parallel to $\mathbf{e}_a$ since the set $\{\mathbf{Q}^a(\mathbf{x}(s)\cdot\mathbf{f}_a)\mathbf{r}_a, \mathbf{Q}^a(\mathbf{x}(s)\cdot\mathbf{f}_a)\mathbf{W}^a\mathbf{r}_a, \mathbf{e}_a\}$ forms an orthogonal basis of $\mathbb{R}^3$. But $\mathbf{e}_a\times\mathbf{e}_b \neq 0$ by hypothesis. So we conclude $\mathbf{f}_a\cdot\mathbf{t} = 0$. Now, we instead dot the equations in (2.40) with $\mathbf{e}_a$ so that the right-hand sides vanish. By a similar argument, we conclude $\mathbf{f}_b\cdot\mathbf{t} = 0$. Substituting $\mathbf{f}_{a,b}\cdot\mathbf{t} = 0$ back into (2.39), we see that the left-hand side vanishes. It, therefore, follows that $\mathbf{g}_a\cdot\mathbf{t} = \mathbf{g}_b\cdot\mathbf{t} = 0$ since $\mathbf{e}_a\times\mathbf{e}_b \neq 0$. In summary, we have deduced that $\mathbf{f}_{a,b}$ and $\mathbf{g}_{a,b}$ are all parallel for this case. But this means that $\mathbf{f}_a\cdot\mathbf{g}_a^{\perp} = 0$, and this violates the non-degeneracy condition given in the start of this section. This is the desired contradiction, proving that, if $\kappa(s) = 0$ for all $s \in (s_1, s_2)$, then $(\mathbf{e}_a\times\mathbf{e}_b) = 0$. $\square$

2.5 Classification of all local solutions

Locally compatible interfaces with zero curvature or nonzero curvature can be further classified.

2.5.1 Vertical, horizontal and helical interfaces

Theorem 2.5.1 (Case 1: Interfaces with zero curvature)**.** *Assume the conditions of Section 2.4 on group parameters and assume without loss of generality that* $\mathbf{e}_a \cdot \mathbf{e}_b > 0$*. Assume that the curvature* $\kappa(s) = 0$ *on* (s_1, s_2)*. Each locally compatible interface is contained in one of the following cases:*

(i) (Vertical interfaces). $\mathbf{e}_a = \mathbf{e}_b$*,* $\mathbf{t} \cdot \mathbf{f}_a = \mathbf{t} \cdot \mathbf{f}_b = 0$*, and* $\mathbf{t} \cdot \mathbf{g}_a = \mathbf{t} \cdot \mathbf{g}_b \neq 0$*;*

(ii) (Horizontal interfaces). $\mathbf{e}_a = \mathbf{e}_b$*,* $\mathbf{t} \cdot \mathbf{f}_a = \mathbf{t} \cdot \mathbf{f}_b \neq 0$*,* $\mathbf{g}_a \cdot \mathbf{t} = \mathbf{g}_b \cdot \mathbf{t} = 0$*, and*

$$\mathbf{r}_a = \mathbf{Q}^b(\mathbf{x}(s_1) \cdot (\mathbf{f}_b - \mathbf{f}_a))\mathbf{r}_b; \tag{2.41}$$

(iii) (Helical interfaces). The same as the horizontal interface except that $\mathbf{g}_a \cdot \mathbf{t} = \mathbf{g}_b \cdot \mathbf{t} \neq 0$*.*

The interface is given by $\mathbf{x}(s) = (s - s_1)\mathbf{t} + \mathbf{c}$ *for some* $\mathbf{c} \in \mathbb{R}^2$*.*

Proof. Since $\mathbf{t}(s) = \mathbf{t} = const$, we have $\mathbf{e}_a \times \mathbf{e}_b \neq 0$ by Lemma 2.4.1 and so $\mathbf{e}_a = \mathbf{e}_b = \mathbf{e}$. Thus, $\mathbf{Q}^a(\cdot) = \mathbf{Q}^b(\cdot) = \mathbf{Q}(\cdot)$ and $\mathbf{W}^a = \mathbf{W}^b = \mathbf{W}$. Hence, by explicitly differentiating the compatibility equation in (2.37) and pre-multiplying this equation by $\mathbf{Q}(-\mathbf{x}(s) \cdot \mathbf{f}_a)$, we obtain a condition equivalent to local compatibility in this case:

$$(\mathbf{t} \cdot \mathbf{f}_b)\mathbf{Q}\big(\mathbf{x}(s) \cdot (\mathbf{f}_b - \mathbf{f}_a)\big)\mathbf{W}\mathbf{r}_b - (\mathbf{t} \cdot \mathbf{f}_a)\mathbf{W}\mathbf{r}_a = (\mathbf{g}_a \cdot \mathbf{t} - \mathbf{g}_b \cdot \mathbf{t})\mathbf{e} \tag{2.42}$$

for $s \in (s_1, s_2)$. Here, $\mathbf{W}\mathbf{r}_a$ and $\mathbf{Q}\big(\mathbf{x}(s) \cdot (\mathbf{f}_b - \mathbf{f}_a)\big)\mathbf{W}\mathbf{r}_b$ are both perpendicular to $\mathbf{e}$. Thus, by dotting this quantity with $\mathbf{e}$, we see that $\mathbf{g}_a \cdot \mathbf{t}$ must equal $\mathbf{g}_b \cdot \mathbf{t}$. This condition is necessary in all cases as stated in the theorem.

Substituting this back into (2.42), the right-hand side vanishes. Then, by differentiating this equation, we obtain the necessary condition

$$(\mathbf{t} \cdot \mathbf{f}_b)(\mathbf{t} \cdot (\mathbf{f}_b - \mathbf{f}_a))\mathbf{Q}\big(\mathbf{x}(s) \cdot (\mathbf{f}_b - \mathbf{f}_a)\big)\mathbf{r}_b = 0 \tag{2.43}$$

for $s \in (s_1, s_2)$. By assumption $\mathbf{r}_b \neq 0$ cannot be zero, so $\mathbf{Q}\big(\mathbf{x}(s) \cdot (\mathbf{f}_b - \mathbf{f}_a)\big)\mathbf{r}_b$ is not zero. Thus, there are only two possibilities for local compatibility in this case:

(a) Either, $\mathbf{t} \cdot \mathbf{f}_b = 0$;

(b) Or, $\mathbf{t}\cdot\mathbf{f}_b \neq 0$ and $\mathbf{t}\cdot(\mathbf{f}_b - \mathbf{f}_a) = 0$.

We suppose (a). Then, in substituting $\mathbf{t}\cdot\mathbf{f}_b = 0$ back into the first in (2.42), we have a locally compatible helical structure if and only if $(\mathbf{t}\cdot\mathbf{f}_a)\mathbf{W}\mathbf{r}_a = 0$, that is, if and only if $\mathbf{t}\cdot\mathbf{f}_a = 0$. In combining all the identities, we obtain Case (i) in the theorem. The inequalitites $\mathbf{g}_{a,b}\cdot\mathbf{t} \neq 0$ are a restatement of the nondegeneracy conditions assumed on the group parameters. That is, suppose $\mathbf{g}_{a,b}\cdot\mathbf{t} = 0$. Together with $\mathbf{f}_{a,b}\cdot\mathbf{t} = 0$, we have that $\mathbf{g}_{a,b}$ is parallel to $\mathbf{f}_{a,b}$. In other words, we have that $\mathbf{f}_{a,b}\cdot\mathbf{g}_{a,b}^{\perp} = 0$, which is ruled out by our hypotheses on the groups. Thus, hypothesis (a) give Case (i) of the theorem.

Now, we suppose (b) above. Note that since $\mathbf{x}'(s) = \mathbf{t} = const$, the curve in this case is given by $\mathbf{x}(s) = (s - s_1)\mathbf{t} + \mathbf{c}$ for some $\mathbf{c} \in \mathbb{R}^2$ (as stated in the theorem). Making use of this fact, we observe that $\mathbf{Q}(\mathbf{x}(s)\cdot(\mathbf{f}_b - \mathbf{f}_a)) = \mathbf{Q}(\mathbf{c}\cdot(\mathbf{f}_b - \mathbf{f}_a)) = const.$ since $\mathbf{t}\cdot(\mathbf{f}_b - \mathbf{f}_a) = 0$. Substituting this into (2.42), we have a locally compatible interface if and only if

$$(\mathbf{t}\cdot\mathbf{f}_b)\mathbf{Q}\big(\mathbf{c}\cdot(\mathbf{f}_b - \mathbf{f}_a)\big)\mathbf{W}\mathbf{r}_b = (\mathbf{t}\cdot\mathbf{f}_a)\mathbf{W}\mathbf{r}_a. \tag{2.44}$$

Noting that $\mathbf{Q}(\cdot)$ and $\mathbf{W}$ commute, we can remove $\mathbf{W}$ from (2.44), and we can cancel the nonzero terms $\mathbf{t}\cdot\mathbf{f}_b = \mathbf{t}\cdot\mathbf{f}_a$. Thus, we have necessarily that $|\mathbf{r}_b| = |\mathbf{r}_a|$ and $\mathbf{Q}(\mathbf{x}(s_1)\cdot(\mathbf{f}_b - \mathbf{f}_a))\mathbf{r}_b = \mathbf{r}_a$. This condition is also sufficient for (2.44). Therefore, necessary and sufficient conditions for local compatibility under hypotheses (b) are given in Cases (ii) and (iii) of the theorem. □

2.5.2 Elliptic interfaces

Theorem 2.5.2 (Case 2: Interfaces with nonzero curvature)**.** *Assume the conditions of Section 2.4 on group parameters and assume that the curvature $\kappa(s) \neq 0$ on (s_1, s_2). Each locally compatible interface is contained in one of the following cases:*

(i) (Type 1 Elliptic interfaces). $\mathbf{e}_a \times \mathbf{e}_b \neq 0$, $\mathbf{f}_a = \mathbf{f}_b$, $\mathbf{g}_a = -\mathbf{g}_b$, $\mathbf{f}_b\cdot\mathbf{g}_b^{\perp} \neq 0$, and

$$\mathbf{r}_a = \mathbf{R}_{(\mathbf{e}_a\times\mathbf{e}_b)}\mathbf{r}_b. \tag{2.45}$$

Here, $\mathbf{R}_{(\mathbf{e}_a\times\mathbf{e}_b)} \in \mathrm{SO}(3)$ is the rotation with axis $(\mathbf{e}_a \times \mathbf{e}_b)$ determined by the condition $\mathbf{e}_a = \mathbf{R}_{(\mathbf{e}_a\times\mathbf{e}_b)}\mathbf{e}_b$.

(ii) (Type 2 Elliptic interfaces). $\mathbf{e}_a \times \mathbf{e}_b \neq 0$, $\mathbf{f}_a = -\mathbf{f}_b$, $\mathbf{g}_a = \mathbf{g}_b$, $\mathbf{f}_b \cdot \mathbf{g}_b^{\perp} \neq 0$ *and*

$$\mathbf{r}_a = \mathbf{R}_{\mathbf{r}_b}(\pi)\mathbf{R}_{(\mathbf{e}_a \times \mathbf{e}_b)}\mathbf{r}_b. \tag{2.46}$$

Here, $\mathbf{R}_{(\mathbf{e}_a \times \mathbf{e}_b)}$ *is determined as in the Type 1 case, and* $\mathbf{R}_{\mathbf{r}_b}(\pi)$ *is a rotation by* π *with axis* $\mathbf{r}_b$*.*

A formula for the arc-length parameterized curve $\mathbf{x}\colon (s_1, s_2) \to \mathbb{R}^2$ *(under the assumption*[11] *that* $\mathbf{x}(s_1) = 0$*) is determined as follows: Let* $\mathbf{f}^b$ *and* $\mathbf{g}^b$ *be the reciprocal vectors*[12] *of* $\mathbf{f}_b$ *and* $\mathbf{g}_b$*, and let*

$$\tilde{\mathbf{x}}^{\pm}(t) = t\mathbf{f}^b \pm \Big(\frac{\mathbf{e}_a \cdot \mathbf{r}_b - \mathbf{e}_a \cdot \mathbf{Q}^b(t)\mathbf{r}_b}{(1 \pm \mathbf{e}_a \cdot \mathbf{e}_b)}\Big)\mathbf{g}^b. \tag{2.47}$$

Then, for Type 1 interfaces

$$\mathbf{x}(s) = \big(\tilde{\mathbf{x}}^{+} \circ \psi\big)(s - s_1) \tag{2.48}$$

and for Type 2 interfaces

$$\mathbf{x}(s) = \big(\tilde{\mathbf{x}}^{-} \circ \psi\big)(s - s_1). \tag{2.49}$$

Here, $\psi(s)$ *is the inverse*[13] *of the arc-length function* $\varphi(t) = \int_0^t |(\tilde{\mathbf{x}}^{\pm})'(\tilde{t})| d\tilde{t}$*.*

We reserve the proof of this result to A.1; foremost because it is long and tedious, and also because it may not be all that physically relevant. Regarding the latter, these interfaces, though locally compatible, are generally not globally compatible. For instance, Figure 2.4(d) shows one such interface, but we cannot achieve the full helix because adding additional atoms to the structure depicted results in self-intersection. Notice that $\{\mathbf{f}_b, \mathbf{g}_b\}$ and $\{-\mathbf{f}_b, -\mathbf{g}_b\}$ generate the same structure. Therefore, Type 1 elliptical interface and Type 2 elliptical interface are related in some sense. See A.2 for more information. There is also a more pressing matter at hand. Our results on local compatibility implicitly assume the existence of a flat two dimensional reference

[11] This is without loss of generality. We can, of course, provide a formula where $\mathbf{x}(s_1)$ is an arbitrary constant, but that formula is quite messy.

[12] This means that $\mathbf{f}^b \cdot \mathbf{f}_b = 1$, $\mathbf{g}^b \cdot \mathbf{g}_b = 1$, $\mathbf{f}^b \cdot \mathbf{g}_b = 0$ and $\mathbf{g}^b \cdot \mathbf{f}_b = 0$.

[13] This inverse is well-defined on all of $\mathbb{R}$ since $(\tilde{\mathbf{x}}^{\pm})'(t) \neq 0$ for all t (i.e., $\tilde{\mathbf{x}}^{\pm}$ is a regular parameterization).

configuration that is a subset of the $\mathbb{Z}^2$ with the phases in this reference separated by an interface. If the helical structure of two (or more) phases shares an axis (i.e., $\mathbf{e}_a = \mathbf{e}_b$), then this implicit assumption is benign. We can always cut the helical structure, unroll it flat (isometrically), and map it back to a subset of the $\mathbb{Z}^2$ lattice by a continuous pairwise affine transformation. However, if the axes are distinct (i.e., $\mathbf{e}_a \nparallel \mathbf{e}_b$), then there is in general no way to unroll the helical structure flat without tearing the structure along the interface. That is, an interface could be perfectly compatible in the helical structure, but not compatible in the flat plane. An example of this is a *zig-zag twin* provided in our concluding remarks (Figure 2.9). We are aware of no general strategy to investigate notions of global compatibility.

2.5.3 Implications of theory on local compatibility

In Table 2.1, for each type of interface, we have conditions on structural parameters specified as rotation, translation and axis part. Reference interface curves $\mathbf{x}(s)$ are given by arc-length parameterization ($|\mathbf{x}'(s)| = 1$). The first three types of interfaces (vertical, horizontal and helical) have identical axis and zero-curvature reference interface curves. Elliptical interface case has nonparallel axes and reference interface curve with non-trivial curvature.

Table 2.1: Four types of compatible interfaces between phases a and b in helical structures.

Type	Rotation	Translation	Axis	Reference interface
Vertical [a]	$\mathbf{t}\cdot\mathbf{f}_a = \mathbf{t}\cdot\mathbf{f}_b = 0$	$\mathbf{t}\cdot\mathbf{g}_a = \mathbf{t}\cdot\mathbf{g}_b \neq 0$	$\mathbf{e}_a = \mathbf{e}_b$	$\mathbf{x}(s) = (s - s_1)\mathbf{t} + \mathbf{c}$
Horizontal	$\mathbf{t}\cdot\mathbf{f}_a = \mathbf{t}\cdot\mathbf{f}_b \neq 0$	$\mathbf{t}\cdot\mathbf{g}_a = \mathbf{t}\cdot\mathbf{g}_b = 0$	$\mathbf{e}_a = \mathbf{e}_b$	$\mathbf{x}(s) = (s - s_1)\mathbf{t} + \mathbf{c}$
Helical	$\mathbf{t}\cdot\mathbf{f}_a = \mathbf{t}\cdot\mathbf{f}_b \neq 0$	$\mathbf{t}\cdot\mathbf{g}_a = \mathbf{t}\cdot\mathbf{g}_b \neq 0$	$\mathbf{e}_a = \mathbf{e}_b$	$\mathbf{x}(s) = (s - s_1)\mathbf{t} + \mathbf{c}$
Elliptical [b]	$\mathbf{f}_a = \pm\mathbf{f}_b$	$\mathbf{g}_a = \mp\mathbf{g}_b$	$\mathbf{e}_a \nparallel \mathbf{e}_b$	$(\mathbf{e}_a\cdot\mathbf{e}_b \pm 1)(\mathbf{x}(s)\cdot\mathbf{g}_b)$ $+\mathbf{e}_a\cdot\mathbf{Q}^b(\mathbf{x}(s)\cdot\mathbf{f}_b)\mathbf{r}_b = const.$

[a] Identical radius is not necessary for vertical interfaces, but it is necessary for the other three types.

[b] The elliptical interface is the only case that $\mathbf{e}_a \nparallel \mathbf{e}_b$. We only give the implicit reference interface curves here. Arc-length parameterized curves are given in Section 2.5.2.

The names of the different types of interfaces indicate the shape of these interfaces in deformed configuration. The interface curve in deformed configuration $\mathbf{y}_I$ is given by substituting structural parameters and reference curve into

$$\mathbf{y}_I(s) = \mathbf{y}_a(\mathbf{x}(s)) = \mathbf{Q}^a(\mathbf{x}(s) \cdot \mathbf{f}_a)\mathbf{r}_a + (\mathbf{x}(s) \cdot \mathbf{g}_a)\mathbf{e}_a + \mathbf{z}_a. \tag{2.50}$$

(This also satisfies $\mathbf{y}_I(s) = \mathbf{y}_b(\mathbf{x}(s))$ for the structure parameters $\{\mathbf{f}_b, \mathbf{g}_b, \mathbf{r}_b, \mathbf{e}_b, \mathbf{z}_b\}$.) The shape depends not only on the structural parameters, but also on the reference interface curve. For instance, the vertical, horizontal and helical interfaces could each share identical reference interface curves (actually lines), but they have different types of interfaces in deformed configuration, as these correspond to different relationships between the parameters and the reference curve. To clarify this, we provide some simple examples along with further explanation of physical meaning for each case. These examples are depicted in Figure 2.4.

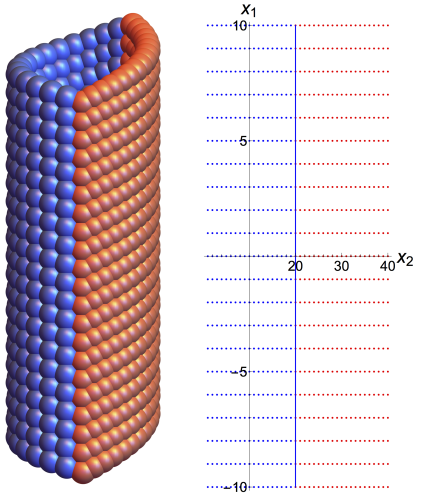

(a) Vertical interface

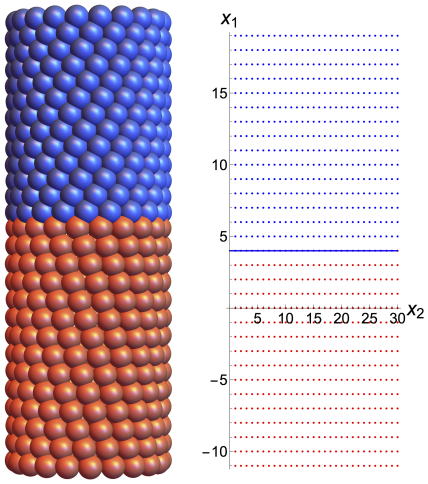

(b) Horizontal interface

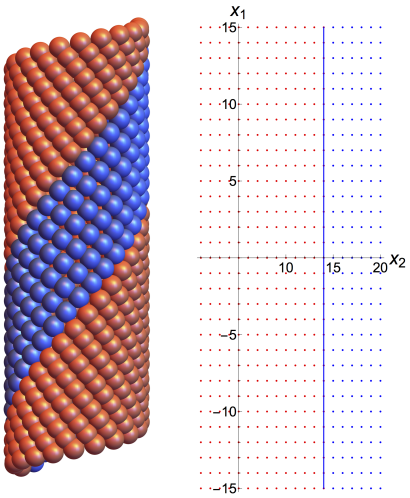

(c) Helical interface

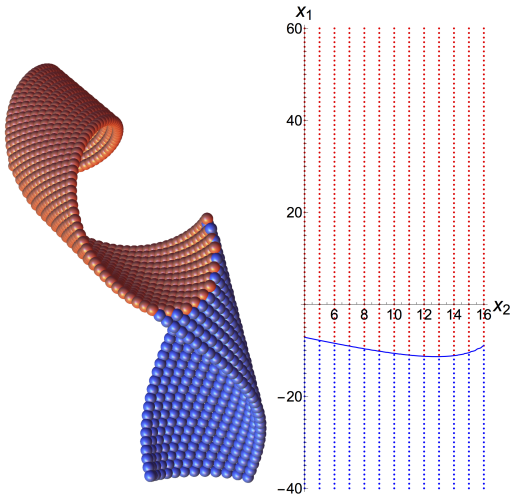

(d) Elliptical interface

Figure 2.4: Examples of four types of compatible interfaces between phase a (blue) and phase b (red) are shown in deformed configuration (left) and reference domain (right). The blue continuous curves represent the interfaces on reference domain. These are the full solutions of compatible interfaces in the local sense, but simply extended to global loops except for (d). See text.

1. *Vertical interface.* In this case, the tangent vector $\mathbf{x}'(s) = \mathbf{t}(s) = \mathbf{t}$ is constant and satisfies $\mathbf{t} \cdot \mathbf{f}_a = 0$. Consequently, the deformed interface curve is given by

$$\mathbf{y}_I'(s) = (\mathbf{t} \cdot \mathbf{g}_a)\mathbf{e}_a. \tag{2.51}$$

Since this quantity must be tangent to the interface, it follows that the interface is a straight line parallel to the axis $\mathbf{e}_a$. Figure 2.4 (a) shows an example of vertical interface with $|\mathbf{r}_a| = |\mathbf{r}_b| = 1$, and nearest neighbor structural parameters

$$\mathbf{f}_a = \begin{pmatrix} 0 \\ 0.25 \end{pmatrix}, \quad \mathbf{f}_b = \begin{pmatrix} 0 \\ 0.15 \end{pmatrix}, \tag{2.52}$$
$$\mathbf{g}_a = \begin{pmatrix} 0.28 \\ -0.08 \end{pmatrix}, \quad \mathbf{g}_b = \begin{pmatrix} 0.28 \\ 0.084 \end{pmatrix}, \quad \mathbf{t} = \begin{pmatrix} 0 \\ 1 \end{pmatrix}.$$

These satisfy the conditions in Table 2.1 for a vertical interface. The reference interface curve $\mathbf{x}(s) = (s, 20)$.

2. *Horizontal interface.* In this case, the tangent vector $\mathbf{x}'(s) = \mathbf{t}(s) = \mathbf{t}$ is constant and satisfies $\mathbf{t} \cdot \mathbf{g}_a = 0$. Consequently, the deformed interface curve is given by

$$\mathbf{y}_I'(s) = (\mathbf{t} \cdot \mathbf{f}_a)\mathbf{Q}^a(\mathbf{x}(s) \cdot \mathbf{f}_a)\mathbf{W}^a\mathbf{r}_a. \tag{2.53}$$

Since this vector is alway perpendicular to the axis $\mathbf{e}_a$, the interface curve lies on a horizontal plane perpendicular to $\mathbf{e}_a$. Figure 2.4(b) shows an example of horizontal interface with $|\mathbf{r}_a| = |\mathbf{r}_b| = 1$, and the nearest neighbor structural parameters satisfying

$$\mathbf{f}_a = \begin{pmatrix} 0.12 \\ \pi/10 \end{pmatrix}, \quad \mathbf{f}_b = \begin{pmatrix} -0.4 \\ \pi/10 \end{pmatrix}, \tag{2.54}$$
$$\mathbf{g}_a = \begin{pmatrix} 0.262 \\ 0 \end{pmatrix}, \quad \mathbf{g}_b = \begin{pmatrix} 0.3 \\ 0 \end{pmatrix}, \quad \mathbf{t} = \begin{pmatrix} 0 \\ 1 \end{pmatrix}.$$

These satisfy the conditions in Table 2.1 for a horizontal interface. The reference interface curve here is $\mathbf{x}(s) = (4, s)$.

3. *Helical interface.* In this case, the tangent vector $\mathbf{x}'(s) = \mathbf{t}(s) = \mathbf{t}$ is constant, but it is not orthogonal to either $\mathbf{f}_a$ or $\mathbf{f}_b$. Consequently, the deformed interface curve is given by

$$\mathbf{y}_I'(s) = (\mathbf{t} \cdot \mathbf{f}_a)\mathbf{Q}(\mathbf{x}(s) \cdot \mathbf{f}_a)\mathbf{W}^a\mathbf{r}_a + (\mathbf{t} \cdot \mathbf{g}_a)\mathbf{e}_a. \tag{2.55}$$

Notice that the first component of this deformed tangent describes an interface which is winding around in a circle. But the winding has a constant tilt along the helical axis given by the second component. Thus, the interface is itself helical. Figure 2.4 (c) shows an example of a helical interface with $|\mathbf{r}_a| = |\mathbf{r}_b| = 1$, and the nearest neighbor structural parameters satisfying

$$\mathbf{f}_a = \begin{pmatrix} 0.2 \\ 0.22 \end{pmatrix}, \quad \mathbf{f}_b = \begin{pmatrix} 0.2 \\ 0.33 \end{pmatrix}, \tag{2.56}$$
$$\mathbf{g}_a = \begin{pmatrix} 0.27 \\ -0.18 \end{pmatrix}, \quad \mathbf{g}_b = \begin{pmatrix} 0.27 \\ 0.081 \end{pmatrix}, \quad \mathbf{t} = \begin{pmatrix} 1 \\ 0 \end{pmatrix}.$$

These satisfy the conditions in Table 2.1 for a helical interface. The reference interface curve here is $\mathbf{x}(s) = (s, 14)$.

4. *Elliptical interface.* In this case, we use the fact that $\mathbf{y}_I(s) = \mathbf{y}_b(\mathbf{x}(s))$ (for convenience, as the theorem and table are notated with respect to the "b" phase). Thus, the deformed interface satisfies

$$\mathbf{y}_I'(s) = (\mathbf{t}(s) \cdot \mathbf{f}_b)\mathbf{Q}^b(\mathbf{x}(s) \cdot \mathbf{f}_b)\mathbf{W}^b\mathbf{r}_b + (\mathbf{t}(s) \cdot \mathbf{g}_b)\mathbf{e}_b. \tag{2.57}$$

By differentiating the corresponding reference interface curves in Table 2.1, we have

$$(\mathbf{e}_a \cdot \mathbf{e}_b \pm 1)(\mathbf{t}(s) \cdot \mathbf{g}_b) + (\mathbf{t}(s) \cdot \mathbf{f}_b)\mathbf{e}_a \cdot \mathbf{Q}^b(\mathbf{x}(s) \cdot \mathbf{f}_b)\mathbf{W}^b\mathbf{r}_b = 0. \tag{2.58}$$

Then $\mathbf{y}_I'(s) \cdot (\mathbf{e}_a \pm \mathbf{e}_b) = 0$ after substituting the differentiated reference curve. Thus, the interface in deformed configuration is on a plane perpendicular to $(\mathbf{e}_a \pm \mathbf{e}_b)$, but not perpendicular to $\mathbf{e}_b$ (because $\mathbf{e}_a \nparallel \mathbf{e}_b$). Then the intersection of the plane and the cylinder with axis $\mathbf{e}_b$ is an ellipse. Figure 2.4(d) shows an example

of elliptical interface with $|\mathbf{r}_a| = |\mathbf{r}_b| = 1$, and the nearest neighbor structural parameters satsifying

$$\mathbf{f}_a = \mathbf{f}_b = \begin{pmatrix} \pi/35 \\ 2\pi/35 \end{pmatrix}, \quad \mathbf{g}_a = -\mathbf{g}_b = \begin{pmatrix} -0.12 \\ 0.06 \end{pmatrix}. \tag{2.59}$$

These satisfy the conditions in Table 2.1 for an elliptic interface. Finally, the reference interface curve satisfies

$$(\mathbf{e}_a \cdot \mathbf{e}_b + 1)(\mathbf{x}(s) \cdot \mathbf{g}_b) + \mathbf{e}_a \cdot \mathbf{Q}^b(\mathbf{x}(s) \cdot \mathbf{f}_b)\mathbf{r}_b = const. \tag{2.60}$$

Notice that for locally compatible horizontal, vertical and helical interfaces, we were able to extend the interface to form a globally compatible helical structure. This appears to be a generic property of these interfaces. In contrast, extending the interface for the elliptical case above beyond what we have shown results in self-intersection of the structure. This, unfortunately, appears to be a generic properties of this interface.

2.6 Slip and mechanical twinning in helical structures

The structure seen in Figure 2.4(b) shares features in common with twins in crystals, including mirror symmetry and equal energy density of the pure phases. In this section we consider the two phases a and b to be the same, in the sense that they are related by an orthogonal transformation and translation. In that case compatible deformations are analogous to slip or twinning. Our main question is whether we can have compatible interfaces, such as horizontal, vertical, helical or elliptical interfaces, between two copies of the same phase that are oriented differently.

2.6.1 Alternative choices of group generators

As noted above, there may be several choices of neighbors with the same or an acceptable distance from a given atom. In such cases it is useful to have efficient ways of checking the hypotheses of Theorems 2.5.1 and 2.5.2 for group parameters corresponding to other choices of close neighbors.

First we recall the basic invariance of the $\mathbb{Z}^2$ lattice [61]. The set of invertible linear transformations mapping $\mathbb{Z}^2$ to $\mathbb{Z}^2$ is

$$GL(\mathbb{Z}^2) = \Big\{ \boldsymbol{\mu} \in \mathbb{R}^{2\times 2} \colon \mu_{ij} \in \mathbb{Z},\ i = 1,2,\ j = 1,2, \quad \det \boldsymbol{\mu} \in \{\pm 1\} \Big\}. \tag{2.61}$$

Consider the parameterizations of the two helical phases given by (2.31), and bring out the dependence of these formulas on the group parameters by writing these positions as $\mathbf{y}_a(p,q) = \mathbf{y}(p,q;\mathbf{f}_a,\mathbf{g}_a,\mathbf{z}_a)$ and $\mathbf{y}_b(p,q) = \mathbf{y}(p,q;\mathbf{f}_b,\mathbf{g}_b,\mathbf{z}_b)$. Each element $\boldsymbol{\mu} \in GL(\mathbb{Z}^2)$ gives an alternative parameterization of these same two given helical phases by replacing $(p,q) = \boldsymbol{\mu}(p',q')$, with (p',q') in the domains $\mathcal{D}'_{a,b} = \boldsymbol{\mu}^{-1}(\mathbb{Z} \times \{1,\dots,q^\star_{a,b}\}$, respectively. As can be seen from the formulas (2.31), the matrix $\boldsymbol{\mu}$ can be moved onto the group parameters. In summary, the positions

$$\mathbf{y}(p',q';\boldsymbol{\mu}^T\mathbf{f}_a,\boldsymbol{\mu}^T\mathbf{g}_a,\mathbf{z}_a), \quad (p',q') \in \mathcal{D}'_a, \quad \mathbf{y}(p',q';\boldsymbol{\mu}^T\mathbf{f}_b,\boldsymbol{\mu}^T\mathbf{g}_b,\mathbf{z}_b), \quad (p',q') \in \mathcal{D}'_b, \tag{2.62}$$

are the same two sets of atomic positions as given by $\mathbf{y}_a(p,q), \mathbf{y}_b(p,q)$. If the two phases are compatible across an interface $p(s), q(s)$, then the positions (2.62) are compatible across the interface $(p'(s),q'(s)) = \boldsymbol{\mu}^{-1}(p(s),q(s))$ in the sense described above.

The transformation of group parameters from $(\mathbf{f},\mathbf{g})$ to $(\boldsymbol{\mu}^T\mathbf{f},\boldsymbol{\mu}^T\mathbf{g})$ is equivalent to a change of generators, by the same operation. Thus, it may happen that the generators for the new group parameters $(\boldsymbol{\mu}^T\mathbf{f},\boldsymbol{\mu}^T\mathbf{g})$ are not nearest neighbor generators. This is not a problem in the case discussed so far, because we have assumed compatibility for one set of nearest neighbor generators.

We can also transform group parameters using different elements of $GL(\mathbb{Z}^2)$ for the two lattices. (By the remarks above, we can without loss of generality leave one lattice unchanged.) Let us transform phase a with $\boldsymbol{\mu}_a = id$ and phase b with $\boldsymbol{\mu}_b \in GL(\mathbb{Z}^2)$. Again, if we use the appropriate domains of integers, both structures are exactly the same. However, the meaning of the compatibility conditions changes, because nearby pairs of integers do not in general give nearby points (in the helical structures) for phases a and b. They do conveniently give alternative choices of nearest neighbor generators as well as close neighbors as long as we restrict $|\boldsymbol{\mu}_b - id|$ to be relatively small. These considerations of smallness of these lattice invariant deformations of $\mathbb{Z}^2$ are closely related to the ideas behind the Ericksen-Pitteri neighborhood of crystalline

phase transformations.

With these physical considerations of smallness in mind, we can state a Corollary to Theorems 2.5.1 and 2.5.2.

Corollary 2.6.1. *Let $\mathbf{f}_{a,b}$ and $\mathbf{g}_{a,b}$ be group parameters associated to nearest neighbor generators. Then, there exists a locally compatible interface if and only if, for some $\boldsymbol{\mu}_a$ and $\boldsymbol{\mu}_b \in GL(\mathbb{Z}^2)$, one of the sets of conditions in the theorems holds after replacing $\{\mathbf{f}_a, \mathbf{f}_b, \mathbf{g}_a, \mathbf{g}_b\}$ with $\{\boldsymbol{\mu}_a\mathbf{f}_a, \boldsymbol{\mu}_b\mathbf{f}_b, \boldsymbol{\mu}_a\mathbf{g}_a, \boldsymbol{\mu}_b\mathbf{g}_b\}$.*

2.6.2 Local compatibility of helical structures in the same phase

Let phase a be given with nearest neighbor group parameterization $\mathbf{f}, \mathbf{g}, \mathbf{z}$, where we drop the subscript "a" for simplicity. The positions of phase a are $\mathbf{y}(p, q; \mathbf{f}, \mathbf{g}, \mathbf{z})$, where $(p, q) \in \mathcal{D} = (\mathbb{Z} \times \{1, \dots, q^\star\}$. In view of the remarks of Section 2.6.1 we have assumed nearest neighbor generators. As above, to describe local compatibility, we extend the definition of $\mathbf{y}$ to $(p, q) \in \mathcal{D}^c := \mathbb{R} \times (0, q^\star)$.

Following the basic invariance of quantum mechanics – orthogonal transformations with determinant ± 1 and translations – we consider another copy of phase a, allowing for a change of generators as described in Section 2.6.1. Thus, we consider

$$\hat{\mathbf{Q}}\mathbf{y}(p, q; \boldsymbol{\mu}\mathbf{f}, \boldsymbol{\mu}\mathbf{g}, \mathbf{z}) + \hat{\mathbf{c}}, \quad \hat{\mathbf{Q}} \in \mathrm{O}(3), \quad \hat{\mathbf{c}} \in \mathbb{R}^3, \quad \boldsymbol{\mu} \in GL(3, \mathbb{Z}), \quad (p, q) \in \boldsymbol{\mu}^{-T}\mathcal{D}^c. \tag{2.63}$$

We consider local compatibility of $\mathbf{y}(p, q; \mathbf{f}, \mathbf{g}, \mathbf{z})$ and $\hat{\mathbf{Q}}\mathbf{y}(p, q; \boldsymbol{\mu}\mathbf{f}, \boldsymbol{\mu}\mathbf{g}, \mathbf{z}) + \hat{\mathbf{c}}$ at an interface $(p(s), q(s)) \in \mathcal{D}^c \cap \boldsymbol{\mu}^{-T}\mathcal{D}^c$. The interfaces of Theorems 2.5.1 and 2.5.2 are treated separately.

Vertical, horizontal and helical interfaces In this case the two phases have a common axis, so that necessarily $\hat{\mathbf{Q}}\mathbf{e} = \pm\mathbf{e}$, and, without loss of generality we can choose $+$, as in Theorem 2.5.1. The second copy of phase a can then be expressed in the form

$$\hat{\mathbf{Q}}\mathbf{y}(\mathbf{x}; \boldsymbol{\mu}\mathbf{f}, \boldsymbol{\mu}\mathbf{g}, \mathbf{z}) + \hat{\mathbf{c}} = \mathbf{Q}_{\pm\mathbf{x}\cdot\boldsymbol{\mu}\mathbf{f}}\hat{\mathbf{Q}}\mathbf{r} + (\mathbf{x} \cdot \boldsymbol{\mu}\mathbf{g})\mathbf{e} + \mathbf{c}, \quad \mathbf{x} \in \boldsymbol{\mu}^{-T}\mathcal{D}^c, \tag{2.64}$$

where $\mathbf{c} = \hat{\mathbf{Q}}\mathbf{z} + \hat{\mathbf{c}}$. Here, the $\pm$ arises because $\hat{\mathbf{Q}}\mathbf{Q}_\theta = \mathbf{Q}_{\pm\theta}\hat{\mathbf{Q}}$ if $\det \hat{\mathbf{Q}} = \pm 1$, respectively. We treat separately the three subcases of Theorem 2.5.1, identifying phase b with the copy of phase a described in (2.64). Thus, we can assume $\mathbf{f}_a = \mathbf{f}$, $\mathbf{g}_a = \mathbf{g}$ for phase a, and $\mathbf{f}_b = \sigma\boldsymbol{\mu}\mathbf{f}$, $\mathbf{g}_b = \boldsymbol{\mu}\mathbf{g}$ for phase b. Here $\sigma = +$ for slips and $\sigma = -$ for twins.

(i) (Vertical interfaces). $\mathbf{t} \cdot \mathbf{f}_a = \mathbf{t} \cdot \mathbf{f}_b = 0$, and $\mathbf{t} \cdot \mathbf{g}_a = \mathbf{t} \cdot \mathbf{g}_b \neq 0$. Necessary and sufficient conditions in this case are therefore $\sigma\boldsymbol{\mu}\mathbf{f} \parallel \mathbf{f}$, $\mathbf{t} \cdot \mathbf{f} = 0$, $\mathbf{t} \cdot (\boldsymbol{\mu}\mathbf{g} - \mathbf{g}) = 0$, $\mathbf{t} \cdot \mathbf{g} \neq 0$. To solve these equations, we recall the nondegeneracy conditions (2.36) that $\mathbf{f} \cdot \mathbf{g}^\perp \neq 0$ and write $\boldsymbol{\mu}$ in the orthonormal basis $\hat{\mathbf{f}} = \mathbf{f}/|\mathbf{f}|$, $\hat{\mathbf{t}} = \mathbf{t}/|\mathbf{t}|$. The general form of $\boldsymbol{\mu}$ satisfying these restrictions is

$$\boldsymbol{\mu} = \delta\hat{\mathbf{f}} \otimes \hat{\mathbf{f}} + (\hat{\mathbf{t}} + \xi\hat{\mathbf{f}}) \otimes \hat{\mathbf{t}}, \tag{2.65}$$

and it follows from $\det \boldsymbol{\mu} = \pm 1$ that $\delta = \pm 1$. Therefore, $\boldsymbol{\mu}$ is expressible in the following forms corresponding, respectively, to $\delta = 1$ and $\delta = -1$:

$$\boldsymbol{\mu} = \mathbf{I} + \xi\hat{\mathbf{f}} \otimes \hat{\mathbf{t}} \quad \text{or} \quad \mathbf{I} + \hat{\mathbf{f}} \otimes (\xi\hat{\mathbf{t}} - 2\hat{\mathbf{f}}). \tag{2.66}$$

These both have the form $\mathbf{I} + \mathbf{a} \otimes \mathbf{n}$ where, respectively, $\mathbf{a} \cdot \mathbf{n} = 0$ or $\mathbf{a} \cdot \mathbf{n} = -2$. We express these forms in the basis $\mathbf{e}_1 = (1, 0), \mathbf{e}_2 = (0, 1)$ where the components of $\boldsymbol{\mu}$ are integers and obtain the general solution in that basis:

$$\boldsymbol{\mu} = \begin{pmatrix} 1+\alpha & \beta \\ -\gamma & 1-\alpha \end{pmatrix}, \text{where } \gamma\beta = \alpha^2,\ \mathbf{f} \parallel (\alpha, -\gamma),\ \mathbf{t} \parallel (\alpha, \beta), \tag{2.67}$$

$$\boldsymbol{\mu} = \begin{pmatrix} 1+\alpha & \beta \\ -\gamma & -(1+\alpha) \end{pmatrix}, \text{where } \gamma\beta = \alpha^2 + 2\alpha,\ \mathbf{f} \parallel (\alpha, -\gamma),\quad \mathbf{t} \parallel (\alpha + 2, \beta),$$
$$\alpha, \beta, \gamma \in \mathbb{Z}. \tag{2.68}$$

In any of the cases that the pair of integers to the right of $\parallel$ are both zero, then the condition $\hat{\mathbf{f}} \cdot \hat{\mathbf{t}} = 0$ is imposed separately. The vector $\mathbf{g}$ is unrestricted except for (2.36). These conditions are necessary and sufficient for the existence of vertical interfaces. Figure 2.5 shows the examples of vertical slip and vertical twin.

(ii) (Horizontal interfaces). $\mathbf{e}_a = \mathbf{e}_b$, $\mathbf{t} \cdot \mathbf{f}_a = \mathbf{t} \cdot \mathbf{f}_b \neq 0$, $\mathbf{g}_a \cdot \mathbf{t} = \mathbf{g}_b \cdot \mathbf{t} = 0$, and

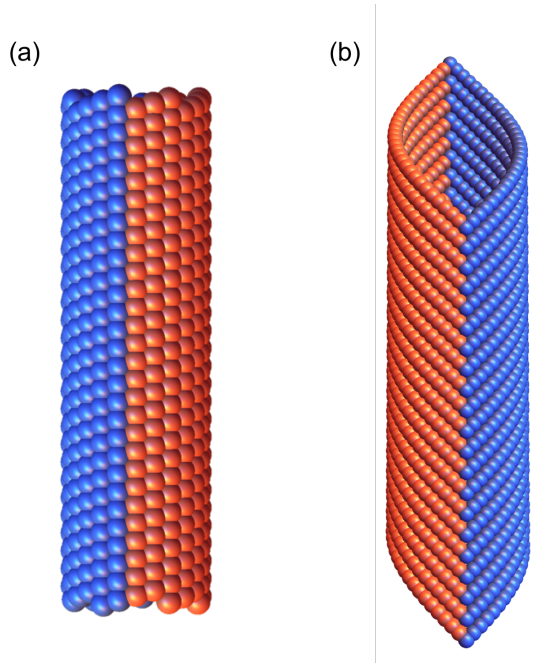

Figure 2.5: Examples of (a) vertical slip and (b) vertical twin.

$\mathbf{r}_a = \mathbf{Q}_{\pm\mathbf{x}(s_1)\cdot(\boldsymbol{\mu}\mathbf{f}-\mathbf{f})}\hat{\mathbf{Q}}\mathbf{r}$. **check the latter** These conditions are formally similar to those above if we switch the roles of $\mathbf{f}$ and $\mathbf{g}$, as long as we keep in mind the slightly different restrictions on these vectors in (2.36). Identifying again phase b with the copy of a given by (2.64), we have

$$\begin{aligned}
\boldsymbol{\mu} &= \begin{pmatrix} 1+\alpha & \beta \\ -\gamma & 1-\alpha \end{pmatrix}, \text{where } \gamma\beta = \alpha^2,\ \mathbf{g} \parallel (\alpha, -\gamma),\ \mathbf{t} \parallel (\alpha, \beta), \\
\boldsymbol{\mu} &= \begin{pmatrix} 1+\alpha & \beta \\ -\gamma & -(1+\alpha) \end{pmatrix}, \text{where } \gamma\beta = \alpha^2 + 2\alpha,\ \mathbf{g} \parallel (\alpha, -\gamma), \quad \mathbf{t} \parallel (\alpha+2, \beta), \\
&\alpha, \beta, \gamma \in \mathbb{Z}.
\end{aligned} \tag{2.69}$$

In any of the cases that the pair of integers to the right of $\parallel$ are both zero, then the condition $\hat{\mathbf{g}} \cdot \hat{\mathbf{t}} = 0$ is imposed separately, respecting (2.36). Note that $\mathbf{f} \neq 0$ is otherwise unrestricted, except for the non-degeneracy condition (2.36). These conditions are necessary and sufficient for the existence of vertical interfaces.

Figure 2.6 shows the examples of horizontal slip and horizontal twin.

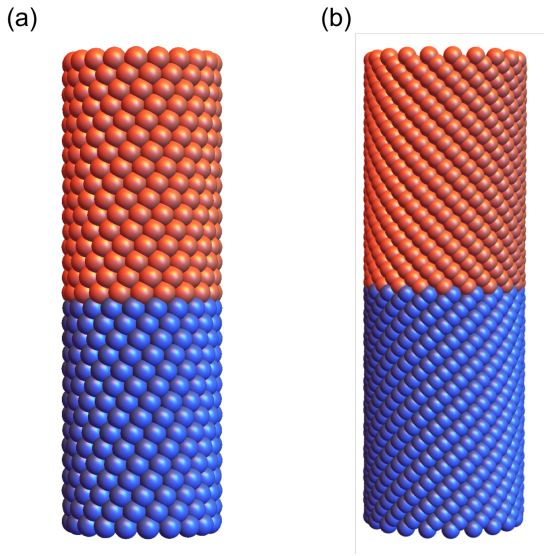

Figure 2.6: Examples of (a) horizontal slip and (b) horizontal twin.

(iii) (Helical interfaces). The same as the horizontal interface except that $\mathbf{g}_a \cdot \mathbf{t} = \mathbf{g}_b \cdot \mathbf{t} \neq 0$. Using $\mathbf{t} \neq 0$ we write $\hat{\mathbf{t}} = \mathbf{t}/|\mathbf{t}|$. The given conditions are $\hat{\mathbf{t}} \cdot (\sigma \boldsymbol{\mu}\mathbf{f} - \mathbf{f}) = 0$, $\sigma = \pm 1$ and $\hat{\mathbf{t}} \cdot (\boldsymbol{\mu}\mathbf{g} - \mathbf{g}) = 0$, subject to $\mathbf{f} \cdot \hat{\mathbf{t}} \neq 0$, $\mathbf{g} \cdot \hat{\mathbf{t}} \neq 0$. We treat the subcases $\sigma = +1, -1$ separately.

(a) $\sigma = 1$ or, equivalently, $(\boldsymbol{\mu}^T - \mathbf{I})\hat{\mathbf{t}} \cdot \mathbf{f} = 0$ and $(\boldsymbol{\mu}^T - \mathbf{I})\hat{\mathbf{t}} \cdot \mathbf{g} = 0$. We have that $\mathbf{f}$ and $\mathbf{g}$ are linearly independent by (2.36), so necessary and sufficient conditions are $(\boldsymbol{\mu}^T - \mathbf{I})\hat{\mathbf{t}} = 0$. The latter, in turn is equivalent to $\boldsymbol{\mu} = \mathbf{I} + \hat{\mathbf{t}}^{\perp} \otimes \mathbf{a}$ for some $\mathbf{a} \in \mathbb{R}^2$, where $\hat{\mathbf{t}}, \hat{\mathbf{t}}^{\perp}$ are orthonormal, and $\det \boldsymbol{\mu} = \pm 1$ implies that $\mathbf{a} = \xi\hat{\mathbf{t}}$ or $\mathbf{a} = (\xi\hat{\mathbf{t}} - 2\hat{\mathbf{t}}^{\perp})$, i.e.,

$$\boldsymbol{\mu} = \mathbf{I} + \xi\hat{\mathbf{t}}^{\perp} \otimes \hat{\mathbf{t}} \quad \text{or} \quad \mathbf{I} + \hat{\mathbf{t}}^{\perp} \otimes (\xi\hat{\mathbf{t}} - 2\hat{\mathbf{t}}^{\perp}). \tag{2.70}$$

As above, the forms of $\boldsymbol{\mu}$ satisfying (2.70) in the basis $\mathbf{e}_1 = (1, 0)$ and $\mathbf{e}_2 =$

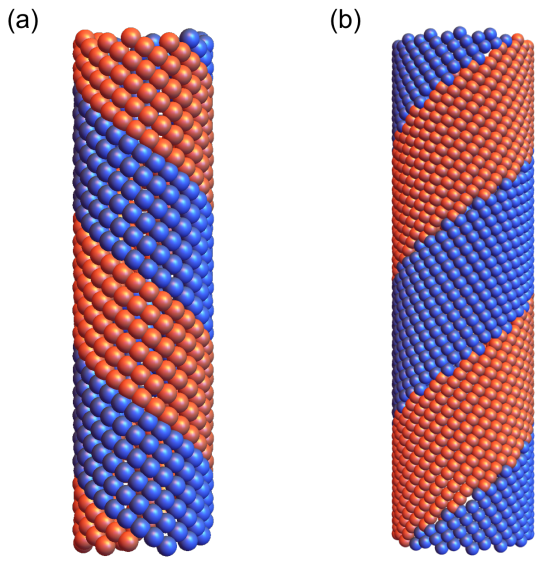

Figure 2.7: Examples of (a) helical slip and (b) helical twin.

$(0,1)$ are

$$\begin{aligned}
\boldsymbol{\mu} &= \begin{pmatrix} 1+\alpha & \beta \\ -\gamma & 1-\alpha \end{pmatrix}, \text{where } \gamma\beta = \alpha^2,\ \mathbf{t} \parallel (\alpha,\beta), \\
\boldsymbol{\mu} &= \begin{pmatrix} 1+\alpha & \beta \\ -\gamma & -(1+\alpha) \end{pmatrix}, \text{where } \gamma\beta = \alpha^2+2\alpha, \quad \mathbf{t} \parallel (\alpha+2,\beta), \\
&\alpha,\beta,\gamma \in \mathbb{Z}.
\end{aligned} \tag{2.71}$$

The vectors $\mathbf{f}$ and $\mathbf{g}$ are any linearly independent vectors in $\mathbb{R}^2$ satisfying $\mathbf{f}\cdot\hat{\mathbf{t}} \neq 0,\ \mathbf{g}\cdot\hat{\mathbf{t}} \neq 0$.

(b) $\sigma = -1$ or, equivalently, $\mathbf{f}\cdot(\boldsymbol{\mu}^T + \mathbf{I})\hat{\mathbf{t}} = 0$ and $\mathbf{g}\cdot(\boldsymbol{\mu}^T - \mathbf{I})\hat{\mathbf{t}} = 0$. There are linearly independent solutions $(\mathbf{f},\mathbf{g})$ of these two equations if and only if $(\boldsymbol{\mu}^T + \mathbf{I})\hat{\mathbf{t}}$ and $(\boldsymbol{\mu}^T - \mathbf{I})\hat{\mathbf{t}}$ are not parallel. Note also that the conditions $\mathbf{f}\cdot\hat{\mathbf{t}} \neq 0,\ \mathbf{g}\cdot\hat{\mathbf{t}} \neq 0$ imply that $\boldsymbol{\mu}^T\hat{\mathbf{t}} \neq \pm\hat{\mathbf{t}}$. Hence, $(\boldsymbol{\mu}^T + \mathbf{I})\hat{\mathbf{t}}$ and $(\boldsymbol{\mu}^T - \mathbf{I})\hat{\mathbf{t}}$ are not parallel if and only if $\hat{\mathbf{t}}$ is not an eigenvector of $\boldsymbol{\mu}^T$. Hence, necessary

and sufficient conditions in this case are

$$\mathbf{t} \text{ is not an eigenvector of } \boldsymbol{\mu}^T \tag{2.72}$$

The vectors $\mathbf{f}$ and $\mathbf{g}$ are given by $0 \neq \mathbf{f} \parallel ((\boldsymbol{\mu}^T + \mathbf{I})\hat{\mathbf{t}})^{\perp}$ and $0 \neq \mathbf{g} \parallel ((\boldsymbol{\mu}^T - \mathbf{I})\hat{\mathbf{t}})^{\perp}$.

Figure 2.7 shows the examples of helical slip and helical twin.

Elliptical interface In this case, $\mathbf{e}_a \nparallel \mathbf{e}_b$ for different phase a and b. For Type I elliptical interface, $\mathbf{f}_a = \mathbf{f}_b$, $\mathbf{g}_a = -\mathbf{g}_b$. We need to solve $\sigma\boldsymbol{\mu}\mathbf{f} = \mathbf{f}$ and $\boldsymbol{\mu}\mathbf{g} = -\mathbf{g}$, where $\sigma = \pm 1$.

(a) $\sigma = 1$. $\boldsymbol{\mu}\mathbf{f} = \mathbf{f}$ implies

$$\boldsymbol{\mu} = \mathbf{I} + \delta\hat{\mathbf{f}} \otimes \hat{\mathbf{f}}^{\perp} + \xi\hat{\mathbf{f}}^{\perp} \otimes \hat{\mathbf{f}}^{\perp}, \tag{2.73}$$

where $\hat{\mathbf{f}} = \mathbf{f}/|\mathbf{f}|$, $\hat{\mathbf{f}}^{\perp} = \mathbf{f}^{\perp}/|\mathbf{f}^{\perp}|$ and $\mathbf{f} \cdot \mathbf{f}^{\perp} = 0$. we can write $\mathbf{g}$ in $\hat{\mathbf{f}}, \hat{\mathbf{f}}^{\perp}$ basis as $\mathbf{g} = |\mathbf{g}|(\cos\theta\,\hat{\mathbf{f}} + \sin\theta\,\hat{\mathbf{f}}^{\perp})$ with $\sin\theta \neq 0$ and substitute $\boldsymbol{\mu}\mathbf{g} = -\mathbf{g}$ to have

$$\xi = -2, \quad \delta = -\frac{2\cos\theta}{\sin\theta}. \tag{2.74}$$

Then $\det\boldsymbol{\mu} = -1$ and therefore we can express $\boldsymbol{\mu}$ in $\mathbf{e}_1, \mathbf{e}_2$ basis as

$$\boldsymbol{\mu} = \begin{pmatrix} 1+\alpha & \beta \\ -\gamma & -(1+\alpha) \end{pmatrix}, \text{where } \gamma\beta = \alpha^2 + 2\alpha,\ \mathbf{f} \parallel (\beta, -\alpha),\ \ \mathbf{g} \parallel (-\alpha, \gamma),$$
$$\alpha, \beta, \gamma \in \mathbb{Z}. \tag{2.75}$$

Non-degeneracy condition 2.36 requires $\alpha \neq 0$. For the Type II elliptical interface, we can exchange $\mathbf{f}$ and $\mathbf{g}$ to have the condition

$$\boldsymbol{\mu} = \begin{pmatrix} 1+\alpha & \beta \\ -\gamma & -(1+\alpha) \end{pmatrix}, \text{where } \gamma\beta = \alpha^2 + 2\alpha,\ \mathbf{f} \parallel (-\alpha, \gamma),\ \ \mathbf{g} \parallel (\beta, -\alpha),$$
$$\alpha, \beta, \gamma \in \mathbb{Z}. \tag{2.76}$$

Also, non-degeneracy condition requires $\alpha \neq 0$.

(b) $\sigma = -1$. We have $\boldsymbol{\mu}\mathbf{f} = -\mathbf{f}$ and $\boldsymbol{\mu}\mathbf{g} = -\mathbf{g}$ with linearly independent $\mathbf{f}$ and $\mathbf{g}$. Thus, $\boldsymbol{\mu} = -\mathbf{I}$. The vectors $\mathbf{f}$ and $\mathbf{g}$ are unrestricted except for $\mathbf{f} \cdot \mathbf{g}^{\perp} \neq 0$.

Figure 2.8 shows the examples of elliptical slip and elliptical twin.

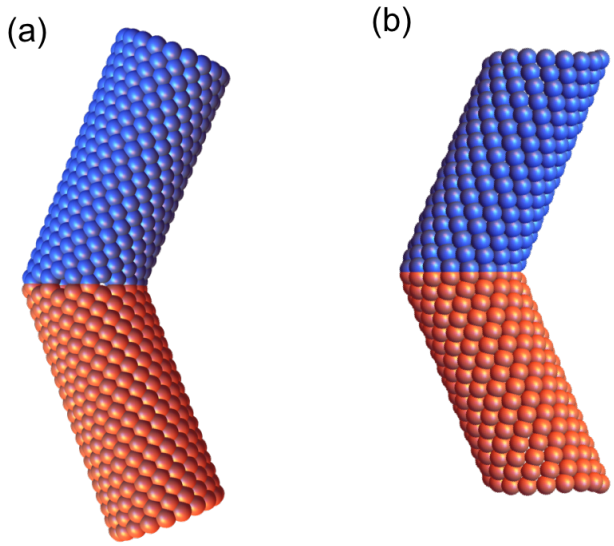

Figure 2.8: Examples of (a) elliptical slip and (b) elliptical twin.

2.6.3 A brief summary and discussion

Here we provide a brief summary and discussion for the slip and mechanical twinning of helical structures. The examples of shown above indicate that, physically, a slip has a compatible interface between two same structures, and a twin has a compatible interface between two mirror-related structures. This is basically because parameters $\{\sigma\boldsymbol{\mu}\mathbf{f}, \boldsymbol{\mu}\mathbf{g}\}, \boldsymbol{\mu} \in GL(\mathbb{Z}^2)$, generate the same structure as $\{\mathbf{f}, \mathbf{g}\}$ if $\sigma = +1$, or generate the mirror image if $\sigma = -1$.

So far, we have constructed slips and twins in helical structures, without introducing any information of the reference domains. Actually, this is cheating, because we may have this situation: Points on the different sides of reference interface curve are mapped

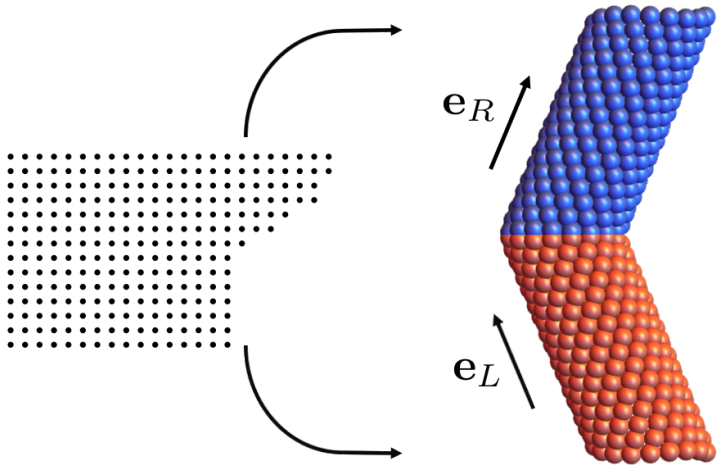

Figure 2.9: Elliptical twin constructed by mapping the same reference domain.

to the same points in the deformed configuration, and same points on the reference domain are mapped to the different sides of the deformed interface curve by deformations of the two phases. In other words, the deformation is not "invertible". As shown in Figure 2.8, by choosing the same reference domain, we can eliminate global self-intersection in elliptical slips and twins. The invertibility issue needs a further investigation.

2.7 Outlook

We end up this chapter with some exciting future work and applications regarding helical twin without rigorous analysis. Figure 2.10 shows two examples similar to austenite/martensite interface in crystal. In this figure, the blue phase and red phase are mirror related. They are able to form a compatible horizontal twin. Also, the "average" deformation of these two phases is compatible with the third green phase by a helical interface. If the area ratio of blue and red phase has to be fixed, it is similar to "average compatibility" in crystal [53]. If the area ratio can be arbitrary, it is similar to "super compatibility" in crystal [55, 58].

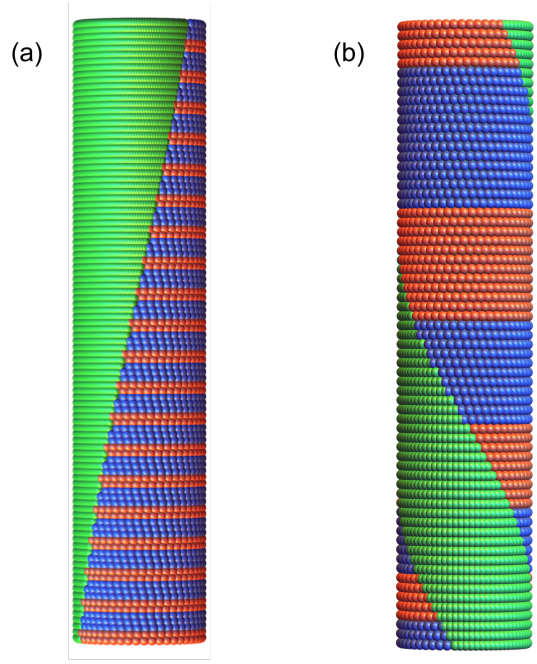

Figure 2.10: (a) Microstructure and average compatibility. (b) Supercompatibility.

As show in Figure 2.11, horizontal twin can provide some overall twist by transforming the blue phase to red phase without any stress. This is useful for developing new actuators. Also, in the next chapter, we provide a far more interesting application – helical Miura origami – using this horizontal twin.

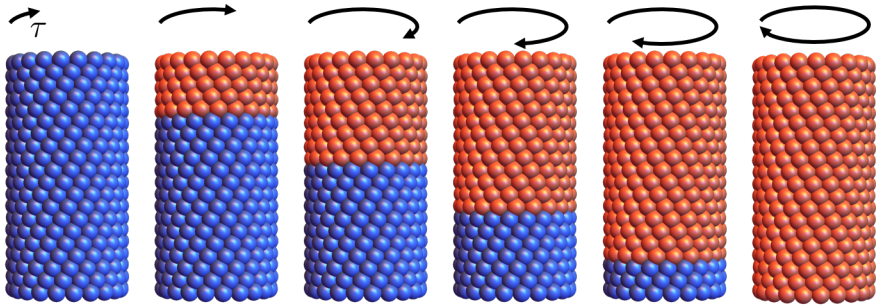

Figure 2.11: Twist by horizontal twin.

Chapter 3

Phase-transforming helical Miura origami

This chapter presents a promising example − the helical Miura origami (HMO), as an application of the theory we developed in the previous chapter. We formulate the design criteria here to obtain a closed HMO numerically. These structures have bistable solutions (variants) basically because there are two different paths to fold the same four-fold intersection. We show that these two variants can form helical and horizontal interfaces. Despite the rigidity of the single variant, by transforming one variant to the other through compatible interfaces, we can have multiple elastic-free states and obtain overall twist/extension actuation. A mechanism of the transformation is possibly bending and buckling. The material of this chapter is adopted mainly from [62] and partially from [63].

3.1 Introduction

Origami is an ancient art form about folding papers originated possibly together with the invention of paper. In the point of view of mechanician, an origami could be obtained by applying a continuous piecewise affine deformation from $\mathbb{R}^2$ to $\mathbb{R}^3$ on a reference domain (flat sheet). A flat sheet could be partially folded in $\mathbb{R}^3$ or fully folded flat onto $\mathbb{R}^2$ as an embedded domain of $\mathbb{R}^3$. An increasing number of studies of origami have been conducted in different areas, including origami design [64, 65, 66], space technology [67],

architectures [68], physical properties [69, 70, 71], biology [72], metamaterials [73, 74, 75] and mechanics [76, 77].

Researchers in origami and mechanics community are particularly interested in the rigid foldability (rigidity) and flat foldability of an origami structure. A rigidly foldable origami can be folded from a flat sheet to some folded sheet in $\mathbb{R}^3$ continuously without any bending or stretching. A flat foldable origami can be folded from a flat sheet to a folded flat sheet. The rigid foldability and flat foldability of origami are well known in the local sense. For instance, a four-fold origami is rigidly and flat foldable if and only if the opposite sector angles sum to π (Kawasaki's theorem). However, the global properties (such as rigidity, flat foldability, self-intersection) of origami structures are very problematic. Many studies, for example, algorithmic and analytical studies [78, 66, 74], have been carried out on the global rigidity and flat foldability of some special origami structures. In our recent work [63], we have developed an algorithm to generate all possible rigid and flat foldable quadrilateral patterns absent global intersections.

Searching for creative and artistic origami from origamists, we notice that a broad set of origami structures have structural symmetry. For example, the famous Miura pattern has two-dimensional translation symmetry. It also preserves the symmetry during the folding process. Yoshimura pattern is an example with helical symmetry [79]. Our previous work of helical structures has inspired us naturally to investigate properties of origami in the objective structure regime − we call it *objective origami* (OO). An OO is an origami structure that each *unit origami cell* sees the same environment, up to orthogonal transformations and translations. The unit origami cell here is a partially folded origami structure. Followed by the fundamental symmetry, if one local part of OO has some physical properties (compatibility, rigidity, ect.), the other corresponding parts also have the same features.

A helical Miura origami (HMO) is an OO having helical symmetry. It is constructed by applying an Abelian helical group on a partially folded Miura parallelogram (four-fold intersection with opposite sector angles sum to π) as the unit origami cell. In this chapter, we study the rigid foldability of the HMO. To do this, we firstly analyze the full kinematics of the Miura parallelogram in Section 3.2. We show that two branches of solutions occur for the same reference domain during the folding process. Then the generators of the helical group are derived in Section 3.3. One side of the partially

folded Miura parallelogram is mapped to its opposite side by the associated generator. The local compatibility of an HMO follows by the commutativity of the generators, but the global compatibility[1] requires more restrictive conditions on parameters. Not as one degree of freedom in quadrilateral origami [63], the HMO has two degrees of freedom, with two free parameters (ω, φ) in our content. Here ω denotes one folding angle of the unit origami cell and φ relates to the axial direction of the structure. The isolated dots of (ω, φ) shown in Figure 3.6 illustrate that the structures are rigid in our computational domain.

The main weakness of the HMO is that the structure is not applicable to the devices that need shape changing, such as robotics [80] and deformable antenna [81]. Therefore, it is worth to explore how to deform a helical Miura-ori in different ways. Inspired by phase transformation in helical structures [38], we investigate phase transformation in helical Miura-ori in Section 3.5. To do this, we firstly introduce variants in helical Miura-ori. The variants here are defined as the two different branches of solutions for the same reference unit origami cell. We denote these two variants by *plus*-phase and *minus*-phase. Then we check the compatible interface between the two variants of the HMO. The result shows that only horizontal and helical interfaces occur in HMO. Despite the rigidity of the single phase, we can obtain motions like twist and extension by transforming one phase to the other. Unfortunately, the transformation here is still not by a rigid folding, because it needs buckling and bending to "jump" from one variant to the other. But the most striking result is that the structure consisting of two variants has multiple elastic-free states. This property is useful for developing novel actuators, sensors, and artificial muscles.

[1] An HMO is globally compatible if the structure is a closed cylindrical origami. See the numerical results in Section 3.4.

3.2 Unit cell of a helical Miura-ori

3.2.1 Basic Miura four-fold pattern and its kinematics

Let $\{\mathbf{e}_1, \mathbf{e}_2, \mathbf{e}_3\}$ be right-handed orthonormal basis and consider lines coming out of the origin in directions

$$\begin{aligned} \mathbf{t}_1 &= \mathbf{e}_1, \quad \mathbf{t}_2 = \cos\alpha\,\mathbf{e}_1 + \sin\alpha\,\mathbf{e}_2, \quad \mathbf{t}_3 = \cos(\alpha+\beta)\,\mathbf{e}_1 + \sin(\alpha+\beta)\,\mathbf{e}_2, \\ \mathbf{t}_4 &= \cos(\pi+\beta)\,\mathbf{e}_1 + \sin(\pi+\beta)\,\mathbf{e}_2 = -\cos\beta\,\mathbf{e}_1 - \sin\beta\,\mathbf{e}_2, \end{aligned} \tag{3.1}$$

where $\alpha \in (0,\pi)$ and $\beta \in (0,\pi)$. Here the sector angles satisfy the well-known Kawasaki theorem about flat foldability that the sum of opposite angles is π, as shown in Figure 3.1. Let the reference domain Ω be specified as the convex hull of $\delta_1\mathbf{t}_1, \delta_2\mathbf{t}_2, \delta_3\mathbf{t}_3, \delta_4\mathbf{t}_4$, where $\delta_1 > 0, \delta_2 > 0, \delta_3 > 0, \delta_4 > 0$. Then $\mathbf{x}_i = \delta_i\mathbf{t}_i, i = 1,2,3,4$ are the corner points in the reference domain. Let $\mathbf{R}_i : [-\pi,\pi] \to \mathrm{SO}(3)$ be given by

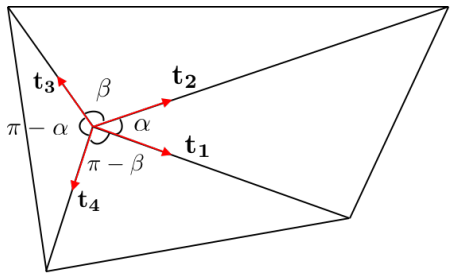

Figure 3.1: Miura four-fold pattern: the opposite sector angles sum to π.

$$\mathbf{R}_i(\theta) = \mathbf{R}_i\mathbf{R}_1(\theta)\mathbf{R}_i^T \tag{3.2}$$

where $\mathbf{R}_1(\theta)$ is a rotation of θ about $\mathbf{e}_1$ and $\mathbf{R}_i\mathbf{e}_3 = \mathbf{e}_3$, $\mathbf{R}_i\mathbf{e}_1 = \mathbf{t}_i$, as above. Notice that $\mathbf{R}_i(\theta)\mathbf{t}_i = \mathbf{t}_i$. Physically, $\mathbf{R}_i(\theta)$ is a rotation about $\mathbf{t}_i$ with angle θ. Let $\mathbf{n}_i = \mathbf{R}_{\mathbf{e}_3}^{\pi/2}\mathbf{t}_i$, $i = 1,2,3,4$, where $\mathbf{R}_{\mathbf{e}_3}^{\pi/2}$ is a counterclockwise 90 degree rotation about $\mathbf{e}_3$. Therefore,

a general Miura folding (up to rotation) is given by

$$\mathbf{y}(\mathbf{x}) = \begin{cases} \mathbf{x}, & \mathbf{x}\cdot\mathbf{e}_3 = 0,\ \mathbf{x}\cdot\mathbf{n}_2 < 0,\ \mathbf{x}\cdot\mathbf{n}_1 \geq 0, \\ \mathbf{R}_2(\eta)\mathbf{x}, & \mathbf{x}\cdot\mathbf{e}_3 = 0,\ \mathbf{x}\cdot\mathbf{n}_3 < 0,\ \mathbf{x}\cdot\mathbf{n}_2 \geq 0, \\ \mathbf{R}_2(\eta)\mathbf{R}_3(\xi)\mathbf{x}, & \mathbf{x}\cdot\mathbf{e}_3 = 0,\ \mathbf{x}\cdot\mathbf{n}_4 < 0,\ \mathbf{x}\cdot\mathbf{n}_3 \geq 0, \\ \mathbf{R}_2(\eta)\mathbf{R}_3(\xi)\mathbf{R}_4(\omega)\mathbf{x}, & \mathbf{x}\cdot\mathbf{e}_3 = 0,\ \mathbf{x}\cdot\mathbf{n}_1 < 0,\ \mathbf{x}\cdot\mathbf{n}_4 \geq 0. \end{cases} \tag{3.3}$$

The angles are restricted to the interval $-\pi \leq \eta, \xi, \omega \leq \pi$. This natural physical restriction avoids paper passing through itself but allows the structure to be folded flat ($\eta, \xi, \omega = \pm\pi$). A general Miura folding deformation $\mathbf{y}(\mathbf{x})$ is a continuous piecewise affine function. The expression of $\mathbf{y}(\mathbf{x})$ satisfies compatibility condition along $\mathbf{t}_2$, $\mathbf{t}_3$, $\mathbf{t}_4$ trivially, which means $\mathbf{y}(x)$ is continuous across those three folding lines. More explicitly,

$$\mathbf{t}_2 = \mathbf{R}_2(\eta)\mathbf{t}_2,\ \mathbf{R}_2(\eta)\mathbf{t}_3 = \mathbf{R}_2(\eta)\mathbf{R}_3(\xi)\mathbf{t}_3,\ \mathbf{R}_2(\eta)\mathbf{R}_3(\xi)\mathbf{t}_4 = \mathbf{R}_2(\eta)\mathbf{R}_3(\xi)\mathbf{R}_4(\omega)\mathbf{t}_4 \tag{3.4}$$

(recall that $\mathbf{R}_i(\theta)\mathbf{t}_i = \mathbf{t}_i$). However, we still need the compatibility condition for $\mathbf{t}_1$, which is

$$\mathbf{R}_2(\eta)\mathbf{R}_3(\xi)\mathbf{R}_4(\omega)\mathbf{t}_1 = \mathbf{t}_1. \tag{3.5}$$

Here we derive a theorem for the kinematics of a Miura four-fold intersection. The proof is given in B.1. A more generalized version relaxing Kawasaki's condition (the opposite sector angles sum to π) is derived in [63].

Theorem 3.2.1. *The Miura folding deformation* $\mathbf{y}(\mathbf{x})$ *defined in (3.3) is continuous if and only if*[2] η, ξ, ω *satisfy one of the following cases:*

1. $\eta = \omega$ *(plus-phase)*

   (a) $\omega = 0,\ \alpha + \beta = \pi,\ -\pi \leq \xi \leq \pi$

   (b) $\omega = \pm\pi,\ \alpha = \beta,\ -\pi \leq \xi \leq \pi$

[2]The statement "only if" is valid unless we distinct $\pm\pi$ cases, because of the fact $\cos(\pm\pi) = -1$, $\sin(\pm\pi) = 0$. We have more explanation on this argument in $B.1$.

(c) *Otherwise,* $\xi = \xi^+(\omega)$ *is uniquely determined and given by*

$$c_{\xi^+(\omega)} = \frac{(1 - c_\alpha c_\beta)c_\omega + s_\alpha s_\beta}{(1 - c_\alpha c_\beta) + s_\alpha s_\beta c_\omega},\ s_{\xi^+(\omega)} = \frac{(c_\beta - c_\alpha)s_\omega}{(1 - c_\alpha c_\beta) + s_\alpha s_\beta c_\eta},\ \textit{if } \omega \in (-\pi, \pi),$$
$$\xi^+(\pi) = -sign(c_\beta - c_\alpha)\pi,\ \xi^+(-\pi) = sign(c_\beta - c_\alpha)\pi. \tag{3.6}$$

2. $\eta = -\omega$ *(minus-phase)*

(a) $\omega = 0,\ \alpha + \beta = \pi,\ -\pi \le \xi \le \pi$

(b) $\omega = \pm\pi,\ \alpha = \beta,\ -\pi \le \xi \le \pi$

(c) *Otherwise,* $\xi = \xi^-(\omega)$ *is uniquely determined and given by*

$$c_{\xi^-(\omega)} = \frac{(1 + c_\alpha c_\beta)c_\omega - s_\alpha s_\beta}{(1 + c_\alpha c_\beta) - s_\alpha s_\beta c_\omega},\ s_{\xi^-(\omega)} = \frac{(c_\beta + c_\alpha)s_\omega}{(1 + c_\alpha c_\beta) - s_\alpha s_\beta c_\eta},\ \textit{if } \omega \in (-\pi, \pi),$$
$$\xi^-(\pi) = -sign(c_\beta + c_\alpha)\pi,\ \xi^-(-\pi) = sign(c_\beta + c_\alpha)\pi. \tag{3.7}$$

Here c_θ, s_θ *denote* $\cos(\theta)$ *and* $\sin(\theta)$ *respectively.*

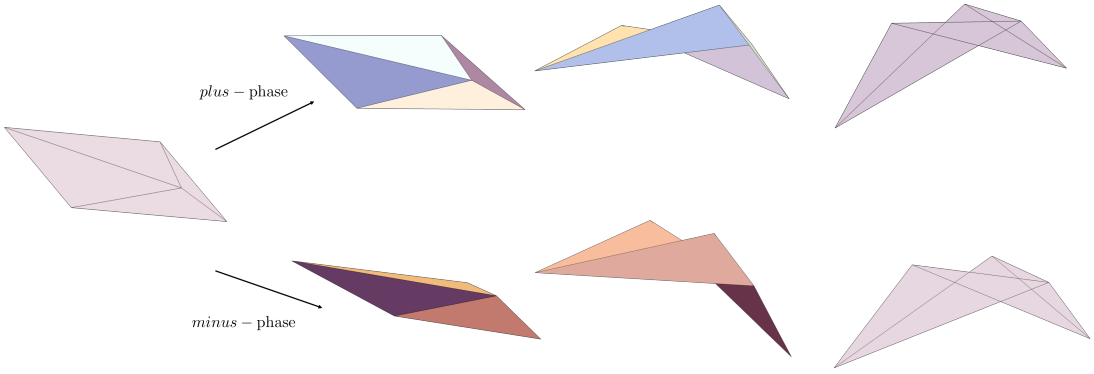

Figure 3.2: Two branches of the regular solution. Left: reference domain. Top: *plus*-phase with $\omega = 1, 2, \pi$. Bottom: *minus*-phase with $\omega = 1, 2, \pi$.

Note. In this chapter, we focus on the regular solutions 1 (c) and 2 (c) in Theorem 3.2.1. Despite the lack of full solutions, the regular solutions have already contained the most important features:

1. There are two branches of solutions corresponding to the same reference domain Ω. We denote the two branches by *plus*-phase and *minus*-phase. For the *plus*-phase, the folding angles are: $\omega, \xi = \xi^{+}(\omega), \eta = \omega$. For the *minus*-phase, the folding angles are: $\omega, \xi = \xi^{-}(\omega), \eta = -\omega$. Physically, they have different mountain-valley distributions. It is important for the concept of variants in Section 3.5 .

2. Each branch of solution has only one free parameter ω. In other words, both η and ξ are functions of ω. Figure 3.2 shows the evolution of the two branches of the regular solution in Theorem 3.2.1.

These features are also investigated in the regime of generalized Miura pattern in our recent work [63].

3.2.2 Miura parallelogram as the unit cell

Theorem 3.2.1 points out the kinematics of a four-fold Miura reference domain rigorously and explicitly. To apply the terminology of objective origami, we attempt to map one side of the partially folded reference domain to its opposite side by the generator of a helical group. The generator is an isometry so that the map preserves distances. Then, more restrictions on the reference domain are required: The lengths of opposite sides have to be equal, say, $|\mathbf{x}_1 - \mathbf{x}_2| = |\mathbf{x}_4 - \mathbf{x}_3|$ and $|\mathbf{x}_1 - \mathbf{x}_4| = |\mathbf{x}_2 - \mathbf{x}_3|$. Therefore, the reference domain is a Miura parallelogram as shown in Figure 3.3. In this subsection, we reparameterize the reference domain in terms of "$\mathbf{p}$-vector" or "$\hat{\mathbf{p}}$-vector" to satisfy the equal-length restrictions automatically.

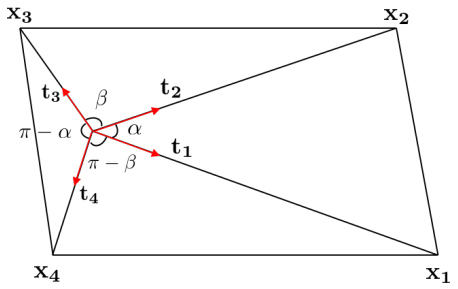

Figure 3.3: Miura parallelogram: the opposite sector angles sum to π.

The side lengths of a Miura parallelogram are

$$\begin{aligned}
|\mathbf{x}_1 - \mathbf{x}_2|^2 &= \delta_1^2 + \delta_2^2 - 2\delta_1\delta_2\cos\alpha, \\
|\mathbf{x}_2 - \mathbf{x}_3|^2 &= \delta_2^2 + \delta_3^2 - 2\delta_2\delta_3\cos\beta, \\
|\mathbf{x}_3 - \mathbf{x}_4|^2 &= \delta_3^2 + \delta_4^2 - 2\delta_3\delta_4\cos(\pi - \alpha), \\
|\mathbf{x}_4 - \mathbf{x}_1|^2 &= \delta_4^2 + \delta_1^2 - 2\delta_4\delta_1\cos(\pi - \beta).
\end{aligned} \tag{3.8}$$

The equalities of lengths imply

$$\begin{aligned}
\cos\alpha &= \frac{\delta_1^2 + \delta_2^2 - \delta_3^2 - \delta_4^2}{2\delta_1\delta_2 + 2\delta_3\delta_4}, \\
\cos\beta &= \frac{\delta_2^2 + \delta_3^3 - \delta_1^2 - \delta_4^2}{2\delta_2\delta_3 + 2\delta_1\delta_4},
\end{aligned} \tag{3.9}$$

where $\delta_i > 0$ for $i = 1, 2, 3, 4$ and $\alpha, \beta \in (0, \pi)$. Since $\cos\alpha, \cos\beta \in (-1, 1)$, we have

$$\begin{aligned}
(\delta_1 - \delta_2)^2 - (\delta_3 + \delta_4)^2 &< 0, \\
(\delta_1 + \delta_2)^2 - (\delta_3 - \delta_4)^2 &> 0, \\
(\delta_2 - \delta_3)^2 - (\delta_1 + \delta_4)^2 &< 0, \\
(\delta_2 + \delta_3)^2 - (\delta_1 - \delta_4)^2 &< 0.
\end{aligned} \tag{3.10}$$

Then the inequalities above can be simplified as

$$\begin{aligned}
-\delta_1 + \delta_2 + \delta_3 + \delta_4 &> 0, \\
\delta_1 - \delta_2 + \delta_3 + \delta_4 &> 0, \\
\delta_1 + \delta_2 - \delta_3 + \delta_4 &> 0, \\
\delta_1 + \delta_2 + \delta_3 - \delta_4 &> 0.
\end{aligned} \tag{3.11}$$

Define the invertible matrix

$$\mathbf{A} = \begin{pmatrix} -1 & 1 & 1 & 1 \\ 1 & -1 & 1 & 1 \\ 1 & 1 & -1 & 1 \\ 1 & 1 & 1 & -1 \end{pmatrix}, \tag{3.12}$$

$\det \mathbf{A} = -16$. Let $\Delta = (\delta_1, \delta_2, \delta_3, \delta_4)$ and $\mathbf{p} = (p_1, p_2, p_3, p_4)$. We assign four positive numbers $(p_1, p_2, p_3, p_4) = \mathbf{p}$ satisfying $p_i + p_j + p_k - p_l > 0$ for all permutations (i, j, k, l) of $(1, 2, 3, 4)$, and calculate $\Delta = (\delta_1, \delta_2, \delta_3, \delta_4)$ by $\Delta = \mathbf{A}^{-1}\mathbf{p}$. Here the condition $p_i + p_j + p_k - p_l > 0$ ensures that $\delta_l > 0$. We define the domain of the $\mathbf{p}$-vector as $\mathcal{P}$.

In this reparameterization, the sector angles are uniquely determined by

$$\sin\alpha = \frac{2\sqrt{p_1p_2p_3p_4}}{p_1p_2 + p_3p_4}, \quad \cos\alpha = \frac{-p_1p_2 + p_3p_4}{p_1p_2 + p_3p_4}, \tag{3.13}$$

$$\sin\beta = \frac{2\sqrt{p_1p_2p_3p_4}}{p_2p_3 + p_1p_4}, \quad \cos\beta = \frac{-p_2p_3 + p_1p_4}{p_2p_3 + p_1p_4}. \tag{3.14}$$

The advantage of the parameterization using $\mathbf{p}$-vector is that, if we choose $\mathbf{p}$-vector correctly, the parameters of the reference four-fold Miura domain satisfy the restrictions of the reference domain we need: 1. The length δ_i of folding line is positive; 2. The sum of opposite sector angles is π; 3. The lengths of opposite sides are equal.

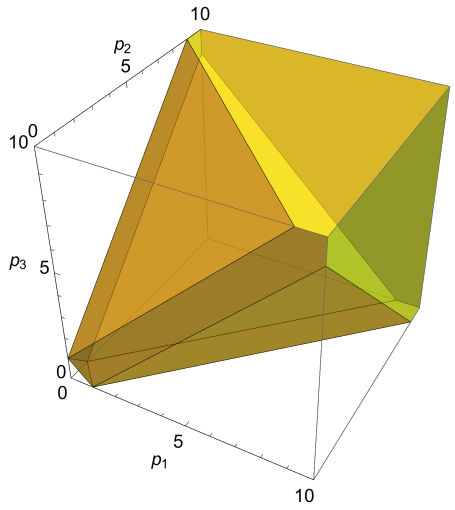

Figure 3.4: The domain $\hat{\mathcal{P}}$ is illustrated as the yellow region. Each point in this region corresponds to a Miura parallelogram.

Notice the fact that we can rescale the reference domain by replacing $\mathbf{p}$ with $\lambda\,\mathbf{p}$ for any $\lambda > 0$. The rescaling preserves the compatibility and rigidity we are about to discuss. In this rescaling, δ_i is replaced by $\lambda\,\delta_i$ and α, β keep the same. Therefore, Instead of using $p_i, i = 1, 2, 3, 4$, we choose $p_4 = 1$ without loss of generality and let

$\hat{\mathbf{p}} = (p_1, p_2, p_3)$. Then the 4-dimensional domain $\hat{\mathcal{P}}$ is dimensionally reduced to a 3-dimensional domain $\hat{\mathcal{P}}$ that can be illustrated. We can define the domain $\mathcal{P}$ by

$$\begin{aligned}\hat{\mathcal{P}} = \{(p_1, p_2, p_3) : p_1 > 0, p_2 > 0, p_3 > 0, p_1 + p_2 + p_3 > 1, \\ 1 + p_1 + p_2 > p_3, 1 + p_1 + p_3 > p_2, 1 + p_2 + p_3 > p_1\}.\end{aligned} \tag{3.15}$$

The domain $\hat{\mathcal{P}}$ of $\hat{\mathbf{p}}$-vector is depicted in Figure 3.4. Then, each $\hat{\mathbf{p}}$-vector that ends in the open yellow region corresponds to a reference Miura parallelogram up to scaling. In principal, we can compute all possible Miura parallelograms by cycling through the points in $\hat{\mathcal{P}}$ domain. However, restricted by the numerical cost, we only choose a finite number of points in $\hat{\mathcal{P}}$ during the following discussion.

3.3 Discrete Abelian group generators for helical Miura-ori

3.3.1 Group generators for the unit cell

Suppose the reference Miura parallelogram is partially folded with some given folding angle $\omega \in (-\pi, 0) \cup (0, \pi)$. As show in Theorem 3.2.1, the system has one degree of freedom so that the deformation $\mathbf{y}(\mathbf{x})$ has been determined. Let $\mathbf{y}_i = \mathbf{y}(\mathbf{x}_i), i = 1, 2, 3, 4$ be the corner points in the deformed domain, and the origin remains fixed after folding. $\mathbf{x}_i$ is the corresponding corner point in reference domain as defined in 3.2. Then the deformed configuration (partially folded domain) is determined by $\mathbf{y}_i, i = 1, 2, , 3, 4$ and the origin. Of course, each $\mathbf{y}_i$ is a function with respect to the folding angle ω, but we drop ω here for the succinct expressions. We construct a screw transformation $g_1 = (\mathbf{R}_1|\mathbf{c}_1)$ mapping $\mathbf{y}_3$ to $\mathbf{y}_2$, $\mathbf{y}_4$ to $\mathbf{y}_1$ respectively. The operation rule is given by $g_1(\mathbf{y}_i) = \mathbf{R}_1\mathbf{y}_i + \mathbf{c}_1$. Let θ_1, τ_1, $\mathbf{e}_1$ and $\mathbf{z}_1$ be the rotation angle, translation, rotation axis and origin of the generator. Then, this isometry is $g_1 = (\mathbf{R}_{\theta_1}|\tau_1\mathbf{e}_1 + (\mathbf{I} - \mathbf{R}_{\theta_1})\mathbf{z}_1)$. By the operation rule, we have

$$\begin{aligned}\mathbf{R}_{\theta_1}\mathbf{y}_3 + (\mathbf{I} - \mathbf{R}_{\theta_1})\mathbf{z}_1 + \tau_1\mathbf{e}_1 = \mathbf{y}_2, \\ \mathbf{R}_{\theta_1}\mathbf{y}_4 + (\mathbf{I} - \mathbf{R}_{\theta_1})\mathbf{z}_1 + \tau_1\mathbf{e}_1 = \mathbf{y}_1.\end{aligned} \tag{3.16}$$

Subtract the first from the second to have

$$\mathbf{R}_{\theta_1}\mathbf{u}_a = \mathbf{u}_b, \tag{3.17}$$

where $\mathbf{u}_a = \mathbf{y}_3 - \mathbf{y}_4$, $\mathbf{u}_b = \mathbf{y}_2 - \mathbf{y}_1$. We notice that $\mathbf{e}_1$ is perpendicular to $\mathbf{u}_a - \mathbf{u}_b$ by the equation

$$(\mathbf{u}_a - \mathbf{u}_b) \cdot \mathbf{e}_1 = (\mathbf{R}_{\theta_1}\mathbf{u}_a - \mathbf{u}_b) \cdot \mathbf{e}_1 = 0. \tag{3.18}$$

Thus, we can establish the right-handed orthonormal basis $\{\mathbf{f}_1, \mathbf{f}_2, \mathbf{f}_3\}$ with

$$\mathbf{f}_1 = \frac{\mathbf{u}_a + \mathbf{u}_b}{|\mathbf{u}_a + \mathbf{u}_b|}, \quad \mathbf{f}_2 = \frac{\mathbf{u}_a \times \mathbf{u}_b}{|\mathbf{u}_a \times \mathbf{u}_b|}, \quad \mathbf{f}_3 = \frac{\mathbf{u}_a - \mathbf{u}_b}{|\mathbf{u}_a - \mathbf{u}_b|}, \tag{3.19}$$

and $\mathbf{e}_1$ is on the span of $\mathbf{f}_1$, $\mathbf{f}_2$. τ_1 can be obtained by dotting the first equation in (3.16) with $\mathbf{e}_1$, which is

$$\tau_1 = \mathbf{e}_1 \cdot (\mathbf{y}_2 - \mathbf{y}_3). \tag{3.20}$$

By projecting $\mathbf{u}_a, \mathbf{u}_b$ on the plane perpendicular to $\mathbf{e}_a$ and using (3.17), we have the formula for θ_1:

$$\cos\theta_1 = \frac{(\mathbf{u}_a - (\mathbf{e}_1 \cdot \mathbf{u}_a)\mathbf{e}_1) \cdot (\mathbf{u}_b - (\mathbf{e}_1 \cdot \mathbf{u}_b)\mathbf{e}_1))}{|\mathbf{u}_a|^2 - (\mathbf{u}_a \cdot \mathbf{e}_1)^2}. \tag{3.21}$$

Finally, substitute $\mathbf{e}_1$, θ_1, τ_1 into the first equation in (3.16) to calculate $\mathbf{z}_1$.

In summary, we have

$$\begin{aligned}
\mathbf{e}_1 &= \mathbf{e}_1(\omega,\varphi) = \cos\varphi\ \mathbf{f}_1 + \sin\varphi\ \mathbf{f}_2, \quad \mathbf{f}_1 = \frac{\mathbf{u}_a + \mathbf{u}_b}{|\mathbf{u}_a + \mathbf{u}_b|}, \quad \mathbf{f}_2 = \frac{\mathbf{u}_a \times \mathbf{u}_b}{|\mathbf{u}_a \times \mathbf{u}_b|}, \\
\theta_1 &= \theta_1(\omega,\varphi) = \pm \arccos \frac{(\mathbf{u}_a - (\mathbf{e}_1 \cdot \mathbf{u}_a)\mathbf{e}_1) \cdot (\mathbf{u}_b - (\mathbf{e}_1 \cdot \mathbf{u}_b)\mathbf{e}_1))}{|\mathbf{u}_a|^2 - (\mathbf{u}_a \cdot \mathbf{e}_1)^2}, \\
\tau_1 &= \tau_1(\omega,\varphi) = \mathbf{e}_1 \cdot (\mathbf{y}_2 - \mathbf{y}_3), \\
\mathbf{z}_1 &= \mathbf{z}_1(\omega,\varphi) = (\mathbf{I} - \mathbf{R}_{\theta_1})^{-1}(\mathbf{I} - \mathbf{e}_1 \otimes \mathbf{e}_1)(\mathbf{y}_2 - \mathbf{R}_{\theta_1}\mathbf{y}_3), \quad \mathbf{z}_1 \cdot \mathbf{e}_1 = 0.
\end{aligned} \tag{3.22}$$

Here, $\pm$ is chosen to satisfy $\mathbf{R}_{\theta_1}\mathbf{u}_a = \mathbf{u}_b$, and $(\mathbf{I} - \mathbf{R}_{\theta_1})^{-1}$ is an inverse on the plane perpendicular to $\mathbf{e}_1$. We also restrict $\varphi \in (0, \pi]$ without loss of generality since φ and $\varphi \pm \pi$ lead to two sets of parameters $\{\mathbf{e}_1, \theta_1, \tau_1, \mathbf{z}_1\}$ and $\{-\mathbf{e}_1, -\theta_1, -\tau_1, \mathbf{z}_1\}$ which generate the same structure up to some rotation and translation.

Similarly, following precisely the argument, we have a second family of screw transformations mapping $\mathbf{y}_1$ to $\mathbf{y}_2$, $\mathbf{y}_4$ to $\mathbf{y}_3$ respectively. Let $\mathbf{v}_a = \mathbf{y}_1 - \mathbf{y}_4$, $\mathbf{v}_b = \mathbf{y}_2 - \mathbf{y}_3$. This procedure leads to an isometry $g_2 = (\mathbf{R}_{\theta_2}|\tau_2\mathbf{e}_2 + (\mathbf{I} - \mathbf{R}_{\theta_2})\mathbf{z}_2)$, where

$$\begin{aligned}
\mathbf{e}_2 &= \mathbf{e}_2(\omega,\psi) = \cos\psi\ \mathbf{g}_1 + \sin\psi\ \mathbf{g}_2, \quad \mathbf{g}_1 = \frac{\mathbf{v}_a + \mathbf{v}_b}{|\mathbf{v}_a + \mathbf{v}_b|}, \quad \mathbf{g}_2 = \frac{\mathbf{v}_a \times \mathbf{v}_b}{|\mathbf{v}_a \times \mathbf{v}_b|}, \\
\theta_2 &= \theta_2(\omega,\psi) = \pm \arccos \frac{(\mathbf{v}_a - (\mathbf{e}_2 \cdot \mathbf{v}_a)\mathbf{e}_2) \cdot (\mathbf{v}_b - (\mathbf{e}_2 \cdot \mathbf{v}_b)\mathbf{e}_2))}{|\mathbf{v}_a|^2 - (\mathbf{v}_a \cdot \mathbf{e}_2)^2}, \\
\tau_2 &= \tau_2(\omega,\psi) = \mathbf{e}_2 \cdot (\mathbf{y}_2 - \mathbf{y}_1), \\
\mathbf{z}_2 &= \mathbf{z}_2(\omega,\psi) = (\mathbf{I} - \mathbf{R}_{\theta_2})^{-1}(\mathbf{I} - \mathbf{e}_2 \otimes \mathbf{e}_2)(\mathbf{y}_2 - \mathbf{R}_{\theta_2}\mathbf{y}_1), \quad \mathbf{z}_2 \cdot \mathbf{e}_2 = 0. \qquad (3.23)
\end{aligned}$$

Here, $\pm$ is chosen to satisfy $\mathbf{R}_{\theta_2}\mathbf{v}_a = \mathbf{v}_b$, and $(\mathbf{I} - \mathbf{R}_{\theta_2})^{-1}$ is an inverse on the plane perpendicular to $\mathbf{e}_2$. Also we restrict ψ in $(0, \pi]$.

The rough strategy for constructing a helical Miura origami is the following. Under some restrictions on the parameters derived above, g_1 and g_2 are commutative, then $G = \{g_1^p g_2^q : p, q \in \mathbb{Z}\}$ forms a group. Then we apply this group on the unit origami cell (partially folded Miura parallelogram) to have a global structure. In the following subsections, we discuss the requirements of parameters in g_1 and g_2.

3.3.2 Commutativity and discreteness of the generators

In this subsection, we derive the conditions for the commutativity of g_1 and g_2. To do this, firstly, we derive a lemma about commutativity for the two general isometries. Then we check the consistency of the generators for Miura parallelogram with respect to the lemma. Finally, we arrive at the commutativity condition for the specific generators derived above.

Lemma 3.3.1. *Two isometries $g_1 = (\mathbf{R}_1|\mathbf{c}_1)$ and $g_2 = (\mathbf{R}_2|\mathbf{c}_2)$ with $\mathbf{R}_i \in SO(3)$ are commutative ($g_1 g_2 = g_2 g_1$) if and only if one of the following holds:*

1. $\mathbf{e}_1 \parallel \mathbf{e}_2$, $(\mathbf{R}_1 - \mathbf{I})\mathbf{c}_2 = (\mathbf{R}_2 - \mathbf{I})\mathbf{c}_1$.
2. $\mathbf{e}_1 \perp \mathbf{e}_2$, $\mathbf{R}_1 = \mathbf{I} - 2\,\mathbf{e}_2 \otimes \mathbf{e}_2$, $\mathbf{R}_2 = \mathbf{I} - 2\,\mathbf{e}_1 \otimes \mathbf{e}_1$, $\mathbf{c}_1 \cdot \mathbf{e}_1 = \mathbf{c}_2 \cdot \mathbf{e}_2 = 0$.

Proof. By the multiplication rule of isometries, $g_1 g_2 = g_2 g_1$ implies

$$(\mathbf{R}_1\mathbf{R}_2|\mathbf{c}_1 + \mathbf{R}_1\mathbf{c}_2) = (\mathbf{R}_2\mathbf{R}_1|\mathbf{c}_2 + \mathbf{R}_2\mathbf{c}_1). \qquad (3.24)$$

Then we have

$$\mathbf{R}_1\mathbf{R}_2 = \mathbf{R}_2\mathbf{R}_1, \tag{3.25}$$

$$\mathbf{c}_1 + \mathbf{R}_1\mathbf{c}_2 = \mathbf{c}_2 + \mathbf{R}_2\mathbf{c}_1. \tag{3.26}$$

$\mathbf{R}_1\mathbf{R}_2\mathbf{e}_1 = \mathbf{R}_2\mathbf{R}_1\mathbf{e}_1 = \mathbf{R}_2\mathbf{e}_1$, then we have

$$\mathbf{R}_2\mathbf{e}_1 = \pm\mathbf{e}_1. \tag{3.27}$$

If $\mathbf{R}_2\mathbf{e}_1 = \mathbf{e}_1$, we have $\mathbf{e}_1 \parallel \mathbf{e}_2$. (3.26) gives $(\mathbf{R}_1 - \mathbf{I})\mathbf{c}_2 = (\mathbf{R}_2 - \mathbf{I})\mathbf{c}_1$. If $\mathbf{R}_2\mathbf{e}_1 = -\mathbf{e}_1$, we have $\mathbf{R}_2 = \mathbf{I} - 2\,\mathbf{e}_1 \otimes \mathbf{e}_1$ and $\mathbf{e}_1 \cdot \mathbf{e}_2 = 0$. Similarly, $\mathbf{R}_1 = \mathbf{I} - 2\,\mathbf{e}_2 \otimes \mathbf{e}_2$. Substitute $\mathbf{R}_1$ and $\mathbf{R}_2$ into (3.26) to get $\mathbf{c}_1 \cdot \mathbf{e}_1 = 0$ and $\mathbf{c}_2 \cdot \mathbf{e}_2 = 0$. □

Lemma 3.3.2. *If the rotation axes of the two generators g_1 and g_2 for the Miura parallelogram defined in 3.3.1 are the same, say $\mathbf{e}_1 = \mathbf{e}_2$, then the two generators have the same origin ($\mathbf{z}_1 = \mathbf{z}_2$).*

Proof. Since $\mathbf{e}_1 = \mathbf{e}_2$, then we have

$$\begin{aligned}(\mathbf{I} - \mathbf{R}_{\theta_i})^{-1}(\mathbf{I} - \mathbf{e}_i \otimes \mathbf{e}_i) &= (\mathbf{I} - \mathbf{e}_i \otimes \mathbf{e}_i)(\mathbf{I} - \mathbf{R}_{\theta_i})^{-1},\\ (\mathbf{I} - \mathbf{R}_{\theta_1})(\mathbf{I} - \mathbf{R}_{\theta_2})^{-1} &= (\mathbf{I} - \mathbf{R}_{\theta_2})^{-1}(\mathbf{I} - \mathbf{R}_{\theta_1}),\end{aligned} \tag{3.28}$$

for $i = 1, 2$. Recall

$$\begin{aligned}\mathbf{z}_1 &= (\mathbf{I} - \mathbf{R}_{\theta_1})^{-1}(\mathbf{I} - \mathbf{e}_1 \otimes \mathbf{e}_1)(\mathbf{y}_2 - \mathbf{R}_{\theta_1}\mathbf{y}_3),\\ \mathbf{z}_2 &= (\mathbf{I} - \mathbf{R}_{\theta_2})^{-1}(\mathbf{I} - \mathbf{e}_2 \otimes \mathbf{e}_2)(\mathbf{y}_2 - \mathbf{R}_{\theta_2}\mathbf{y}_1),\end{aligned} \tag{3.29}$$

then

$$\begin{aligned}\mathbf{z}_1 - \mathbf{z}_2 &= (\mathbf{I} - \mathbf{e}_1 \otimes \mathbf{e}_1)[(\mathbf{I} - \mathbf{R}_{\theta_1})^{-1}(\mathbf{y}_2 - \mathbf{R}_{\theta_1}\mathbf{y}_3) - (\mathbf{I} - \mathbf{R}_{\theta_2})^{-1}(\mathbf{y}_2 - \mathbf{R}_{\theta_2}\mathbf{y}_1)]\\ &= \hat{\mathbf{R}}(\mathbf{I} - \mathbf{e}_1 \otimes \mathbf{e}_1)[(\mathbf{I} - \mathbf{R}_{\theta_2})(\mathbf{y}_2 - \mathbf{R}_{\theta_1}\mathbf{y}_3) - (\mathbf{I} - \mathbf{R}_{\theta_1})(\mathbf{y}_2 - \mathbf{R}_{\theta_2}\mathbf{y}_1)]\end{aligned} \tag{3.30}$$

where $\hat{\mathbf{R}} = (\mathbf{I} - \mathbf{R}_{\theta_1})^{-1}(\mathbf{I} - \mathbf{R}_{\theta_2})^{-1}$. We notice that

$$\begin{aligned}&(\mathbf{I} - \mathbf{e}_1 \otimes \mathbf{e}_1)[(\mathbf{I} - \mathbf{R}_{\theta_2})(\mathbf{y}_2 - \mathbf{R}_{\theta_1}\mathbf{y}_3) - (\mathbf{I} - \mathbf{R}_{\theta_1})(\mathbf{y}_2 - \mathbf{R}_{\theta_2}\mathbf{y}_1)] \\ &= (\mathbf{I} - \mathbf{e}_1 \otimes \mathbf{e}_1)[\mathbf{R}_{\theta_1}(\mathbf{y}_2 - \mathbf{y}_3) + \mathbf{R}_{\theta_2}(\mathbf{y}_1 - \mathbf{y}_2) + \mathbf{R}_{\theta_1}\mathbf{R}_{\theta_2}(\mathbf{y}_3 - \mathbf{y}_1)] \qquad (3.31)\end{aligned}$$

and also

$$\begin{aligned}(\mathbf{I} - \mathbf{e}_1 \otimes \mathbf{e}_1)\mathbf{R}_{\theta_1}\mathbf{y}_3 &= (\mathbf{I} - \mathbf{e}_1 \otimes \mathbf{e}_1)\mathbf{y}_2, \\ (\mathbf{I} - \mathbf{e}_1 \otimes \mathbf{e}_1)\mathbf{R}_{\theta_2}\mathbf{y}_1 &= (\mathbf{I} - \mathbf{e}_1 \otimes \mathbf{e}_1)\mathbf{y}_2. \qquad (3.32)\end{aligned}$$

By substituting equations above into (3.31), we have

$$(33) = (\mathbf{I} - \mathbf{e}_1 \otimes \mathbf{e}_1)[\mathbf{R}_{\theta_1}\mathbf{y}_2 - \mathbf{R}_{\theta_2}\mathbf{y}_2 + \mathbf{R}_{\theta_1}\mathbf{R}_{\theta_2}(\mathbf{y}_3 - \mathbf{y}_1)] = 0 \qquad (3.33)$$

(recall $\mathbf{R}_{\theta_1}\mathbf{R}_{\theta_2} = \mathbf{R}_{\theta_2}\mathbf{R}_{\theta_1}$). Thus, $\mathbf{z}_1 - \mathbf{z}_2 = 0$.

□

Theorem 3.3.1. *The generators g_1 and g_2 of the Miura parallelogram are commutative if and only if $\mathbf{e}_1 = \mathbf{e}_2$.*

Proof. $\mathbf{e}_1 = \mathbf{e}_2$ implies $\mathbf{R}_{\theta_1}\mathbf{R}_{\theta_2} = \mathbf{R}_{\theta_2}\mathbf{R}_{\theta_1}$. By Lemma 3.3.1, we only need to check the equality $(\mathbf{R}_{\theta_1} - \mathbf{I})\mathbf{c}_2 = (\mathbf{R}_{\theta_2} - \mathbf{I})\mathbf{c}_1$ with

$$\begin{aligned}\mathbf{c}_1 &= \tau_1\mathbf{e}_1 + (\mathbf{I} - \mathbf{R}_{\theta_1})\mathbf{z}_1, \\ \mathbf{c}_2 &= \tau_2\mathbf{e}_2 + (\mathbf{I} - \mathbf{R}_{\theta_2})\mathbf{z}_2. \qquad (3.34)\end{aligned}$$

By direct calculation, we have

$$\begin{aligned}(\mathbf{R}_{\theta_1} - \mathbf{I})\mathbf{c}_2 &= (\mathbf{R}_{\theta_1} + \mathbf{R}_{\theta_2} - \mathbf{R}_{\theta_1+\theta_2} - \mathbf{I})\mathbf{z}_2, \\ (\mathbf{R}_{\theta_2} - \mathbf{I})\mathbf{c}_1 &= (\mathbf{R}_{\theta_1} + \mathbf{R}_{\theta_2} - \mathbf{R}_{\theta_1+\theta_2} - \mathbf{I})\mathbf{z}_1. \qquad (3.35)\end{aligned}$$

Obviously, the equality holds (recall $\mathbf{z}_1 = \mathbf{z}_2$ by Lemma 3.3.2). The necessity of $\mathbf{e}_1 = \mathbf{e}_2$ is given by Lemma 3.3.1.

□

By Theorem 3.3.1, we can choose (ω, φ) such that $\mathbf{e}_1(\omega, \varphi) = \mathbf{e}_2(\omega, \varphi)$ to have two commutative generators g_1 and g_2 as defined in Section 3.3.

Next, we consider the discreteness of the generators. We derive Theorem 3.3.2 regarding the discreteness of the generators g_1 and g_2. The proof is given in B.2.

Theorem 3.3.2. *Suppose* $g_1 = (\mathbf{R}_{\theta_1}|(\mathbf{I}-\mathbf{R}_{\theta_1})\mathbf{z}+\tau_1\mathbf{e})$ *and* $g_2 = (\mathbf{R}_{\theta_2}|(\mathbf{I}-\mathbf{R}_{\theta_2})\mathbf{z}+\tau_2\mathbf{e})$ *are isometries with the same axis and* $\tau_2\theta_1 \neq \tau_1\theta_2$[3]. *Then the group* $G = \{g_1^p g_2^q | (p,q) \in \mathbb{Z}^2\}$ *is discrete if and only if there exists* $(p^\star, q^\star) \in \mathbb{Z}^2 \setminus (0,0)$ *such that* $g_1^{p^\star} g_2^{q^\star} = id$.

The previous results are summarized as follows.

Commutativity and discreteness of the non-degenerate generators[4] for helical Miura origami. The group generated by non-degenerate generators $g_1 = (\mathbf{R}_{\theta_1}|\tau_1\mathbf{e}_1+(\mathbf{I}-\mathbf{R}_{\theta_1})\mathbf{z}_1)$ and $g_2 = (\mathbf{R}_{\theta_2}|\tau_2\mathbf{e}_2+(\mathbf{I}-\mathbf{R}_{\theta_2})\mathbf{z}_2)$ with parameters given by (3.22) (3.23) are Abelian and discrete if and only if the generators satisfy ALL of the following conditions:

1. (Commutativity). $\mathbf{e}_1 = \mathbf{e}_2$.
2. (Discreteness). There exits $(p^\star, q^\star) \in \mathbb{Z}^2 \setminus (0,0)$ such that

$$\begin{aligned} p^\star\theta_1 + q^\star\theta_2 &= 2k\pi, \quad k \in \mathbb{Z}, \\ p^\star\tau_1 + q^\star\tau_2 &= 0. \end{aligned} \tag{3.36}$$

3.4 Design a closed helical Miura-ori

The results of the previous section indicate that if the parameters given by (3.22) and (3.23) satisfy

$$\mathbf{e}_1 = \mathbf{e}_2, \tag{3.37}$$

$$p^\star\theta_1 + q^\star\theta_2 = 2k\pi, \tag{3.38}$$

$$p^\star\tau_1 + q^\star\tau_2 = 0, \tag{3.39}$$

[3]This is the non-degenerate condition and ensures that $g_1^p g_2^q(\mathbf{x})$ is not a single helix.

[4]Here the non-degenerate generators satisfy $\tau_1\theta_2 \neq \tau_2\theta_1$

the group $G = \{g_1^p g_2^q | (p,q) \in \mathbb{Z}^2\}$ is a discrete helical group (we assume $\mathbf{e}_1 = \mathbf{e}_2$ here). $\mathbf{e}_1 = \mathbf{e}_2$, i.e.

$$\cos\varphi\ \mathbf{f}_1 + \sin\varphi\ \mathbf{f}_2 = \cos\psi\ \mathbf{g}_1 + \sin\psi\ \mathbf{g}_2. \tag{3.40}$$

Then $\psi = \psi(\omega, \varphi)$ is uniquely determined by

$$\begin{aligned} \sin\psi &= \cos\varphi\ (\mathbf{f}_1 \cdot \mathbf{g}_2) + \sin\varphi\ (\mathbf{f}_2 \cdot \mathbf{g}_2), \\ \cos\psi &= \cos\varphi\ (\mathbf{f}_1 \cdot \mathbf{g}_1) + \sin\varphi\ (\mathbf{f}_2 \cdot \mathbf{g}_1). \end{aligned} \tag{3.41}$$

Thus, all the parameters can be written as the functions of (ω, φ). In the following discussion, we assume that $\mathbf{e}_1 = \mathbf{e}_2 = \mathbf{e}$ and $\mathbf{z}_1 = \mathbf{z}_2 = \mathbf{z}$, i.e., the generators g_1 and g_2 are commutative. Also, we conclude that, for a physically realistic helical origami structure, k is 1 or -1, otherwise, part of the origami structure will be overlapped with some other part (even if the group of generators is discrete). The fact is given by the following theorem.

Theorem 3.4.1. *Suppose the group parameters $\theta_1, \theta_2, \tau_1, \tau_2$ of g_1, g_2 satisfy*

$$\begin{aligned} p^\star\theta_1 + q^\star\theta_2 &= \pm 2\pi, \\ p^\star\tau_1 + q^\star\tau_2 &= 0, \end{aligned} \tag{3.42}$$

for some $(p^\star, q^\star) \in \mathbb{Z}^2 \setminus (0,0)$ and $\theta_1\tau_2 \neq \theta_2\tau_1$. Define the extended domain $\tilde{\Omega} \subset \mathbb{R} \times \mathbb{R}$ of powers of generators as

$$\tilde{\Omega} = \begin{cases} \mathbb{R} \times (0, |q^\star|] & \text{if } q^\star \neq 0 \\ (0, |p^\star|] \times \mathbb{R} & \text{otherwise.} \end{cases} \tag{3.43}$$

The cylindrical surface $\mathcal{C} \subset \mathbb{R}^3$ is defined by

$$\mathcal{C} = \{\mathbf{z} + |\mathbf{x} - \mathbf{z}| \cos\theta\, \hat{\mathbf{e}}_1 + |\mathbf{x} - \mathbf{z}| \sin\theta\, \hat{\mathbf{e}}_2 + \rho\, \hat{\mathbf{e}}_3 : \theta \in (0, 2\pi], \rho \in \mathbb{R}\} \tag{3.44}$$

where $\hat{\mathbf{e}}_3 = \mathbf{e}$ is the rotation axis of the generators and $(\mathbf{x} - \mathbf{z}) \cdot \mathbf{e} = 0$. Then the map $\tilde{\mathbf{y}} : \tilde{\Omega} \to \mathcal{C}$ defined as $\tilde{\mathbf{y}}(\tilde{p}, \tilde{q}) = g_1^{\tilde{p}} g_2^{\tilde{q}}(\mathbf{x})$ is bijective.

Proof. To simplify the proof, we assume $q^\star > 0$ without loss of generality, because we

can exchange g_1, g_2 and flip the sign of (3.42).

(*Step 1:* $\tilde{\mathbf{y}}(\tilde{\Omega}) \subset \mathcal{C}$.) By the multiplication rule of generator, we have

$$\tilde{\mathbf{y}}(\tilde{p},\tilde{q}) = \mathbf{R}_{\tilde{p}\theta_1+\tilde{q}\theta_2}(\mathbf{x}-\mathbf{z}) + (\tilde{p}\tau_1+\tilde{q}\tau_2)\mathbf{e} + \mathbf{z}. \tag{3.45}$$

Because

$$\begin{aligned} \mathbf{R}_{\tilde{p}\theta_1+\tilde{q}\theta_2}(\mathbf{x}-\mathbf{z})+\mathbf{z} &\in \{|\mathbf{x}-\mathbf{z}|\cos\theta\,\mathbf{e}_1 + |\mathbf{x}-\mathbf{z}|\sin\theta\,\mathbf{e}_2 + \mathbf{z} : \theta\in(0,2\pi]\}, \\ (\tilde{p}\tau_1+\tilde{q}\tau_2)\mathbf{e} &\in \{\rho\mathbf{e}_3 : \rho\in\mathbb{R}\}, \end{aligned} \tag{3.46}$$

it is obvious that $\tilde{\mathbf{y}}(\tilde{p},\tilde{q}) \in \mathcal{C}$.

(*Step 2: Injection.*) Suppose $\tilde{\mathbf{y}}(p_1,q_1) = \tilde{\mathbf{y}}(p_2,q_2)$ with $(p_1,q_1),(p_2,q_2) \in \tilde{\Omega}$. We have

$$\begin{aligned} (p_1-p_2)\theta_1 + (q_1-q_2)\theta_2 &= 2k\pi, \quad k\in\mathbb{Z}, \\ (p_1-p_2)\tau_1 + (q_1-q_2)\tau_2 &= 0. \end{aligned} \tag{3.47}$$

Since $\theta_2\tau_1 \neq \theta_1\tau_2$, the previous equations have solutions as

$$(p_1-p_2, q_1-q_2) \in \{\pm(kp^\star, kq^\star)\}. \tag{3.48}$$

$|q_1-q_2| < |q^\star|$ implies that $k=0$. Thus $p_1=p_2$ and $q_1=q_2$.

(*Step 3: Surjection.*) The map $\tilde{\mathbf{y}}$ is surjective if for any $\theta\in(0,2\pi], \rho\in\mathbb{R}$, there exists $(\tilde{p},\tilde{q}) \in \tilde{\Omega}$ such that

$$\begin{aligned} \tilde{p}\theta_1 + \tilde{q}\theta_2 &= \theta + 2k\pi, \quad k\in\mathbb{Z}, \\ \tilde{p}\tau_1 + \tilde{q}\tau_2 &= \rho. \end{aligned} \tag{3.49}$$

Suppose (p_0,q_0) satisfies

$$\begin{aligned} p_0\theta_1 + q_0\theta_2 &= \theta, \\ p_0\tau_1 + q_0\tau_2 &= \rho. \end{aligned} \tag{3.50}$$

Let $(\tilde{p},\tilde{q}) = (p_0+mp^\star, q_0+mq^\star)$ where m is an integer such that $q_0+mq^\star = q_0 \mod q^\star$.

Then $(\tilde{p}, \tilde{q}) \in \tilde{\Omega}$ is a solution to (3.49). □

We call the condition (3.42) *special discreteness condition*. It tells us not only the discreteness of the generators but also the one-one correspondence from an appropriate reference domain to deformed domain. For the purpose of our origami construction, if g_1 and g_2 satisfy the special discreteness condition, $g_1^p g_2^q(\mathbf{y}(\Omega))$ is an origami without overlapping in the sense that $g_1^{\hat{p}} g_2^{\hat{q}}(\mathbf{y}_1), (\hat{p}, \hat{q}) \in \hat{\Omega}$ has no overlapping region. Then the problem is to find pairs of real numbers $(\omega, \varphi) \in (-\pi, 0) \cup (0, \pi) \times (0, \pi]$ such that

$$p^\star \theta_1 + q^\star \theta_2 = \pm 2\pi, \tag{3.51}$$

$$p^\star \tau_1 + q^\star \tau_2 = 0. \tag{3.52}$$

We summarize the design strategy for a closed helical Miura-ori as follows.

Design equation for a closed helical Miura-ori. The unit origami cell (Miura parallelogram) is parameterized by some constant $\hat{\mathbf{p}}$-vector in the domain $\hat{\mathcal{P}}$ defined by 3.15. If there exists $(\omega, \varphi) \in (-\pi, 0) \cup (0, \pi) \times (0, \pi]$ satisfying the special discreteness condition

$$p^\star \theta_1(\omega, \varphi) + q^\star \theta_2(\omega, \varphi) = \sigma 2\pi, \tag{3.53}$$

$$p^\star \tau_1(\omega, \varphi) + q^\star \tau_2(\omega, \varphi) = 0, \tag{3.54}$$

for some $(p^\star, q^\star) \in \mathbb{Z}^2 \backslash (0, 0)$, $\sigma \in \{\pm\}$, then $\{g_1^p g_2^q(\mathbf{y}(\mathbf{x})) : (p, q) \in \mathbb{Z} \times \{1, 2, \ldots, |q^\star|\}, \mathbf{x} \in \Omega\}$ forms a closed helical Miura-ori. Here $\mathbf{y}(\mathbf{x})$ is the origami deformation given in 3.2.

We provide some important explanations about the design equation here.

1. We assume $q^\star \neq 0$ here. Of course, one can choose $q^\star \neq 0$ and $(p, q) \in \{1, 2, \ldots, |p^\star|\} \times \mathbb{Z}$.

2. Different sets of $\{\hat{\mathbf{p}}, (p^\star, q^\star), \sigma\}$ determine the different structures of closed HMO. Since $\{\hat{\mathbf{p}}, (p^\star, q^\star), \sigma\}$ and $\{\hat{\mathbf{p}}, (-p^\star, -q^\star), \sigma\}$ have the identical solution for (ω, φ), without loss of generality, we assume $p^\star \geq 0$.

3. Define the *computational domain* as

$$\mathcal{C}_d = \hat{\mathcal{P}} \times \{\mathbb{N} \times \mathbb{Z}\} \times \{\pm\}. \tag{3.55}$$

Every closed HMO corresponds to some generalized *computational vector*

$$(p_1, p_2, p_3) \times (p^\star, q^\star) \times \{\sigma\} \in \mathcal{C}_d. \tag{3.56}$$

But unfortunately, an arbitrary vector in $\mathcal{C}_d$ is not able to secure a physical relevant solution. We need to solve the design equation and check.

3.4.1 Compatibility of translations τ_1 and τ_2

Now we give the method for solving the design equations (3.53) and (3.54). Suppose we have $\mathbf{e}_1 = \mathbf{e}_2$. The two translations are

$$\begin{aligned} \tau_1 &= \mathbf{e}_1 \cdot (\mathbf{y}_2 - \mathbf{y}_3) = \mathbf{e}_2 \cdot \mathbf{v}_b = \cos\psi\, \mathbf{g}_1 \cdot \mathbf{v}_b, \\ \tau_2 &= \mathbf{e}_2 \cdot (\mathbf{y}_2 - \mathbf{y}_1) = \mathbf{e}_1 \cdot \mathbf{u}_b = \cos\varphi\, \mathbf{f}_1 \cdot \mathbf{u}_b. \end{aligned} \tag{3.57}$$

Recall that $\cos\psi = \cos\varphi\, \mathbf{f}_1 \cdot \mathbf{g}_1 + \sin\varphi\, \mathbf{f}_2 \cdot \mathbf{g}_1$. (3.54) is equivalent to

$$p^\star \cos\varphi\ (\mathbf{g}_1 \cdot \mathbf{f}_1)(\mathbf{g}_1 \cdot \mathbf{v}_b) + q^\star \cos\varphi\ \mathbf{f}_1 \cdot \mathbf{u}_b + p^\star \sin\varphi\ (\mathbf{g}_1 \cdot \mathbf{f}_2)(\mathbf{g}_1 \cdot \mathbf{v}_b) = 0. \tag{3.58}$$

We assume $p^\star > 0$ here, then $\tau_2 \neq 0$, which means $\cos\varphi\, \mathbf{f}_1 \cdot \mathbf{u}_b \neq 0$. Here we firstly prove that $(\mathbf{g}_1 \cdot \mathbf{f}_2)(\mathbf{g}_1 \cdot \mathbf{v}_b) \neq 0$ for any $\omega \in (-\pi, 0) \cup (0, \pi)$. $\mathbf{g}_1 \cdot \mathbf{v}_b = 0$ implies that $\mathbf{v}_a = -\mathbf{v}_b$ (recall $\mathbf{g}_1 = \frac{\mathbf{v}_a + \mathbf{v}_b}{|\mathbf{v}_a + \mathbf{v}_b|}$). Then $\mathbf{y}_1, \mathbf{y}_2, \mathbf{y}_3, \mathbf{y}_4$ are on the same plane, which implies that $\omega \in \{0, \pm\pi\}$ by the similar argument in 3.5.4. Next we assume $\mathbf{g}_1 \cdot \mathbf{f}_2 = 0$. Substitute $\mathbf{g}_1 = \frac{\mathbf{v}_q + \mathbf{v}_b}{|\mathbf{v}_a + \mathbf{v}_b|}$ and $\mathbf{f}_2 = \frac{\mathbf{u}_a \times \mathbf{u}_b}{|\mathbf{u}_a \times \mathbf{u}_b|}$ to have

$$(\mathbf{v}_a + \mathbf{v}_b) \cdot (\mathbf{u}_a \times \mathbf{u}_b) = 0. \tag{3.59}$$

Notice that $\mathbf{u}_a + \mathbf{v}_b = \mathbf{v}_a + \mathbf{u}_b$. We have

$$\begin{aligned} 0 &= (\mathbf{v}_a + \mathbf{v}_b) \cdot ((\mathbf{v}_a - \mathbf{v}_b) \times \mathbf{u}_b) \\ &= (\mathbf{v}_a + \mathbf{v}_b) \cdot (\mathbf{v}_b \times \mathbf{u}_b) \\ &= \mathbf{v}_a \cdot (\mathbf{v}_b \times \mathbf{u}_b). \end{aligned} \tag{3.60}$$

Then $\mathbf{y}_1, \mathbf{y}_2, \mathbf{y}_3, \mathbf{y}_4$ are on the same plane and $\omega \in \{0, \pm\pi\}$. Thus,

$$\tan\varphi = -\frac{\mathbf{g}_1 \cdot \mathbf{f}_1}{\mathbf{g}_1 \cdot \mathbf{f}_2} - \frac{q^\star \mathbf{f}_1 \cdot \mathbf{u}_b}{p^\star(\mathbf{g}_1 \cdot \mathbf{f}_2)(\mathbf{g}_1 \cdot \mathbf{v}_b)} = \Gamma(\omega) \tag{3.61}$$

has no singularities for $\omega \in (-\pi, 0) \cup (0, \pi)$. Then $\varphi = \varphi(\omega) \in (0, \pi]$ is given by

$$\varphi(\omega) = \begin{cases} (1 - \text{sign}(\Gamma(\omega))\pi/2 + \arctan\Gamma(\omega), & \text{if } \Gamma(\omega) \neq 0 \\ \pi, & \text{if } \Gamma(\omega) = 0 \end{cases} \tag{3.62}$$

3.4.2 Compatibility of rotations θ_1 and θ_2

$\cos\theta_1$ and $\cos\theta_2$ could be simplified as

$$\begin{aligned} \cos\theta_1 &= \frac{\mathbf{u}_a \cdot \mathbf{u}_b - \tau_2^2}{|\mathbf{u}_a|^2 - \tau_2^2}, \\ \cos\theta_2 &= \frac{\mathbf{v}_a \cdot \mathbf{v}_b - \tau_1^2}{|\mathbf{v}_a|^2 - \tau_1^2}. \end{aligned} \tag{3.63}$$

Then

$$\begin{aligned} \theta_1 &= \pm\arccos\frac{\mathbf{u}_a \cdot \mathbf{u}_b - \tau_2^2}{|\mathbf{u}_a|^2 - \tau_2^2}, \\ \theta_2 &= \pm\arccos\frac{\mathbf{v}_a \cdot \mathbf{v}_b - \tau_1^2}{|\mathbf{v}_a|^2 - \tau_1^2}. \end{aligned} \tag{3.64}$$

The signs of θ_1 and θ_2 are chosen to satisfy

$$\mathbf{R}_{\theta_1}(\mathbf{u}_a - (\mathbf{e} \cdot \mathbf{u}_a)\mathbf{e}) = \mathbf{u}_b - (\mathbf{e} \cdot \mathbf{u}_b)\mathbf{e} \tag{3.65}$$

and

$$\mathbf{R}_{\theta_2}(\mathbf{v}_a - (\mathbf{e} \cdot \mathbf{v}_a)\mathbf{e}) = \mathbf{v}_b - (\mathbf{e} \cdot \mathbf{v}_b)\mathbf{e} \tag{3.66}$$

respectively, where $\mathbf{e} = \mathbf{e}_1 = \mathbf{e}_2$. Substitute $\varphi_i(\omega)$ into the rotation part (3.53) to have

$$p^\star\theta_1(\omega, \varphi_i(\omega)) + q^\star\theta_2(\omega, \varphi_i(\omega)) = \sigma 2\pi, \tag{3.67}$$

where $\sigma \in \{\pm\}$ We can solve this equation numerically and the algorithm is:

1. Discretize $\omega \in (-\pi, 0) \cup (0, \pi)$.

2. Calculate solution ω such that $|p^\star \theta_1(\omega, \varphi) + q^\star \theta_2(\omega, \varphi)| < \epsilon$, where $\varphi = \varphi(\omega)$ and ϵ is the numerical tolerance.

3.4.3 Some numerical results

Since we have two branches of the solution for the same reference domain as discussed in 3.2, it is possible to have two different closed HMO corresponding to the same computational vector as depicted in Figure 3.5. We call them *plus*-phase and *minus*-phase. These two phases have different parameters in their group generators, and therefore, they have different radiuses, pitches, and twists. These remarkable features are useful for actuation. In Figure 3.6 and 3.7, we also show some solutions with different computational vectors for *plus*-phase and *minus*-phase. Notice that the solutions of (ω, φ) are isolated, which also means the structures are rigid.

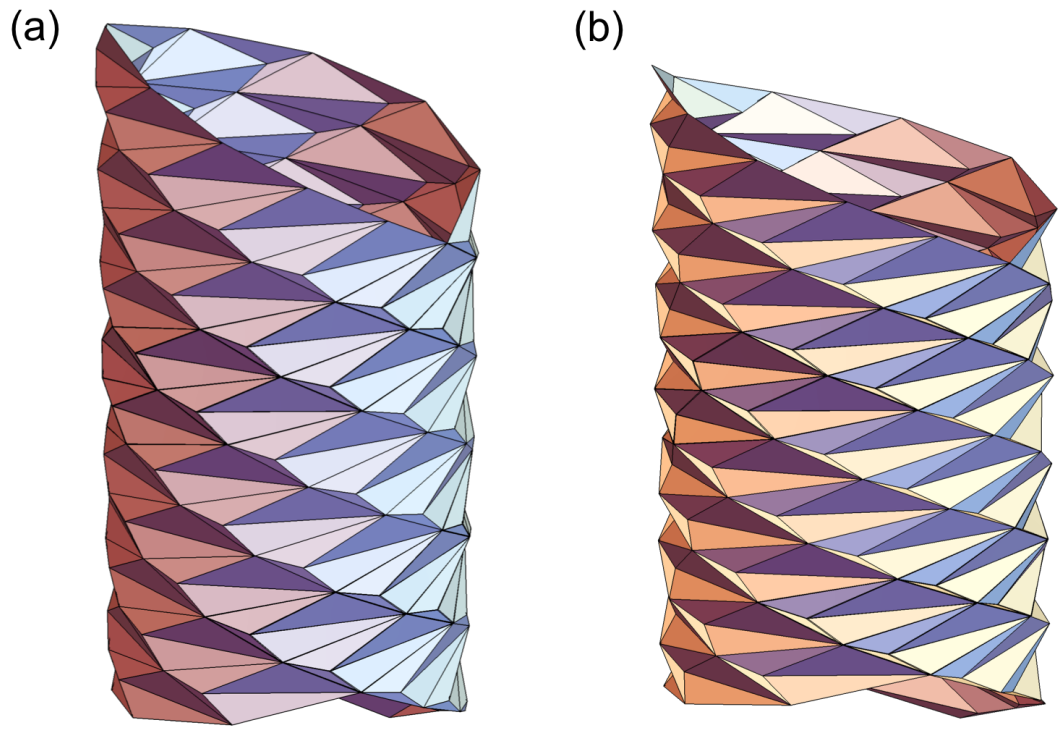

Figure 3.5: Bistable solutions corresponding to the same computational vector $\hat{\mathbf{p}} \times (p^\star, q^\star) \times \{\sigma\} = (1.603, 1.667, 0.178) \times (5, 5) \times \{+\}$: (a) *plus*-phase and (b) *minus*-phase.

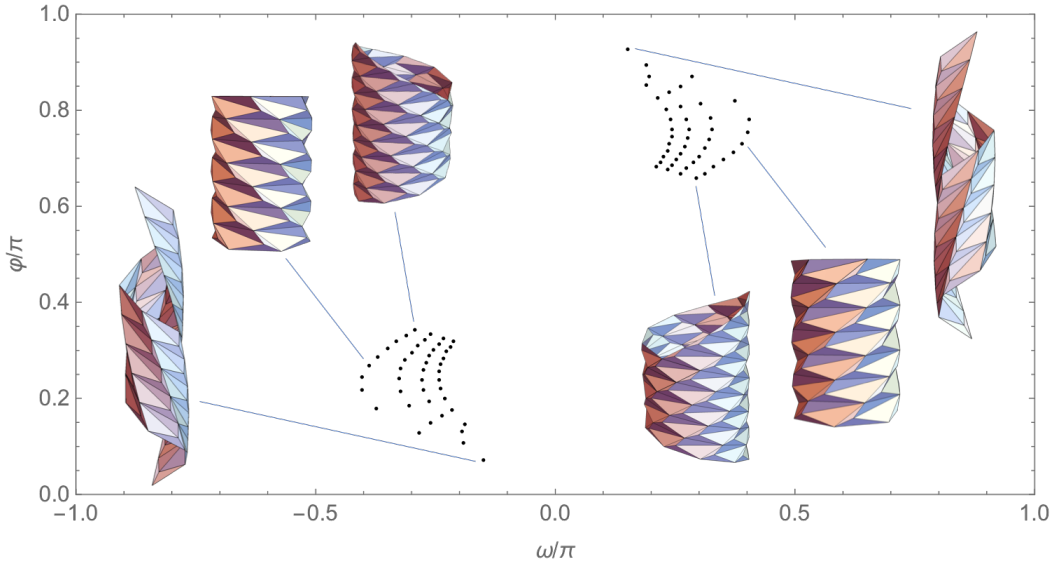

Figure 3.6: Solutiuons in *plus*-phase with the same reference unit cell ($\hat{\mathbf{p}} = (1.603, 1.667, 0.178)$) but different $(p^\star, q^\star)$ and σ. Each black dot denotes a closed HMO. ω and φ are normalized by π.

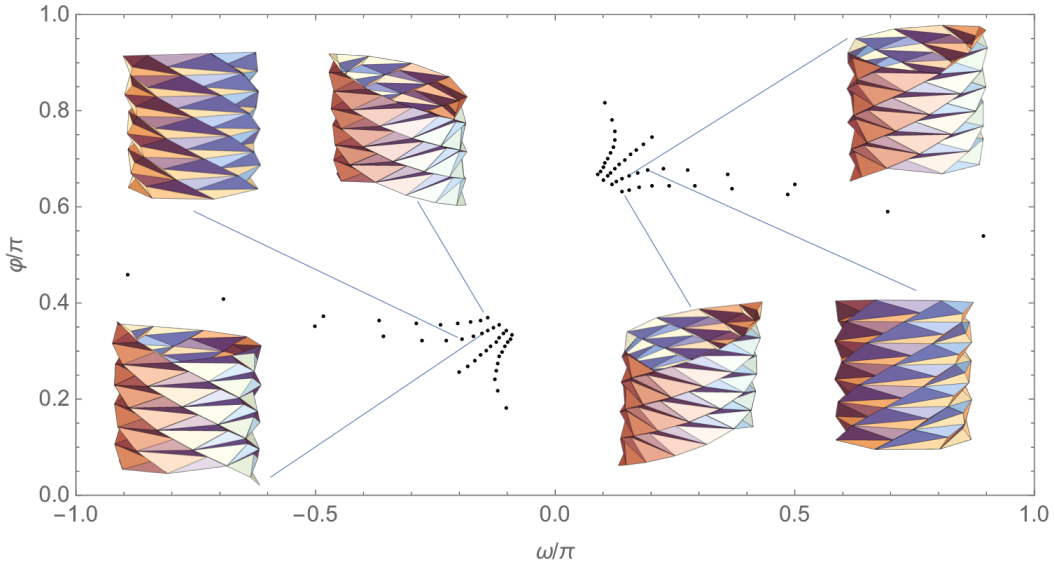

Figure 3.7: Solutiuons in *minus*-phase with the same reference unit cell ($\hat{\mathbf{p}} = (1.603, 1.667, 0.178)$) but different $(p^\star, q^\star)$ and σ. Each black dot denotes a closed HMO. ω and φ are normalized by π.

3.5 Phase transformations in helical Miura-ori

In this section, we explore the idea of phase transformation in HMO. Despite the rigidity of a closed HMO shown in the previous section, phase-transforming helical Miura origami can achieve some actuations as desired.

3.5.1 Two variants for the same reference domain

Suppose we have the reference domain ($\omega = 0$) with vertices $\{\mathbf{x}_1, \mathbf{x}_2, \mathbf{x}_3, \mathbf{x}_4\}$ as defined in Section 3.2, and the piecewise affine deformation is

$$\mathbf{y}^{\pm}(\mathbf{x}) = \begin{cases} \mathbf{x}, & \mathbf{x}\cdot\mathbf{e}_3 = 0,\ \mathbf{x}\cdot\mathbf{n}_2 < 0,\ \mathbf{x}\cdot\mathbf{n}_1 \geq 0, \\ \mathbf{R}_2(\pm\omega)\mathbf{x}, & \mathbf{x}\cdot\mathbf{e}_3 = 0,\ \mathbf{x}\cdot\mathbf{n}_3 < 0,\ \mathbf{x}\cdot\mathbf{n}_2 \geq 0, \\ \mathbf{R}_2(\pm\omega)\mathbf{R}_3(\xi^{\pm}(\omega))\mathbf{x}, & \mathbf{x}\cdot\mathbf{e}_3 = 0,\ \mathbf{x}\cdot\mathbf{n}_4 < 0,\ \mathbf{x}\cdot\mathbf{n}_3 \geq 0, \\ \mathbf{R}_2(\pm\omega)\mathbf{R}_3(\xi^{\pm}(\omega))\mathbf{R}_4(\omega)\mathbf{x}, & \mathbf{x}\cdot\mathbf{e}_3 = 0,\ \mathbf{x}\cdot\mathbf{n}_1 < 0,\ \mathbf{x}\cdot\mathbf{n}_4 \geq 0. \end{cases} \tag{3.68}$$

Here we have two solutions $\mathbf{y}^{\pm}(\mathbf{x})$ for the same reference domain as discussed in Section

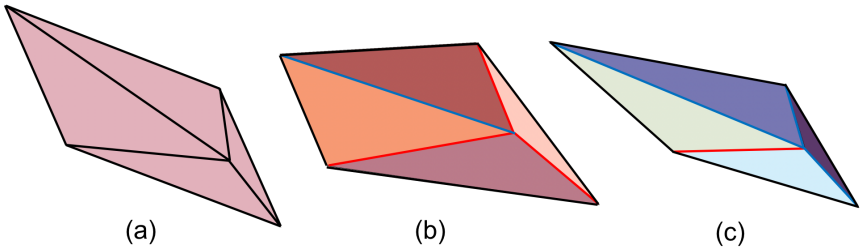

Figure 3.8: (a) Reference domain. (b) *plus*-phase. (c) *minus*-phase.

3.2. Consequently, we have the set of vertices

$$\{\mathbf{y}_{ip} : \mathbf{y}_{ip} = \mathbf{y}^{+}(\mathbf{x}_i), i = 1, 2, 3, 4\} \tag{3.69}$$

for *plus*-phase, and

$$\{\mathbf{y}_{im} : \mathbf{y}_{im} = \mathbf{y}^{-}(\mathbf{x}_i), i = 1, 2, 3, 4\} \tag{3.70}$$

for *minus*-phase. The corresponding generators for these two sets of vertices are

$$\begin{cases} g_{1p}(\omega_p, \varphi_p) = (\mathbf{R}_{\theta_{1p}} | (\mathbf{I} - \mathbf{R}_{\theta_{1p}})\mathbf{z}_p + \tau_{1p}\mathbf{e}_p) \\ g_{2p}(\omega_p, \varphi_p) = (\mathbf{R}_{\theta_{2p}} | (\mathbf{I} - \mathbf{R}_{\theta_{2p}})\mathbf{z}_p + \tau_{2p}\mathbf{e}_p) \end{cases} \tag{3.71}$$

and

$$\begin{cases} g_{1m}(\omega_m, \varphi_m) = (\mathbf{R}_{\theta_{1m}} | (\mathbf{I} - \mathbf{R}_{\theta_{1m}})\mathbf{z}_m + \tau_{1m}\mathbf{e}_m) \\ g_{2m}(\omega_m, \varphi_m) = (\mathbf{R}_{\theta_{2m}} | (\mathbf{I} - \mathbf{R}_{\theta_{2m}})\mathbf{z}_m + \tau_{2m}\mathbf{e}_m) \end{cases} \tag{3.72}$$

with group parameters $\{\theta_{1p}, \theta_{2p}, \tau_{1p}, \tau_{2p}, \mathbf{z}_p, \mathbf{e}_p\}$ and $\{\theta_{1m}, \theta_{2m}, \tau_{1m}, \tau_{2m}, \mathbf{z}_m, \mathbf{e}_m\}$ as functions of (ω_p, φ_p) and (ω_m, φ_m) respectively. Finally, we have two sets of group parameters for *plus*-phase and *minus*-phase. We will discuss phase transformation between these two phases and make a perfect analog to the idea of helical phase transformation. For the convenience to construct compatible interfaces, we firstly clarify some concepts.

Definition 3.5.1. *We define two generators* $g = (\mathbf{R}_\theta | (\mathbf{I} - \mathbf{R}_\theta)\mathbf{z} + \tau\mathbf{e})$ *and* $g^\star = (\mathbf{R}^\star_{\theta^\star} | (\mathbf{I} - \mathbf{R}^\star_{\theta^\star})\mathbf{z}^\star + \tau^\star\mathbf{e}^\star)$ *to be equivalent generators if*

$$\theta = \theta^\star,\ \tau = \tau^\star. \tag{3.73}$$

The relationship between two equivalent generators is denoted by $g = g^\star$.

Lemma 3.5.1. *If* $g_{1p} = g_{1m}$, *then* $r_p = r_m$. *Here* $r_p = |(\mathbf{I} - \mathbf{e}_p \otimes \mathbf{e}_p)(\mathbf{y}_{3p} - \mathbf{z}_p)|$ *and* $r_m = |(\mathbf{I} - \mathbf{e}_m \otimes \mathbf{e}_m)(\mathbf{y}_{3m} - \mathbf{z}_m)|$ *are the radiuses of the cylindrical surfaces containing* $\mathbf{y}_{ip}$ *and* $\mathbf{y}_{im}$, $i = 1, 2, 3, 4$, *respectively.*

Proof. We calculate r_p first. Substitute the formula of $\mathbf{z}_p$ to have

$$\begin{aligned} r_p &= |(\mathbf{I} - \mathbf{e}_p \otimes \mathbf{e}_p)(\mathbf{y}_{3p} - (\mathbf{I} - \mathbf{R}_{\theta_{1p}})^{-1}(\mathbf{I} - \mathbf{e}_p \otimes \mathbf{e}_p)(\mathbf{y}_{2p} - \mathbf{R}_{\theta_{1p}}\mathbf{y}_{3p}))| \\ &= |(\mathbf{I} - \mathbf{R}_{\theta_{1p}})^{-1}(\mathbf{I} - \mathbf{e}_p \otimes \mathbf{e}_p)((\mathbf{I} - \mathbf{R}_{\theta_{1p}})\mathbf{y}_{3p} - (\mathbf{y}_{2p} - \mathbf{R}_{\theta_{1p}}\mathbf{y}_{3p}))| \\ &= |(\mathbf{I} - \mathbf{R}_{\theta_{1p}})^{-1}(\mathbf{y}_{2p} - \mathbf{y}_{3p} - \tau_{1p}\mathbf{e}_p)| \\ &= \frac{|\mathbf{x}_3 - \mathbf{x}_2|^2 - \tau_{1p}^2}{2\sin(\theta_{1p}/2)}. \end{aligned} \tag{3.74}$$

Here we have substituted the formula $\tau_{1p} = \mathbf{e}_p \cdot (\mathbf{y}_{2p} - \mathbf{y}_{3p})$. Notice the fact that

$\mathbf{y}_{2p} - \mathbf{y}_{3p} - \tau_{1p}\mathbf{e}_p$ is on the plane perpendicular to $\mathbf{e}_p$. Then the last equality follows by the triangular calculation on this plane:

$$\begin{aligned} 2r_p \sin(\theta_{1p}/2) &= |\mathbf{y}_{2p} - \mathbf{y}_{3p} - \tau_{1p}\mathbf{e}_p| \\ &= |\mathbf{y}_{3p} - \mathbf{y}_{2p}|^2 - \tau_{1p}^2 \\ &= |\mathbf{x}_3 - \mathbf{x}_2|^2 - \tau_{1p}^2. \end{aligned} \tag{3.75}$$

Similarly, the radius of *minus*-phase is

$$r_m = \frac{|\mathbf{x}_3 - \mathbf{x}_2|^2 - \tau_{1m}^2}{2\sin(\theta_{1m}/2)}. \tag{3.76}$$

$g_{1p} = g_{1m}$ gives $\theta_{1p} = \theta_{1m}$ and $\tau_{1p} = \tau_{1m}$. Thus, $r_m = r_p$. □

Lemma 3.5.2. *Suppose g and $g^\star$ defined above are equivalent generators, i.e., $g = g^\star$. If $|(\mathbf{I} - \mathbf{e}\otimes\mathbf{e})(\mathbf{x} - \mathbf{z})| = |(\mathbf{I} - \mathbf{e}^\star\otimes\mathbf{e}^\star)(\mathbf{x}^\star - \mathbf{z}^\star)|$, then there exits $\mathbf{R} \in SO(3)$ and $\mathbf{t} \in \mathbb{R}^3$ such that*

$$\mathbf{R}g^p(\mathbf{x}) + \mathbf{t} = (g^\star)^p(\mathbf{x}^\star) \tag{3.77}$$

for any $p \in \mathbb{R}$.

Proof. By the multiplication rule of generators, we have

$$g^p(\mathbf{x}) = \mathbf{R}_{p\theta}(\mathbf{x} - \mathbf{z}) + p\tau\mathbf{e} + \mathbf{z} \tag{3.78}$$

and

$$(g^\star)^p(\mathbf{x}^\star) = \mathbf{R}^\star_{p\theta^\star}(\mathbf{x}^\star - \mathbf{z}^\star) + p\tau^\star\mathbf{e}^\star + \mathbf{z}^\star. \tag{3.79}$$

$g = g^\star$ gives $\theta = \theta^\star$ and $\tau = \tau^\star$ by definition. Let $\mathbf{R}_{\mathbf{e}\times\mathbf{e}^\star}$ be a rotation about $\mathbf{e}\times\mathbf{e}^\star$ satisfying $\mathbf{R}_{\mathbf{e}\times\mathbf{e}^\star}\mathbf{e} = \mathbf{e}^\star$. Since $|(\mathbf{I} - \mathbf{e}\otimes\mathbf{e})(\mathbf{x} - \mathbf{z})| = |(\mathbf{I} - \mathbf{e}^\star\otimes\mathbf{e}^\star)(\mathbf{x}^\star - \mathbf{z}^\star)|$, there exits $\mathbf{R}_{\mathbf{e}^\star} \in \mathrm{SO}(3)$, $\mathbf{R}_{\mathbf{e}^\star}\mathbf{e}^\star = \mathbf{e}^\star$ and $\rho \in \mathbb{R}$ such that

$$\mathbf{x}^\star - \mathbf{z}^\star = \mathbf{R}_{\mathbf{e}^\star}\mathbf{R}_{\mathbf{e}\times\mathbf{e}^\star}(\mathbf{x} - \mathbf{z}) + \rho\mathbf{e}^\star. \tag{3.80}$$

Let $\mathbf{R} = \mathbf{R}_{\mathbf{e}^\star}\mathbf{R}_{\mathbf{e}\times\mathbf{e}^\star}$ and $\mathbf{t} = \mathbf{z}^\star - \mathbf{R}_{\mathbf{e}^\star}\mathbf{R}_{\mathbf{e}\times\mathbf{e}^\star}\mathbf{z} + \rho\mathbf{e}^\star$. Then

$$\begin{aligned}
\mathbf{R}g^p(\mathbf{x}) + \mathbf{t} &= \mathbf{R}_{\mathbf{e}^\star}\mathbf{R}_{\mathbf{e}\times\mathbf{e}^\star}[\mathbf{R}_{p\theta}(\mathbf{x}-\mathbf{z}) + p\,\tau\mathbf{e} + \mathbf{z}] + \mathbf{t} \\
&= \mathbf{R}_{\mathbf{e}^\star}\mathbf{R}_{\mathbf{e}\times\mathbf{e}^\star}\mathbf{R}_{p\theta}(\mathbf{x}-\mathbf{z}) + p\,\tau^\star\mathbf{e}^\star + \mathbf{z}^\star + \rho\mathbf{e}^\star \\
&= \mathbf{R}^\star_{p\theta^\star}(\mathbf{x}^\star - \mathbf{z}^\star) + p\,\tau^\star\mathbf{e}^\star + \mathbf{z}^\star \quad (\text{recall } \mathbf{R}^\star_{p\theta^\star}\mathbf{R}_{\mathbf{e}^\star}\mathbf{R}_{\mathbf{e}\times\mathbf{e}^\star} = \mathbf{R}_{\mathbf{e}^\star}\mathbf{R}_{\mathbf{e}\times\mathbf{e}^\star}\mathbf{R}_{p\theta}) \\
&= (g^\star)^p(\mathbf{x}^\star). \qquad (3.81)
\end{aligned}$$

Then $\mathbf{R}$ and $\mathbf{t}$ are the rotation and translation we need. □

Theorem 3.5.1. *For the same reference domain, if $g_{1p} = g_{1m}$, then there exits $\mathbf{R} \in SO(3)$ and $\mathbf{t} \in \mathbb{R}^3$ such that*

$$\mathbf{R}g^n_{1p}(\mathbf{y}_{3p}) + \mathbf{t} = g^n_{1m}(\mathbf{y}_{3m}). \qquad (3.82)$$

for $n \in \mathbb{Z}$.

Proof. By Lemma 3.5.1, we have $|(\mathbf{I} - \mathbf{e}_p \otimes \mathbf{e}_p)(\mathbf{y}_{3p} - \mathbf{z}_p)| = |(\mathbf{I} - \mathbf{e}_m \otimes \mathbf{e}_m)(\mathbf{y}_{3m} - \mathbf{z}_m)|$. Then, the theorem holds naturally by Lemma 3.5.2. □

The helical origami (or helical structure) is generated by two generators. The theorem tells us that, if *plus*-phase and *minus*-phase have the same radius and one equivalent generator (for instance $g_{1p} = g_{1m}$), then there exists a compatible interface between them. The interface is given by

$$g^n_{1m}(\lambda\mathbf{y}_{3m} + (1-\lambda)\mathbf{y}_{2m}), \quad \lambda \in (0, 1]. \qquad (3.83)$$

The type of interface (vertical, horizontal, helical, or elliptical) depends on group parameters, which is about to discuss in detail[5].

3.5.2 Horizontal interface

A horizontal interface requires that $\tau_{1p} = \tau_{1m} = 0$ and $\theta_{1p} = \theta_{1m} \neq 0$. The group generators should also satisfy the special discreteness condition (recall (3.53) and (3.54)).

[5]Actually, we are discussing the special case in Table 2.1, with tangent vector $(1, 0)^T$.

Then $q^\star = 0$, $p^\star \neq 0$. Therefore, we need to solve

$$\begin{cases} p^\star\, \theta_{1p}(\omega_p, \varphi_p) = \sigma 2\pi \\ \tau_{1p}(\omega_p, \varphi_p) = 0 \\ \theta_{1p}(\omega_p, \varphi_p) = \theta_{1m}(\omega_m, \varphi_m) \\ \tau_{1p}(\omega_p, \varphi_p) = \tau_{1m}(\omega_m, \varphi_m) \end{cases} \tag{3.84}$$

for some $(\omega_p, \varphi_p), (\omega_m, \varphi_m) \in (-\pi, 0) \cup (0, \pi) \times (0, \pi]$, $\sigma \in \{\pm\}$. We calculate the interface numerically and give the algorithm here.

1. Solve $\tau_{1p}(\omega_p, \varphi_p) = 0$ for φ_p as a function of ω_p, i.e., $\varphi_p(\omega_p)$.
2. Substitute $\varphi_p(\omega_p)$ into $p^\star \theta_{1p}(\omega_p, \varphi_p) = \sigma 2\pi$. Find $(\omega_p, \varphi_p(\omega_p))$ numerically, such that $|p^\star\, \theta_{1p}(\omega_p, \varphi_p(\omega_p)) - \sigma 2\pi| < \epsilon$, where ϵ is the tolerance and $p^\star \neq 0$ is fixed.
3. Use the similar method to calculate $(\omega_m, \varphi_m(\omega_m))$.
4. Calculate $g_{1p}(\omega_p, \varphi_p(\omega_p))$, $g_{2p}(\omega_p, \varphi_p(\omega_p))$, $g_{1m}(\omega_m, \varphi_m(\omega_p))$, $g_{2m}(\omega_m, \varphi_m(\omega_p))$ and construct the horizontal interface.

Figure 3.9 is an example of the horizontal interface. In this example, we choose $(p^\star, q^\star) = (8, 0)$ and

$$\mathbf{p} = (11.241, 11.687, 1.251, 7.011), \tag{3.85}$$

or

$$\hat{\mathbf{p}} = (1.603, 1.667, 0.178) \tag{3.86}$$

after rescaling, which defines the reference domain (flat configuration). The numerical results for the parameters (before rescaling) are listed in Table 3.1.

3.5.3 Helical interface

Suppose we have a pure *minus*-phase helical Miura-ori and part of the structure transforms to *plus*-phase. If the interface is helical and $g_{1p} = g_{1m}$, we need a generalized

Table 3.1: Parameters for horizontal interface with $\sigma = -$.

ω_p	φ_p	θ_{1p}	τ_{1p}	θ_{2p}	τ_{2p}
-0.867	0.812	-0.785	0	0.386	-2.638
ω_m	φ_m	θ_{1m}	τ_{1m}	θ_{2m}	τ_{2m}
-0.451	0.947	-0.785	0	0.428	-2.214

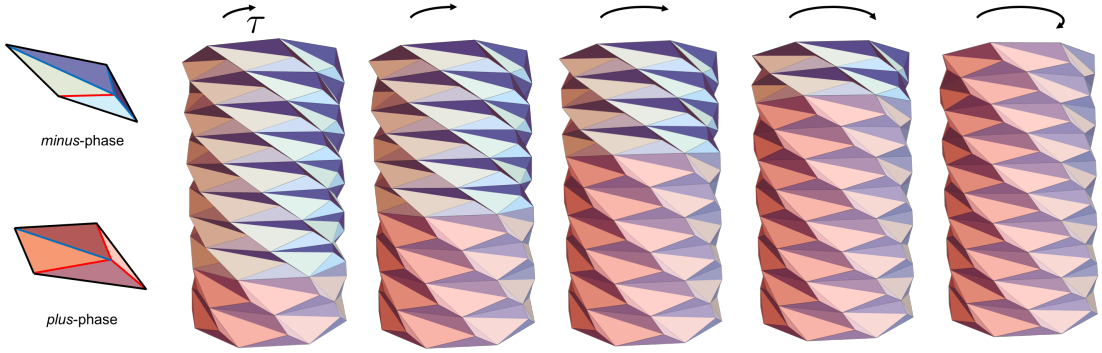

Figure 3.9: Twists by horizontal interface between two variants of the HMO.

compatibility equation for mixed phases to close the structure. The strategy is illustrated in Figure 3.10. Apply corresponding generators along the loop to have

$$g_{1p}^{p^\star} g_{2p}^{q^\star - \delta} g_{2m}^{\delta} = id, \tag{3.87}$$

which is equivalent to

$$\begin{cases} p^\star \theta_{1p}(\omega_p, \varphi_p) + (q^\star - \delta)\theta_{2p}(\omega_p, \varphi_p) + \delta\, \theta_{2m}(\omega_m, \varphi_m) = \sigma 2\pi \\ p^\star \tau_{1p}(\omega_p, \varphi_p) + (q^\star - \delta)\tau_{2p}(\omega_p, \varphi_p) + \delta\, \tau_{2m}(\omega_m, \varphi_m) = 0 \\ \theta_{1p}(\omega_p, \varphi_p) = \theta_{1m}(\omega_m, \varphi_m) \\ \tau_{1p}(\omega_p, \varphi_p) = \tau_{1m}(\omega_m, \varphi_m) \end{cases} \tag{3.88}$$

with $\delta \in \{0, 1, \ldots, q^\star\}$[6], $\sigma \in \{\pm\}$. To solve these equations numerically, we give the following algorithm:

[6] If $\delta = 0$ ($q^\star$), we have a pure *plus* (*minus*)−phase.

1. Let $\theta_{1p} = \theta_{1m} = \theta_{var}$ and $\tau_{1p} = \tau_{1m} = \tau_{var}$.

2. Inverse the last two equations in (3.88) implicitly, then we have

$$(\omega_p, \varphi_p) = (\omega_p(\theta_{var}, \tau_{var}), \varphi_p(\theta_{var}, \tau_{var})) \tag{3.89}$$

   and

$$(\omega_m, \varphi_m) = (\omega_m(\theta_{var}, \tau_{var}), \varphi_m(\theta_{var}, \tau_{var})). \tag{3.90}$$

3. Calculate $\theta_{ip}(\omega_p, \varphi_p)$, $\theta_{im}(\omega_p, \varphi_p)$, $i = 1, 2$. Cycle through θ_{var}, τ_{var}, and check the first two equations in (3.88) to be numerically accurate enough.

4. Check the conditions for the helical interface: $\theta_{1p}(\omega_p, \varphi_p) = \theta_{1m}(\omega_m, \varphi_m) \neq 0$ and $\tau_{1p}(\omega_p, \varphi_p) = \tau_{1m}(\omega_m, \varphi_m) \neq 0$.

We should notice that the group parameters depend on δ. Figure 3.10 is an example for $(p^\star, q^\star) = (10, 8)$, $\delta = 3$ and

$$\mathbf{p} = (2.177, 1.954, 7.172, 4.292). \tag{3.91}$$

The numerical solutions for the parameters are listed in Table 3.2.

Table 3.2: Parameters for helical interface with $\sigma = +$.

ω_p	φ_p	θ_{1p}	τ_{1p}	θ_{2p}	τ_{2p}
-0.282	0.247	0.749	-3.085	-0.149	3.861
ω_m	φ_m	θ_{1m}	τ_{1m}	θ_{2m}	τ_{2m}
-0.113	0.259	0.749	-3.085	-0.156	3.847

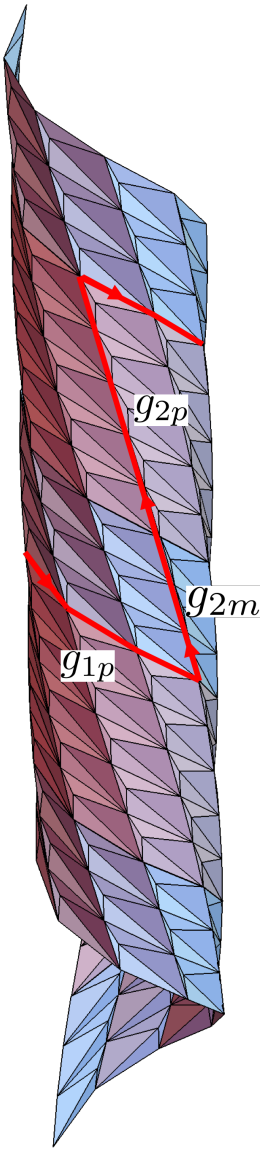

Figure 3.10: Helical interface

3.5.4 Vertical and elliptical interfaces

Vertical interface requires that one of rotation angles in group parameters vanishes. Without loss of generality, we assume that $\theta_{1p} = \theta_{1m} = 0$. For convenience, we eliminate p and m, and discuss in general, say, $\theta_1 = 0$. Then,

$$\frac{(\mathbf{u}_a - (\mathbf{e}_1 \cdot \mathbf{u}_a)\mathbf{e}_1) \cdot (\mathbf{u}_b - (\mathbf{e}_1 \cdot \mathbf{u}_b)\mathbf{e}_1))}{|\mathbf{u}_a|^2 - (\mathbf{u}_a \cdot \mathbf{e}_1)^2} = 1. \tag{3.92}$$

$\mathbf{R}_{\theta_1}\mathbf{u}_a = \mathbf{u}_b$ implies that $\mathbf{u}_a = \mathbf{u}_b$, which also follows by the equation above. We claim that, in this case, all the folding angles are zero, i.e., $\eta = \omega = \xi = 0$. We prove the conjecture by simple geometrical argument. Since $\mathbf{u}_a = \mathbf{u}_b$, we have that $\mathbf{y}_1, \mathbf{y}_2, \mathbf{y}_3, \mathbf{y}_4$ are on the same plane and form a parallelogram. The origin is out of the plane, otherwise, the folding angles are all zero. Now we assume the origin is out of the plane. Then the sum of neighbor angles in the deformed configuration is less or equal to the sum in the flat configuration. The equality only holds when all the folding angles are zero. This completes the proof. Then, in the vertical interface case, there is no difference between *plus*-phase and *minus*-phase, in other words, there is no phase transformation. The elliptical interface has no rational plane as shown in Chapter 2. Therefore, no elastic-free elliptical interfaces occur in helical Miura origami.

3.6 Engineering validation

The engineering validation is conducted by Frank Yu (a high school student in our group) and me, as a joint project of Wayzata Mentor Connection program[7] .

Our attempt was to create a model through 3D printing. In a collaboration with the Earl E. Bakken Medical Device Center 3D prototyping laboratory, we were able to utilize the Stratasys J750 3D printer, which is able to print using multiple materials. The rigid panels were printed out of acrylic compounds. The folding lines were created using a rubber-like photopolymer dubbed Agilus. Our approach was to create .stl (stereolithography) files directly from Wolfram Mathematica. Using various commands on the helical miura-ori 3D graphics, we created one frame composed of cylinders for the

[7]The project review [82] was submitted to *Scholars of Distinction: Mathematics Program* and Frank has been recognized as a Scholar of Distinction in Mathematics.

Agilus and one file for the Acrylic panels (Figure 3.11 (b)). Using Meshmixer (software that combines .stl files), we combined the two .stl files to create a single model (Figure 3.11 (c). Then we printed out the model by Stratasys J750 as depicted in Figure 3.11 (a). The 3D printed model was proved to be a compatible helical origami as we expected. However, the mechanical property (mechanism of transformation) had shown the limitation of these materials: we were not able to transform the model by simple twist. We need to investigate more on the materials we should use in the future.

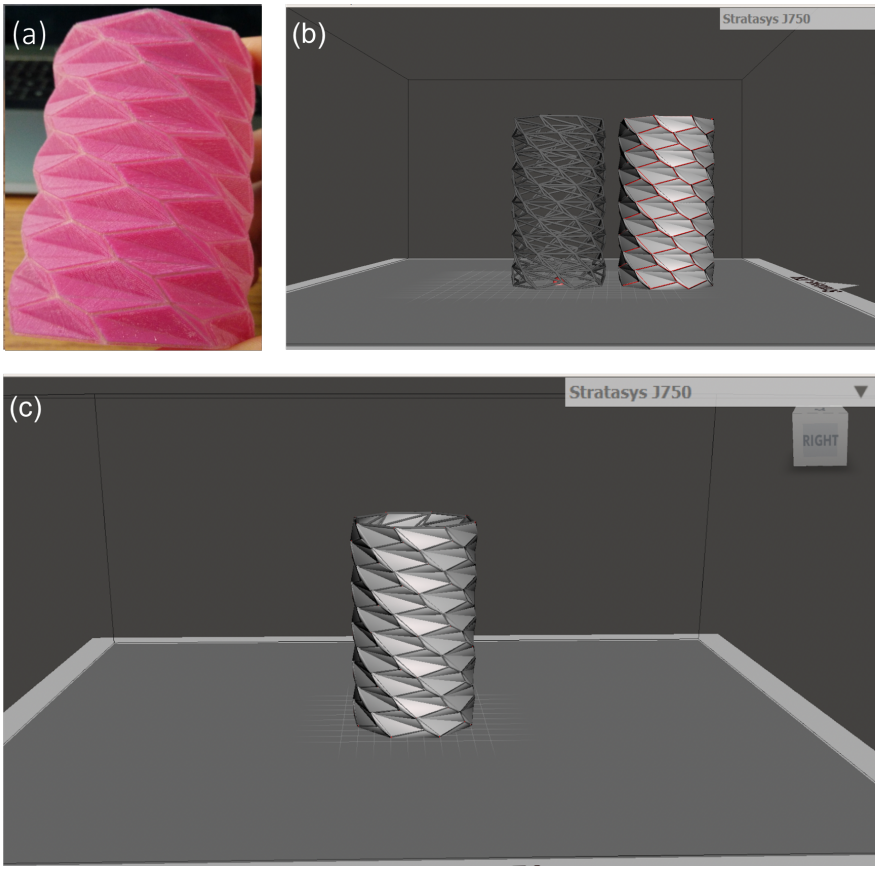

Figure 3.11: Prototype with 3D printing. (a) Stratasys J750 3D printed model. (b) Flexible frame (left) and rigid plates (right). Merging process in Meshmixer. (c) Fully combined structure of flexible frame and rigid plate.

Chapter 4

Conclusions and future work

4.1 Conclusions

In this work, we have developed a martensitic phase transformation theory for helical structures and demonstrated the helical Miura origami as one of its applications. We have achieved the full solution of compatible interfaces − horizontal, vertical, helical and elliptical interfaces − between two different helical structures. Using the theory for examples, the HMO can exhibit twist and extension during the phase transformation between its variants.

In Chapter 2, using nearest neighbor generators, we regenerate the same helical group and apply the rank-one compatibility condition. We have proposed the local compatibility problem in helical structures.The strategy for solving this problem is to divide it into two situations − zero curvature and non-trivial curvature, in a local interval. The results show that zero curvature case corresponds to the horizontal, vertical and helical interface, while non-trivial curvature corresponds to the elliptical interface, depending on group parameters. The conditions on parameters are summarized in Table 2.1, which are analog to $\lambda_2 = 1$ in lattice. We also conjecture that there are microstructures and related "cofactor conditions" in helical structures. These are ongoing work.

In Chapter 3, we have constructed closed helical Miura-ori by using some appropriate group generators applying on partially folded four-fold Miura parallelogram. The kinematics of the fold-fold node is derived mathematically. The result shows that there are two solutions for the same regular reference domain. These two solutions are defined

as variants in our context. Even though the closed HMO is proved to be rigid in our computational domain, we can achieve overall twist and extension by transforming one variant to the other. The compatible interface between these two variants could be a horizontal or a helical interface.

4.2 Future work

We end up the thesis with potential future directions related to isometry groups, objective structures, and origami.

1. **Theory of microstructures in helical structures**. At the end of Chapter 2, we give some examples of microstructures in helical structures. However, a rigorous theory is still needed. Inspired by a lot work about microstructure in lattice using Γ-convergence and Young measure [83, 84, 85, 86], we can develop theory in helical structure and find minimizing sequence with specific boundary conditions.

2. **Non-discrete isometry groups**. A discrete objective structure is generated by applying the corresponding discrete isometry group on some set of points. If the isometry group is non-discrete, the resulting structure can be proved "locally objective" by cutting off the powers of group generators. Indeed, some structures of viruses could be simulated in this way [87, 88, 89, 90]. Here "locally objective" means some atoms see the same local environment, even though the global environments are different.

3. **Objective origami using general four-fold node**. For a four-fold node, we can relax the condition that the opposite sector angles sum to π. The kinematics has been done in [63]. So it is possible to construct objective origami using this general four-fold node. This gives us more freedom and the rigidity of the structure needs more exploration.

4. **Non-isometric origami**. Many active materials, such as liquid crystal elastomer [91, 92, 93], shape memory polymer [94] etc., can exhibit stretch under some specific stimuli. Then the kinematics of these materials regrading origami design should be generalized.

Bibliography

[1] G. Jaeger, "The ehrenfest classification of phase transitions: Introduction and evolution," *Archive for History of Exact Sciences*, vol. 53, pp. 51–81, May 1998.

[2] L. D. Landau and E. M. Lifshitz, *Course of theoretical physics. vol. 5 : Statistical physics.* Pergamon: London, 1951.

[3] X. Chen, *The Influence of Compatibility Conditions on the Microstructure at Phase Transformation.* PhD thesis, University of Minnesota, Minneapolis, 2013.

[4] J. Cui, Y. S. Chu, O. O. Famodu, Y. Furuya, J. Hattrick-Simpers, R. D. James, A. Ludwig, S. Thienhaus, M. Wuttig, Z. Zhang, *et al.*, "Combinatorial search of thermoelastic shape-memory alloys with extremely small hysteresis width," *Nature materials*, vol. 5, no. 4, p. 286, 2006.

[5] R. D. James and K. F. Hane, "Martensitic transformations and shape-memory materials," *Acta Materialia*, vol. 48, pp. 197–222, Jan. 2000.

[6] K. F. Hane and T. W. Shield, "Microstructure in the cubic to monoclinic transition in titanium–nickel shape memory alloys," *Acta Materialia*, vol. 47, no. 9, pp. 2603 – 2617, 1999.

[7] V. Srivastava, X. Chen, and R. D. James, "Hysteresis and unusual magnetic properties in the singular heusler alloy ni45co5mn40sn10," *Applied Physics Letters*, vol. 97, no. 1, p. 014101, 2010.

[8] V. Srivastava, Y. Song, K. Bhatti, and R. D. James, "The direct conversion of heat to electricity using multiferroic alloys," *Advanced Energy Materials*, vol. 1, no. 1, pp. 97–104, 2011.

[9] Y. Song, K. P. Bhatti, V. Srivastava, C. Leighton, and R. D. James, "Thermodynamics of energy conversion via first order phase transformation in low hysteresis magnetic materials," *Energy & Environmental Science*, vol. 6, no. 4, pp. 1315–1327, 2013.

[10] A. Roitburd and G. Kurdjumov, "The nature of martensitic transformations," *Materials Science and Engineering*, vol. 39, no. 2, pp. 141 – 167, 1979.

[11] B. E. Warren, *X-ray Diffraction*. Courier Corporation, 1969.

[12] H. P. Klug and L. E. Alexander, "X-ray diffraction procedures: for polycrystalline and amorphous materials," *X-Ray Diffraction Procedures: For Polycrystalline and Amorphous Materials, 2nd Edition, by Harold P. Klug, Leroy E. Alexander, pp. 992. ISBN 0-471-49369-4. Wiley-VCH, May 1974.*, p. 992, 1974.

[13] R. D. James, "Objective structures," *Journal of the Mechanics and Physics of Solids*, vol. 54, pp. 2354–2390, Nov. 2006.

[14] W. Falk and R. D. James, "Elasticity theory for self-assembled protein lattices with application to the martensitic phase transition in bacteriophage T4 tail sheath," *Phys. Rev. E*, vol. 73, p. 011917, Jan. 2006.

[15] T. Dumitrică and R. D. James, "Objective molecular dynamics," *Journal of the Mechanics and Physics of Solids*, vol. 55, pp. 2206–2236, Oct. 2007.

[16] K. Dayal and R. D. James, "Nonequilibrium molecular dynamics for bulk materials and nanostructures," *Journal of the Mechanics and Physics of Solids*, vol. 58, pp. 145–163, Feb. 2010.

[17] K. Dayal and R. D. James, "Design of viscometers corresponding to a universal molecular simulation method," *Journal of Fluid Mechanics*, vol. 691, pp. 461–486, 2012.

[18] D. Justel, G. Friesecke, and R. D. James, "Bragg-von Laue diffraction generalized to twisted X-rays," *Acta Crystallographica Section A*, vol. 72, no. 2, pp. 190–196, 2016.

[19] G. Friesecke, R. James, and D. Jüstel, "Twisted x-rays: Incoming waveforms yielding discrete diffraction patterns for helical structures," *SIAM Journal on Applied Mathematics*, vol. 76, no. 3, pp. 1191–1218, 2016.

[20] A. S. Banerjee, *Density Functional Methods for Objective Structures: Theory and Simulation Schemes*. PhD thesis, University of Minnesota, Minneapolis, 2013.

[21] A. S. Banerjee, R. S. Elliott, and R. D. James, "A spectral scheme for Kohn–Sham density functional theory of clusters," *Journal of Computational Physics*, vol. 287, pp. 226–253, Apr. 2015.

[22] A. S. Banerjee and P. Suryanarayana, "Cyclic density functional theory: A route to the first principles simulation of bending in nanostructures," *Journal of the Mechanics and Physics of Solids*, vol. 96, pp. 605–631, 2016.

[23] A. S. Banerjee, L. Lin, W. Hu, C. Yang, and J. E. Pask, "Chebyshev polynomial filtered subspace iteration in the discontinuous galerkin method for large-scale electronic structure calculations," *The Journal of Chemical Physics*, vol. 145, no. 15, p. 154101, 2016.

[24] N. C. Darnton and H. C. Berg, "Force-extension measurements on bacterial flagella: Triggering polymorphic transformations," *Biophysical Journal*, vol. 92, pp. 2230–2236, 03 2007.

[25] A. B. Kolomeisky, "How viruses enter cells: A story behind bacteriophage t4," *Biophysical Journal*, vol. 113, pp. 4–5, 2018/06/22 2017.

[26] C. S. Haines, M. D. Lima, N. Li, G. M. Spinks, J. Foroughi, J. D. W. Madden, S. H. Kim, S. Fang, M. Jung de Andrade, F. Göktepe, Ö. Göktepe, S. M. Mirvakili, S. Naficy, X. Lepró, J. Oh, M. E. Kozlov, S. J. Kim, X. Xu, B. J. Swedlove, G. G. Wallace, and R. H. Baughman, "Artificial Muscles from Fishing Line and Sewing Thread," *Science*, vol. 343, pp. 868–872, Feb. 2014.

[27] X. Liu, S. Yao, S. V. Georgakopoulos, B. S. Cook, and M. M. Tentzeris, "Reconfigurable helical antenna based on an origami structure for wireless communication system," in *2014 IEEE MTT-S International Microwave Symposium (IMS2014)*, pp. 1–4, June 2014.

[28] J. L. Ericksen, "On the symmetry and stability of thermoelastic solids," *Journal of Applied Mechanics*, vol. 45, pp. 740–744, 12 1978.

[29] R. L. Fosdick and B. Hertog, "Material Symmetry and Crystals," in *Mechanics and Thermodynamics of Continua: A Collection of Papers Dedicated to B.D. Coleman on His Sixtieth Birthday* (H. Markovitz, V. J. Mizel, and D. R. Owen, eds.), pp. 395–424, Berlin, Heidelberg: Springer Berlin Heidelberg, 1991.

[30] J. M. Ball and R. D. James, "Proposed Experimental Tests of a Theory of Fine Microstructure and the Two-Well Problem," *Philosophical Transactions of the Royal Society of London A: Mathematical, Physical and Engineering Sciences*, vol. 338, pp. 389–450, Feb. 1992.

[31] W. E and P. Ming, "Cauchy–Born Rule and the Stability of Crystalline Solids: Static Problems," *Archive for Rational Mechanics and Analysis*, vol. 183, no. 2, pp. 241–297, 2007.

[32] M. Arroyo and T. Belytschko, "Finite crystal elasticity of carbon nanotubes based on the exponential Cauchy-Born rule," *Phys. Rev. B*, vol. 69, p. 115415, Mar. 2004.

[33] G. Zanzotto, "The Cauchy-Born hypothesis, nonlinear elasticity and mechanical twinning in crystals," *Acta Crystallographica Section A: Foundations of Crystallography*, vol. 52, pp. 839–849, Nov. 1996.

[34] G. Friesecke and R. D. James, "A scheme for the passage from atomic to continuum theory for thin films, nanotubes and nanorods," *Journal of the Mechanics and Physics of Solids*, vol. 48, pp. 1519–1540, June 2000.

[35] J. Z. Yang and W. E, "Generalized cauchy-born rules for elastic deformation of sheets, plates, and rods: Derivation of continuum models from atomistic models," *Phys. Rev. B*, vol. 74, p. 184110, Nov 2006.

[36] K. Bhattacharya, *Microstructure of martensite : why it forms and how it gives rise to the shape-memory effect*. Oxford: Oxford University Press, 2003.

[37] K. Dayal, R. Elliott, and R. D. James, "Objective formulas," 2018. Preprint.

[38] F. Feng, P. Plucinsky, and R. D. James, "Compatibility of phases in helical structures," *ArXiv e-prints*, Sept. 2018.

[39] Y. Ganor, T. Dumitrică, F. Feng, and R. D. James, "Zig-zag twins and helical phase transformations," *Phil. Trans. R. Soc. A*, vol. 374, no. 2066, p. 20150208, 2016.

[40] M. F. Moody, "Structure of the sheath of bacteriophage t4: I. structure of the contracted sheath and polysheath," *Journal of molecular biology*, vol. 25, no. 2, pp. 167–200, 1967.

[41] M. F. Moody, "Sheath of bacteriophage t4: Iii. contraction mechanism deduced from partially contracted sheaths," *Journal of molecular biology*, vol. 80, no. 4, pp. 613–635, 1973.

[42] G. B. Olson and H. Hartman, "Martensite and life: displacive transformations as biological processes," *Le Journal de Physique Colloques*, vol. 43, no. C4, pp. C4–855, 1982.

[43] F. Arisaka, J. Engel, and H. Klump, "Contraction and dissociation of the bacteriophage T4 tail sheath induced by heat and urea," *Progress in clinical and biological research*, vol. 64, pp. 365–379, 1981.

[44] S. Asakura, "Polymerization of flagellin and polymorphism of flagella.," *Advances in biophysics*, vol. 1, p. 99, 1970.

[45] C. R. Calladine, "Construction of bacterial flagella," *Nature*, vol. 255, no. 5504, p. 121, 1975.

[46] K. Yonekura, S. Maki-Yonekura, and K. Namba, "Complete atomic model of the bacterial flagellar filament by electron cryomicroscopy," *Nature*, vol. 424, no. 6949, p. 643, 2003.

[47] R. K. Komai, "Chirality switching by martensitic transformation in protein cylindrical crystals: Application to bacterial flagella," *Doctoral dissertation*, Aug. 2015.

[48] J. Zhou, N. Li, F. Gao, Y. Zhao, L. Hou, and Z. Xu, "Vertically-aligned BCN nanotube arrays with superior performance in electrochemical capacitors," *Scientific reports*, vol. 4, p. 6083, 2014.

[49] J. Goldberger, R. He, Y. Zhang, S. Lee, H. Yan, H.-J. Choi, and P. Yang, "Single-crystal gallium nitride nanotubes," *Nature*, vol. 422, no. 6932, p. 599, 2003.

[50] B. Radisavljevic, A. Radenovic, J. Brivio, I. V. Giacometti, and A. Kis, "Single-layer MoS_2 transistors," *Nature nanotechnology*, vol. 6, no. 3, p. 147, 2011.

[51] D.-B. Zhang, T. Dumitrică, and G. Seifert, "Helical nanotube structures of mos_2 with intrinsic twisting: an objective molecular dynamics study," *Physical review letters*, vol. 104, no. 6, p. 065502, 2010.

[52] A. S. Banerjee and P. Suryanarayana, "Ab initio framework for simulating systems with helical symmetry: formulation, implementation and applications to torsional deformations in nanostructures." preprint, 2018.

[53] J. M. Ball and R. D. James, "Fine phase mixtures as minimizers of energy," *Archive for Rational Mechanics and Analysis*, vol. 100, no. 1, pp. 13–52, 1987.

[54] R. D. James, "Taming the temperamental metal transformation," *Science*, vol. 348, pp. 968–969, May 2015.

[55] Y. Song, X. Chen, V. Dabade, T. W. Shield, and R. D. James, "Enhanced reversibility and unusual microstructure of a phase-transforming material," *Nature*, vol. 502, pp. 85–88, Oct. 2013.

[56] K. Bhattacharya, "Self-accommodation in martensite," *Archive for Rational Mechanics and Analysis*, vol. 120, no. 3, pp. 201–244, 1992.

[57] Y. Ganor, T. Dumitrică, F. Feng, and R. D. James, "Zig-zag twins and helical phase transformations," *Phil. Trans. R. Soc. A*, vol. 374, Mar. 2016.

[58] X. Chen, V. Srivastava, V. Dabade, and R. D. James, "Study of the cofactor conditions: Conditions of supercompatibility between phases," *Journal of the Mechanics and Physics of Solids*, vol. 61, pp. 2566–2587, Dec. 2013.

[59] H. Gu, L. Bumke, C. Chluba, E. Quandt, and R. D. James, "Phase engineering and supercompatibility of shape memory alloys," *Materials Today*, 2017.

[60] Y.-J. He and Q.-P. Sun, "Scaling relationship on macroscopic helical domains in NiTi tubes," *International Journal of Solids and Structures*, vol. 46, no. 24, pp. 4242–4251, 2009.

[61] M. Pitteri and G. Zanzotto, *Continuum models for phase transitions and twinning in crystals*. CRC Press, 2002.

[62] F. Feng, P. Plucinsky, and R. D. James, "Phase-transforming helical miura origami," *preprint*.

[63] P. Plucinsky, F. Feng, and R. D. James, "The design and deformations of generalized miura origami," *preprint*.

[64] R. J. Lang, "A computational algorithm for origami design," in *Proceedings of the Twelfth Annual Symposium on Computational Geometry*, SCG '96, (New York, NY, USA), pp. 98–105, ACM, 1996.

[65] J. C. Bowers and I. Streinu, "Lang's universal molecule algorithm," *Annals of Mathematics and Artificial Intelligence*, vol. 74, no. 3-4, pp. 371–400, 2015.

[66] T. Tachi, "Generalization of rigid foldable quadrilateral mesh origami," in *Symposium of the International Association for Shell and Spatial Structures (50th. 2009. Valencia). Evolution and Trends in Design, Analysis and Construction of Shell and Spatial Structures: Proceedings*, Editorial Universitat Politècnica de València, 2009.

[67] L. Wilson, S. Pellegrino, and R. Danner, "Origami sunshield concepts for space telescopes," in *54th AIAA/ASME/ASCE/AHS/ASC Structures, Structural Dynamics, and Materials Conference*, p. 1594, 2013.

[68] P. M. Reis, F. L. Jiménez, and J. Marthelot, "Transforming architectures inspired by origami," *Proceedings of the National Academy of Sciences*, vol. 112, no. 40, pp. 12234–12235, 2015.

[69] S. Waitukaitis, R. Menaut, B. G.-g. Chen, and M. van Hecke, "Origami multistability: From single vertices to metasheets," *Physical review letters*, vol. 114, no. 5, p. 055503, 2015.

[70] S. Waitukaitis and M. van Hecke, "Origami building blocks: Generic and special four-vertices," *Physical Review E*, vol. 93, no. 2, p. 023003, 2016.

[71] B. G.-g. Chen, B. Liu, A. A. Evans, J. Paulose, I. Cohen, V. Vitelli, and C. Santangelo, "Topological mechanics of origami and kirigami," *Physical review letters*, vol. 116, no. 13, p. 135501, 2016.

[72] J. A. Faber, A. F. Arrieta, and A. R. Studart, "Bioinspired spring origami," *Science*, vol. 359, no. 6382, pp. 1386–1391, 2018.

[73] M. Schenk and S. D. Guest, "Geometry of miura-folded metamaterials," *Proceedings of the National Academy of Sciences*, vol. 110, no. 9, pp. 3276–3281, 2013.

[74] H. Yasuda and J. Yang, "Reentrant origami-based metamaterials with negative poisson's ratio and bistability," *Physical review letters*, vol. 114, no. 18, p. 185502, 2015.

[75] J. L. Silverberg, A. A. Evans, L. McLeod, R. C. Hayward, T. Hull, C. D. Santangelo, and I. Cohen, "Using origami design principles to fold reprogrammable mechanical metamaterials," *science*, vol. 345, no. 6197, pp. 647–650, 2014.

[76] Z. Y. Wei, Z. V. Guo, L. Dudte, H. Y. Liang, and L. Mahadevan, "Geometric mechanics of periodic pleated origami," *Physical review letters*, vol. 110, no. 21, p. 215501, 2013.

[77] L. H. Dudte, E. Vouga, T. Tachi, and L. Mahadevan, "Programming curvature using origami tessellations," *Nature materials*, vol. 15, no. 5, p. 583, 2016.

[78] R. J. Lang and L. Howell, "Rigidly foldable quadrilateral meshes from angle arrays," *Journal of Mechanisms and Robotics*, vol. 10, pp. 021004–021004–11, 02 2018.

[79] F. Bös, M. Wardetzky, E. Vouga, and O. Gottesman, "On the Incompressibility of Cylindrical Origami Patterns," *Journal of Mechanical Design*, vol. 139, pp. 021404–021404–9, Dec. 2016.

[80] S. Miyashita, S. Guitron, S. Li, and D. Rus, "Robotic metamorphosis by origami exoskeletons," *Science Robotics*, vol. 2, no. 10, 2017.

[81] X. Liu, S. Yao, B. S. Cook, M. M. Tentzeris, and S. V. Georgakopoulos, "An origami reconfigurable axial-mode bifilar helical antenna," *IEEE Transactions on Antennas and Propagation*, vol. 63, pp. 5897–5903, Dec 2015.

[82] F. Yu, "Design and prototype of helical miura origami," 2018.

[83] R. V. Kohn and S. Müller, "Branching of twins near an austenite—twinned-martensite interface," *Philosophical Magazine A*, vol. 66, no. 5, pp. 697–715, 1992.

[84] E. De Giorgi and G. Dal Maso, "γ—convergence and calculus of variations," in *Mathematical theories of optimization*, pp. 121–143, Springer, 1983.

[85] H. Knüpfer, R. V. Kohn, and F. Otto, "Nucleation barriers for the cubic-to-tetragonal phase transformation," *Communications on pure and applied mathematics*, vol. 66, no. 6, pp. 867–904, 2013.

[86] S. Müller, "Variational models for microstructure and phase transitions," in *Calculus of variations and geometric evolution problems*, pp. 85–210, Springer, 1999.

[87] J. Patera and R. Twarock, "Affine extension of noncrystallographic coxeter groups and quasicrystals," *Journal of Physics A: Mathematical and General*, vol. 35, no. 7, p. 1551, 2002.

[88] T. Keef, J. P. Wardman, N. A. Ranson, P. G. Stockley, and R. Twarock, "Structural constraints on the three-dimensional geometry of simple viruses: case studies of a new predictive tool," *Acta Crystallographica Section A: Foundations of Crystallography*, vol. 69, no. 2, pp. 140–150, 2013.

[89] E. R. May, J. Feng, and C. L. Brooks III, "Exploring the symmetry and mechanism of virus capsid maturation via an ensemble of pathways," *Biophysical journal*, vol. 102, no. 3, pp. 606–612, 2012.

[90] P.-P. Dechant, J. Wardman, T. Keef, and R. Twarock, "Viruses and fullerenes–symmetry as a common thread?," *Acta Crystallographica Section A: Foundations and Advances*, vol. 70, no. 2, pp. 162–167, 2014.

[91] P. Cesana, P. Plucinsky, and K. Bhattacharya, "Effective Behavior of Nematic Elastomer Membranes," *Archive for Rational Mechanics and Analysis*, vol. 218, pp. 863–905, Nov. 2015.

[92] P. Plucinsky, M. Lemm, and K. Bhattacharya, "Programming complex shapes in thin nematic elastomer and glass sheets," *Phys. Rev. E*, vol. 94, p. 010701, Jul 2016.

[93] P. Plucinsky, M. Lemm, and K. Bhattacharya, "Actuation of Thin Nematic Elastomer Sheets with Controlled Heterogeneity," *Archive for Rational Mechanics and Analysis*, vol. 227, pp. 149–214, Jan. 2018.

[94] Y. Liu, B. Shaw, M. D. Dickey, and J. Genzer, "Sequential self-folding of polymer sheets," *Science Advances*, vol. 3, no. 3, p. e1602417, 2017.

[95] I. M. Niven, *Diophantine approximations*. Courier Corporation, 2008.

Appendix A

Appendix for Chapter 2

A.1 Proof of Theorem 2.5.2: The elliptical interface

In this case, the interface has curvature (i.e., $\kappa(s) \neq 0$ on $(\tilde{s}_1, \tilde{s}_2)$). Making use of this fact, we will arrive at some very strong conditions on the parameters—these are entirely distinct from the conditions in the preceding derivations. It is quite a lot of work to rigorously deduce that all these conditions are necessary. Consequently, this proof is long. For clarity, we break it up into several succinct steps.

Proof of Theorem 2.5.2. (*Step 1: A rewriting of local compatibility in this case.*) Since the interface has curvature, we have that

$$\mathbf{e}_a \times \mathbf{e}_b \neq 0 \quad \text{(by Lemma 2.4.1).} \tag{A.1}$$

That is, the helices of the two phases do not share the same axis. In particular, the set $\{\mathbf{e}_a \times \mathbf{e}_b, \mathbf{e}_a, \mathbf{e}_b\}$ forms a basis of $\mathbb{R}^3$. Consequently, we solve the compatibility conditions (2.37) on the interval $(\tilde{s}_1, \tilde{s}_2)$ if and only if

$$\begin{cases} \Big((\mathbf{e}_a \times \mathbf{e}_b) \cdot \mathbf{Q}^a(\mathbf{x}(s) \cdot \mathbf{f}_a)\mathbf{r}_a\Big)' = \Big((\mathbf{e}_a \times \mathbf{e}_b) \cdot \mathbf{Q}^b(\mathbf{x}(s) \cdot \mathbf{f}_b)\mathbf{r}_b\Big)' \\ (\mathbf{x}(s) \cdot \mathbf{g}_a)' = \Big(\mathbf{e}_a \cdot \mathbf{Q}^b(\mathbf{x}(s) \cdot \mathbf{f}_b)\mathbf{r}_b + (\mathbf{e}_a \cdot \mathbf{e}_b)(\mathbf{x}(s) \cdot \mathbf{g}_b)\Big)' \\ \Big(\mathbf{e}_b \cdot \mathbf{Q}^a(\mathbf{x}(s) \cdot \mathbf{f}_a)\mathbf{r}_a) + (\mathbf{x}(s) \cdot \mathbf{g}_a)(\mathbf{e}_a \cdot \mathbf{e}_b)\Big)' = (\mathbf{x}(s) \cdot \mathbf{g}_b)' \end{cases} \tag{A.2}$$

on this interval (i.e., by dotting the compatibility equation with the $\{\mathbf{e}_a \times \mathbf{e}_b, \mathbf{e}_a, \mathbf{e}_b\}$

basis). Here, we have made use of the definitions: $\mathbf{r}_{a,b} \cdot \mathbf{e}_{a,b} = 0$ and $\mathbf{Q}^{a,b}(\cdot)\mathbf{e}_{a,b} = \mathbf{e}_{a,b}$.

The first of these equations can be rewritten in a more revealing way. Indeed, we observe that

$$\begin{aligned}(\mathbf{e}_a \times \mathbf{e}_b) \cdot \mathbf{Q}^a(\mathbf{x}(s) \cdot \mathbf{f}_a)\mathbf{r}_a &= \Big(\mathbf{e}_a \times \mathbf{Q}^a(\mathbf{x}(s) \cdot \mathbf{f}_a)^T \mathbf{e}_b\Big) \cdot \mathbf{r}_a \\ &= \Big(\mathbf{r}_a \times \mathbf{e}_a\Big) \cdot \mathbf{Q}^a(\mathbf{x}(s) \cdot \mathbf{f}_a)^T \mathbf{e}_b = -\mathbf{e}_b \cdot \mathbf{Q}^a(\mathbf{x}(s) \cdot \mathbf{f}_a)\mathbf{W}^a \mathbf{r}_a,\end{aligned} \tag{A.3}$$

using[1] properties of the cross-product, and the fact that $\{\mathbf{r}_a/|\mathbf{r}_a|, \mathbf{W}^a\mathbf{r}_a/|\mathbf{r}_a|, \mathbf{e}_a\}$ forms a right-hand orthonormal basis. By an analogous argument,

$$(\mathbf{e}_a \times \mathbf{e}_b) \cdot \mathbf{Q}^b(\mathbf{x}(s) \cdot \mathbf{f}_b)\mathbf{r}_b = \mathbf{e}_a \cdot \mathbf{Q}^b(\mathbf{x}(s) \cdot \mathbf{f}_b)\mathbf{W}^b \mathbf{r}_b. \tag{A.4}$$

Thus, given (A.3) and (A.4), we see that the first equation in (A.2) is equivalent to

$$\mathbf{e}_b \cdot \mathbf{Q}^a(\mathbf{x}(s) \cdot \mathbf{f}_a)\mathbf{W}^a \mathbf{r}_a + \mathbf{e}_a \cdot \mathbf{Q}^b(\mathbf{x}(s) \cdot \mathbf{f}_b)\mathbf{W}^b \mathbf{r}_b = c_0, \tag{A.5}$$

for $s \in (\tilde{s}_1, \tilde{s}_2)$ for some constant $c_0 \in \mathbb{R}$ (i.e., by integrating this equation). Further, by explicitly differentiating the other two equations in (A.2), we arrive at

$$\begin{aligned}(\mathbf{t}(s) \cdot \mathbf{f}_b)\Big(\mathbf{e}_a \cdot \mathbf{Q}^b(\mathbf{x}(s) \cdot \mathbf{f}_b)\mathbf{W}^b \mathbf{r}_b\Big) &= (\mathbf{t}(s) \cdot \mathbf{g}_a) - (\mathbf{e}_a \cdot \mathbf{e}_b)(\mathbf{t}(s) \cdot \mathbf{g}_b), \\ (\mathbf{t}(s) \cdot \mathbf{f}_a)\Big(\mathbf{e}_b \cdot \mathbf{Q}^a(\mathbf{x}(s) \cdot \mathbf{f}_a)\mathbf{W}^a \mathbf{r}_a\Big) &= (\mathbf{t}(s) \cdot \mathbf{g}_b) - (\mathbf{e}_a \cdot \mathbf{e}_b)(\mathbf{t}(s) \cdot \mathbf{g}_a),\end{aligned} \tag{A.6}$$

and these must hold for all $s \in (\tilde{s}_1, \tilde{s}_2)$.

(*Step 2: A necessary condition on the parameters.*) The set of equations in (A.5) and (A.6) is equivalent to the set in (A.2). That is, they are equivalent to solving the compatibility equation (2.37) on the interval $(\tilde{s}_1, \tilde{s}_2)$. The important point in this manipulation is that it reveals the terms $\mathbf{e}_{b,a} \cdot \mathbf{Q}^{a,b}(\mathbf{x}(s) \cdot \mathbf{f}_{a,b})\mathbf{W}^{a,b}\mathbf{r}_{a,b}$. These can be substituted for to yield a *non-trivial*[2] necessary condition that is absent the rotations $\mathbf{Q}^{a,b}(\cdot)$. In particular, since $\mathbf{t}(s) \neq const$ on $(\tilde{s}_1, \tilde{s}_2)$ by the hypotheses of this case and

[1] in addition to the oft used identity $\mathbf{Q}^{a,b}(\cdot)\mathbf{e}_{a,b} = \mathbf{e}_{a,b}$

[2] There are less involved ways to arrive at necessary conditions which do not involve the rotations, but these *easier* ways did not turn out to be very useful.

$|\mathbf{f}_{a,b}| \neq 0$, we have that

$$\exists\ (\bar{s}_1, \bar{s}_2) \subset (\tilde{s}_1, \tilde{s}_2) \quad \text{s.t.} \quad (\mathbf{t}(s) \cdot \mathbf{f}_a) \neq 0,\ \ (\mathbf{t}(s) \cdot \mathbf{f}_b) \neq 0,\ \ \mathbf{t}(s) \neq \pm\mathbf{e}_2, \quad \text{on } (\bar{s}_1, \bar{s}_2). \tag{A.7}$$

Hence, on this interval, we can divide through by $(\mathbf{t}(s) \cdot \mathbf{f}_{a,b})$ in the equations in (A.6) and then substitute these relations into (A.5). In doing this, we arrive at the necessary condition

$$\frac{(\mathbf{t}(s) \cdot \mathbf{g}_b) - (\mathbf{e}_a \cdot \mathbf{e}_b)(\mathbf{t}(s) \cdot \mathbf{g}_a)}{(\mathbf{t}(s) \cdot \mathbf{f}_a)} + \frac{(\mathbf{t}(s) \cdot \mathbf{g}_a) - (\mathbf{e}_a \cdot \mathbf{e}_b)(\mathbf{t}(s) \cdot \mathbf{g}_b)}{(\mathbf{t}(s) \cdot \mathbf{f}_b)} = c_0, \tag{A.8}$$

which must hold on the interval $(\bar{s}_1, \bar{s}_2)$. After some algebraic manipulation, this can be written in the more revealing form:

$$\mathbf{t}(s) \cdot \Big(\mathbf{f}_b \otimes \mathbf{g}_b + \mathbf{f}_a \otimes \mathbf{g}_a - (\mathbf{e}_a \cdot \mathbf{e}_b)(\mathbf{f}_b \otimes \mathbf{g}_a + \mathbf{f}_a \otimes \mathbf{g}_b) - c_0(\mathbf{f}_a \otimes \mathbf{f}_b)\Big)\mathbf{t}(s) = 0. \tag{A.9}$$

Now, since (A.9) must hold on the interval $(\bar{s}_1, \bar{s}_2)$, it follows that the parameters *must* satisfy

$$\mathrm{sym}\Big(\mathbf{f}_b \otimes \mathbf{g}_b + \mathbf{f}_a \otimes \mathbf{g}_a - (\mathbf{e}_a \cdot \mathbf{e}_b)(\mathbf{f}_b \otimes \mathbf{g}_a + \mathbf{f}_a \otimes \mathbf{g}_b) - c_0(\mathbf{f}_a \otimes \mathbf{f}_b)\Big) = 0, \tag{A.10}$$

where $\mathrm{sym}(\mathbf{A}) = \frac{1}{2}(\mathbf{A} + \mathbf{A}^T)$. Indeed, since $\mathbf{t}(s) \neq \pm\mathbf{e}_2$ for any s on this interval, we may write $\mathbf{t}(s) = \hat{p}'(s)(1, \lambda(s))$ for $\lambda(s) = \hat{q}'(s)/\hat{p}'(s)$. In substituting this into (A.9) and dividing through by $\hat{p}'(s) \neq 0$, we obtain a quadratic equation in $\lambda(s)$. Moreover, since $\mathbf{t}(s) \neq \mathit{const}$ on this interval, $\lambda(s) \neq \mathit{const}$ on this interval. Consequently, this quadratic equation is solved if and only if the coefficients are all zero. Finally, these coefficients are zero if an only if (A.10) holds.

(*Step 3:* $\mathbf{f}_a = \pm\mathbf{f}_b$ *and* $c_0 = 0$.) The equation in (A.10) is a necessary condition which depends only on the parameters of the helices. That is, it does not depend on the explicit form of the interface[3]. We now show that this is an *exceptionally restrictive* condition on these parameters. In this direction, it turns out to be very useful to derive a necessary condition that is absent the constant c_0 in this tensor. To do this, we

[3]it is arrived at only using the fact that the interface has curvature

contract this tensor by dotting it on both sides with $\mathbf{f}_b^{\perp} = -(\mathbf{f}_b \cdot \mathbf{e}_2)\mathbf{e}_1 + (\mathbf{f}_b \cdot \mathbf{e}_1)\mathbf{e}_2$. We obtain the necessary condition

$$(\mathbf{f}_b^{\perp} \cdot \mathbf{f}_a)\Big(\mathbf{f}_b^{\perp} \cdot \big(\mathbf{g}_a - (\mathbf{e}_a \cdot \mathbf{e}_b)\mathbf{g}_b\big)\Big) = 0. \tag{A.11}$$

This condition holds if and only if:

(a) $\mathbf{f}_b$ is parallel to $\mathbf{f}_a$ (i.e., the parameter $\mathbf{f}_a = \delta \mathbf{f}_b$ for some $\delta \in \mathbb{R}$);

(b) $\mathbf{f}_b$ is parallel to $\mathbf{g}_a - (\mathbf{e}_a \cdot \mathbf{e}_b)\mathbf{g}_b$ (i.e., the parameter $\mathbf{g}_a - (\mathbf{e}_a \cdot \mathbf{e}_b)\mathbf{g}_b = \delta \mathbf{f}_b$ for some $\delta \in \mathbb{R}$).

Let us focus first on the latter case (i.e., (b)). We claim that this is not actually a case at all. It contradicts the fact that the interface has curvature $\kappa(s) \neq 0$. Indeed, we suppose (b), and so $\mathbf{g}_a - (\mathbf{e}_a \cdot \mathbf{e}_b)\mathbf{g}_b = \delta \mathbf{f}_b$ for some $\delta \in \mathbb{R}$. We substitute this into the necessary condition in (A.6) to conclude that the equation

$$(\mathbf{t}(s) \cdot \mathbf{f}_b)\Big(\mathbf{e}_a \cdot \mathbf{Q}^b(\mathbf{x}(s) \cdot \mathbf{f}_b)\mathbf{W}^b \mathbf{r}_b\Big) = \delta(\mathbf{t}(s) \cdot \mathbf{f}_b) \tag{A.12}$$

must hold on the interval $(\bar{s}_1, \bar{s}_2)$. We note that $(\mathbf{t}(s) \cdot \mathbf{f}_b)$ does not equal zero on this interval (recall (A.7)). Thus, we divide through by this quantity to conclude that $\mathbf{e}_a \cdot \mathbf{Q}^b(\mathbf{x}(s) \cdot \mathbf{f}_b)\mathbf{W}^b \mathbf{r}_b = \delta$. We differentiate again and divide through by the quantity $(\mathbf{t}(s) \cdot \mathbf{f}_b) \neq 0$ to conclude $\mathbf{e}_a \cdot \mathbf{Q}^b(\mathbf{x}(s) \cdot \mathbf{f}_b)\mathbf{r}_b = 0$. Finally, we differentiate one last time and divide through by $(\mathbf{t}(s) \cdot \mathbf{f}_b) \neq 0$ to conclude $\mathbf{e}_a \cdot \mathbf{Q}^b(\mathbf{x}(s) \cdot \mathbf{f}_b)\mathbf{W}^b \mathbf{r}_b = 0$. Consequently, $\delta = 0$. Moreover, $\{\mathbf{Q}^b(\mathbf{x}(s) \cdot \mathbf{f}_b)\mathbf{r}_b, \mathbf{Q}^b(\mathbf{x}(s) \cdot \mathbf{f}_b)\mathbf{W}^b \mathbf{r}_b, \mathbf{e}_b\}$ forms an orthogonal basis, and we have just shown that $\mathbf{e}_a$ is perpendicular to the first two vectors in this basis. Therefore, $\mathbf{e}_a$ is parallel to $\mathbf{e}_b$. But this is a contradiction given (A.1). Hence, $\mathbf{g}_a - (\mathbf{e}_a \cdot \mathbf{e}_b)\mathbf{g}_b$ is not parallel to $\mathbf{f}_b$.

Thus, the interface has curvature $\kappa(s) \neq 0$ on some interval only if $\mathbf{f}_a = \delta \mathbf{f}_b$ for some $\delta \in \mathbb{R} \setminus \{0\}$ (δ cannot be zero since this would contradict $|\mathbf{f}_{b,a}| \neq 0$). We now show that δ is, in fact, $+$ or -1. To do this, we substitute $\mathbf{f}_a = \delta \mathbf{f}_b$ into the necessary condition in (A.5) and differentiate this equation to conclude that

$$\delta(\mathbf{t}(s) \cdot \mathbf{f}_b)\Big(\mathbf{e}_b \cdot \mathbf{Q}^a(\delta(\mathbf{x}(s) \cdot \mathbf{f}_b))\mathbf{r}_a\Big) = -(\mathbf{t}(s) \cdot \mathbf{f}_b)\Big(\mathbf{e}_a \cdot \mathbf{Q}^b(\mathbf{x}(s) \cdot \mathbf{f}_b)\mathbf{r}_b\Big) \tag{A.13}$$

is necessary on the interval $(\bar{s}_1, \bar{s}_2)$. We recall, as before, that $(\mathbf{t}(s) \cdot \mathbf{f}_b)$ does not equal zero on this interval. Consequently, we can divide through by this quantity. Further, we can differentiate and divide through by this quantity three more times. In doing all this, we obtain four conditions which must hold on the interval $(\bar{s}_1, \bar{s}_2)$:

$$\begin{cases} \delta\big(\mathbf{e}_b \cdot \mathbf{Q}^a(\delta(\mathbf{x}(s) \cdot \mathbf{f}_b)\mathbf{r}_a\big) = -\big(\mathbf{e}_a \cdot \mathbf{Q}^b(\mathbf{x}(s) \cdot \mathbf{f}_b)\mathbf{r}_b\big), \\ \delta^2\big(\mathbf{e}_b \cdot \mathbf{Q}^a(\delta(\mathbf{x}(s) \cdot \mathbf{f}_b)\mathbf{W}^a\mathbf{r}_a\big) = -\big(\mathbf{e}_a \cdot \mathbf{Q}^b(\mathbf{x}(s) \cdot \mathbf{f}_b)\mathbf{W}^b\mathbf{r}_b\big), \\ -\delta^3\big(\mathbf{e}_b \cdot \mathbf{Q}^a(\delta(\mathbf{x}(s) \cdot \mathbf{f}_b)\mathbf{r}_a\big) = \big(\mathbf{e}_a \cdot \mathbf{Q}^b(\mathbf{x}(s) \cdot \mathbf{f}_b)\mathbf{r}_b\big), \\ -\delta^4\big(\mathbf{e}_b \cdot \mathbf{Q}^a(\delta(\mathbf{x}(s) \cdot \mathbf{f}_b)\mathbf{W}^a\mathbf{r}_a\big) = \big(\mathbf{e}_a \cdot \mathbf{Q}^b(\mathbf{x}(s) \cdot \mathbf{f}_b)\mathbf{W}^b\mathbf{r}_b\big). \end{cases} \tag{A.14}$$

Here, we used the fact that $\mathbf{W}^{a,b}\mathbf{W}^{a,b}\mathbf{r}_{a,b} = -\mathbf{r}_{a,b}$. In adding the first and third of these equations and the second and fourth of these, we obtain the necessary conditions on the interval $(\bar{s}_1, \bar{s}_2)$:

$$\begin{cases} (\delta - \delta^3)\Big(\mathbf{e}_b \cdot \mathbf{Q}^a(\delta(\mathbf{x}(s) \cdot \mathbf{f}_b)\mathbf{r}_a\Big) = 0, \\ (\delta^2 - \delta^4)\Big(\mathbf{e}_b \cdot \mathbf{Q}^a(\delta(\mathbf{x}(s) \cdot \mathbf{f}_b)\mathbf{W}^a\mathbf{r}_a\Big) = 0. \end{cases} \tag{A.15}$$

We claim that these two condition, in combination, imply that $\delta^2 = 1$. Indeed, suppose not. It follows that $(\delta - \delta^3), (\delta^2 - \delta^4) \neq 0$ since $\delta \notin \{0, \pm 1\}$. From this, we conclude that $\mathbf{e}_b$ is perpendicular to $\mathbf{Q}^a(\delta(\mathbf{x}(s) \cdot \mathbf{f}_b)\mathbf{r}_a$ and $\mathbf{Q}^a(\delta(\mathbf{x}(s) \cdot \mathbf{f}_b)\mathbf{W}^a\mathbf{r}_a$. However, $\{\mathbf{Q}^a(\delta(\mathbf{x}(s) \cdot \mathbf{f}_b)\mathbf{r}_a, \mathbf{Q}^a(\delta(\mathbf{x}(s) \cdot \mathbf{f}_b)\mathbf{W}^a\mathbf{r}_a, \mathbf{e}_a\}$ is an orthogonal basis of $\mathbb{R}^3$. Therefore, $\mathbf{e}_b$ is parallel to $\mathbf{e}_a$. This is the desired contradiction (recall (A.1)).

We have determined that $\delta^2 = 1$ (i.e., $\mathbf{f}_a = \mathbf{f}_b$ or $\mathbf{f}_a = -\mathbf{f}_b$). In fact, we also have that the constant $c_0 = 0$. Indeed, we substitute the second identity in (A.14) into the necessary condition (A.5) using the fact that $\mathbf{f}_a = \delta\mathbf{f}_b$ and $\delta^2 = 1$, and the identity $c_0 = 0$ follows. Now, depending on the choice $\mathbf{f}_a = \pm\mathbf{f}_b$, we will derive a different set of necessary conditions on the remaining parameters. We catalogue each case individually in the next two paragraphs.

(*Step 4:* $\mathbf{f}_a = \mathbf{f}_b$ *implies* $\mathbf{g}_a = -\mathbf{g}_b$*, and* $\mathbf{f}_a = -\mathbf{f}_b$ *implies* $\mathbf{g}_a = \mathbf{g}_b$.) We assume $\mathbf{f}_a = \mathbf{f}_b$, and we contract the tensor in (A.9) in two ways by dotting both sides with

$\mathbf{g}_{a,b}^{\perp} = -(\mathbf{g}_{a,b} \cdot \mathbf{e}_2)\mathbf{e}_1 + (\mathbf{g}_{a,b} \cdot \mathbf{e}_1)\mathbf{e}_2$. This gives two necessary conditions:

$$\begin{cases} (1 - \mathbf{e}_a \cdot \mathbf{e}_b)(\mathbf{g}_a^{\perp} \cdot \mathbf{g}_b)(\mathbf{g}_a^{\perp} \cdot \mathbf{f}_b) = 0, \\ (1 - \mathbf{e}_a \cdot \mathbf{e}_b)(\mathbf{g}_a^{\perp} \cdot \mathbf{g}_b)(\mathbf{g}_b^{\perp} \cdot \mathbf{f}_b) = 0. \end{cases} \tag{A.16}$$

Here, we have used the fact that $c_0 = 0$ as well as the identity $\mathbf{g}_a^{\perp} \cdot \mathbf{g}_b = -\mathbf{g}_b^{\perp} \cdot \mathbf{g}_a$. We claim that, in combination, these necessary conditions imply that $\mathbf{g}_a$ is parallel to $\mathbf{g}_b$ (i.e., $\mathbf{g}_a = \delta \mathbf{g}_b$ for some $\delta \neq 0$). Indeed, suppose not. Then $(1 - \mathbf{e}_a \cdot \mathbf{e}_b)(\mathbf{g}_a^{\perp} \cdot \mathbf{g}_b) \neq 0$ since $(1 - \mathbf{e}_a \cdot \mathbf{e}_b) \neq 0$ from (A.1). Consequently, we must have $\mathbf{g}_a$ parallel to $\mathbf{f}_b$ and $\mathbf{g}_b$ parallel to $\mathbf{f}_b$. But then, $\mathbf{g}_a$ is parallel to $\mathbf{g}_b$ since $\mathbf{f}_b$ is a non-zero vector on $\mathbb{R}^2$. This is a contradiction. Hence, we set $\mathbf{g}_a = \delta \mathbf{g}_b$ for $\delta \in \mathbb{R} \setminus \{0\}$ to solve the necessary condition (A.16). Now, we substitute this condition (as well as the necessary condition $c_0 = 0$ and the assumption $\mathbf{f}_b = \mathbf{f}_a$) back into the tensor (A.9). This, after some rearranging of terms, yields the requirement

$$(1 + \delta)(1 - \mathbf{e}_a \cdot \mathbf{e}_b)\mathrm{sym}\Big(\mathbf{f}_b \otimes \mathbf{g}_b\Big) = 0. \tag{A.17}$$

Again $(1 - \mathbf{e}_a \cdot \mathbf{e}_b) \neq 0$ given (A.1) and $\mathbf{f}_b, \mathbf{g}_b \neq 0$ by hypothesis. Thus, we determine that $\delta = -1$ as desired.

We now assume $\mathbf{f}_a = -\mathbf{f}_b$. By contracting the tensor in (A.9) again with $\mathbf{g}_{a,b}^{\perp}$, we conclude that $\mathbf{g}_a = \delta \mathbf{g}_b$ for some $\delta \in \mathbb{R} \setminus \{0\}$ (the argument is completely analogous to the previous case). In substituting this condition, the assumption $\mathbf{f}_a = -\mathbf{f}_b$, and the necessary condition $c_0 = 0$ back into (A.9), we deduce the requirement

$$(1 - \delta)(1 + \mathbf{e}_a \cdot \mathbf{e}_b)\mathrm{sym}\Big(\mathbf{f}_b \otimes \mathbf{g}_b\Big) = 0. \tag{A.18}$$

Again $(1 + \mathbf{e}_a \cdot \mathbf{e}_b) \neq 0$ given (A.1), and $\mathbf{f}_b, \mathbf{g}_b \neq 0$ by hypothesis. Thus for this case, we determine that $\delta = 1$ as desired.

(*Step 5: The two helices have the same radius,* $|\mathbf{r}_a| = |\mathbf{r}_b|$.) In the remainder of this argument, we write $\mathbf{f}_a = \pm \mathbf{f}_b$ and $\mathbf{g}_a = \mp \mathbf{g}_b$ to keep track of the two cases. We now prove that the radius of each helical phase is identical. To do this, we first differentiate the full compatibility equation, and we substitute these parameters into this equation.

That is, on the interval $(\bar{s}_1, \bar{s}_2)$, we must satisfy

$$\begin{aligned}\mathbf{Q}^a(\pm\mathbf{x}(s)\cdot\mathbf{f}_b)\Big(\pm(\mathbf{t}(s)\cdot\mathbf{f}_b)\mathbf{W}^a\mathbf{r}_a \mp (\mathbf{t}(s)\cdot\mathbf{g}_b)\mathbf{e}_a\Big)\\ = \mathbf{Q}^b(\mathbf{x}(s)\cdot\mathbf{f}_b)\Big((\mathbf{t}(s)\cdot\mathbf{f}_b)\mathbf{W}^b\mathbf{r}_b + (\mathbf{t}(s)\cdot\mathbf{g}_b)\mathbf{e}_b\Big).\end{aligned} \tag{A.19}$$

We eliminate $\mathbf{Q}^{a,b}(\cdot)$ by taking the squared norm of both sides. Given that fact that the set $\{\mathbf{W}^{a,b}\mathbf{r}_{a,b}/|\mathbf{r}_{a,b}|, \mathbf{e}_{a,b}\}$ is orthonormal, this yields the necessary condition

$$(\mathbf{t}(s)\cdot\mathbf{f}_b)^2|\mathbf{r}_a|^2 = (\mathbf{t}(s)\cdot\mathbf{f}_b)^2|\mathbf{r}_b|^2 \tag{A.20}$$

on the interval $(\bar{s}_1, \bar{s}_2)$. Again $(\mathbf{t}(s)\cdot\mathbf{f}_b) \neq 0$ on this interval (recall (A.7)), and so we may divide through by this quantity to obtain the desired result.

(*Step 6: Local compatibly given the established necessary conditions.*) We have established the necessary conditions on the parameters in this case: $\mathbf{e}_a \times \mathbf{e}_b \neq 0$, $\mathbf{f}_a = \pm\mathbf{f}_b$, $\mathbf{g}_a = \mp\mathbf{g}_b$ and $|\mathbf{r}_a| = |\mathbf{r}_b|$. Given these, local compatibility (i.e., (A.19)) is equivalent to

$$\begin{aligned}&\mathbf{e}_b\cdot\mathbf{Q}^a(\pm\mathbf{x}(s)\cdot\mathbf{f}_b)\mathbf{W}^a\mathbf{r}_a + \mathbf{e}_a\cdot\mathbf{Q}^b(\mathbf{x}(s)\cdot\mathbf{f}_b)\mathbf{W}^b\mathbf{r}_b = 0,\\ &(\mathbf{t}(s)\cdot\mathbf{f}_b)\Big(\mathbf{e}_a\cdot\mathbf{Q}^b(\mathbf{x}(s)\cdot\mathbf{f}_b)\mathbf{W}^b\mathbf{r}_b\Big) = \mp(1\pm\mathbf{e}_a\cdot\mathbf{e}_b)(\mathbf{t}(s)\cdot\mathbf{g}_b),\\ &(\mathbf{t}(s)\cdot\mathbf{f}_b)\Big(\mathbf{e}_b\cdot\mathbf{Q}^a(\pm\mathbf{x}(s)\cdot\mathbf{f}_b)\mathbf{W}^a\mathbf{r}_a\Big) = \pm(1\pm\mathbf{e}_a\cdot\mathbf{e}_b)(\mathbf{t}(s)\cdot\mathbf{g}_b),\end{aligned} \tag{A.21}$$

on $(\bar{s}_1, \bar{s}_2)$ (substituting in all the necessary conditions). By adding latter two equations, we obtain the first equation. Thus, this set of equations is degenerate[4], and it remains only to solve the first two equations above.

(*Step 7: The rotation between coordinates of each helical phase.*) We focus on the first of the equations in (A.21). Since the sets $\{\mathbf{r}_a/|\mathbf{r}_a|, \mathbf{W}^a\mathbf{r}_a/|\mathbf{r}_a|, \mathbf{e}_a\}$ and $\{\mathbf{r}_b/|\mathbf{r}_a|, \mathbf{W}^b\mathbf{r}_b/|\mathbf{r}_a|, \mathbf{e}_b\}$ each form a right-hand orthonormal basis (recall $|\mathbf{r}_a| = |\mathbf{r}_b|$), we have

$$\exists\ \mathbf{R}\in SO(3), \quad \mathbf{R}\big\{\mathbf{r}_a, \mathbf{W}^a\mathbf{r}_a, \mathbf{e}_a\big\} = \big\{\mathbf{r}_b, \mathbf{W}^b\mathbf{r}_b, \mathbf{e}_b\big\}. \tag{A.22}$$

We solve the first equation in (A.21) by determining $\mathbf{R}$. For this, we note that $\mathbf{Q}^a(\pm\mathbf{x}(s)\cdot\mathbf{f}_b) = \mathbf{R}^T\mathbf{Q}^b(\pm\mathbf{x}(s)\cdot\mathbf{f}_b)\mathbf{R}$, and we observe that the first equation in (A.21) can be

[4]This stems from the fact that we solved (A.9), which is obtained from all these equations.

rewritten as

$$\mathbf{e}_b \cdot \Big(\mathbf{R}^T\mathbf{Q}^b(\pm\mathbf{x}(s)\cdot\mathbf{f}_b) + \mathbf{R}\mathbf{Q}^b(\mathbf{x}(s)\cdot\mathbf{f}_b)\Big)\mathbf{W}^b\mathbf{r}_b = 0. \tag{A.23}$$

This form suggests the substitution $\mathbf{R} = \tilde{\mathbf{R}}\mathbf{R}^{\pm}$ for some $\tilde{\mathbf{R}} \in SO(3)$ where $\mathbf{R}^+ = \mathbf{Id}$ and $\mathbf{R}^-$ is a rotation by π about the vector $\mathbf{r}_b$ so that $\mathbf{R}^-\mathbf{W}^b\mathbf{r}_b = -\mathbf{W}^b\mathbf{r}_b$ and $\mathbf{R}^-\mathbf{e}_b = -\mathbf{e}_b$, and $\mathbf{R}^-\mathbf{Q}^b(\mathbf{x}(s)\cdot\mathbf{f}_b)\mathbf{W}^b\mathbf{r}_b = -\mathbf{Q}^b(-\mathbf{x}(s)\cdot\mathbf{f}_b)\mathbf{W}^b\mathbf{r}_b$. Indeed, we obtain

$$\mathbf{e}_b \cdot \Big(\tilde{\mathbf{R}}^T + \tilde{\mathbf{R}}\Big)\mathbf{Q}^b(\pm\mathbf{x}(s)\cdot\mathbf{f}_b)\mathbf{W}^b\mathbf{r}_b = 0 \tag{A.24}$$

from (A.23) following this substitution. Further by differentiation and dividing through by $\pm\mathbf{t}(s)\cdot\mathbf{f}_b$ which is non-vanishing $(\bar{s}_1, \bar{s}_2)$, we deduce that the identity

$$\mathbf{e}_b \cdot \Big(\tilde{\mathbf{R}}^T + \tilde{\mathbf{R}}\Big)\mathbf{Q}^b(\pm\mathbf{x}(s)\cdot\mathbf{f}_b)\mathbf{r}_b = 0 \tag{A.25}$$

must also hold on the interval $(\bar{s}_1, \bar{s}_2)$. Combining these two observations, we conclude that $(\tilde{\mathbf{R}}^T + \tilde{\mathbf{R}})\mathbf{e}_b$ is perpendicular to $\{\mathbf{Q}^b(\pm\mathbf{x}(s)\cdot\mathbf{f}_b)\mathbf{r}_b, \mathbf{Q}^b(\pm\mathbf{x}(s)\cdot\mathbf{f}_b)\mathbf{W}^b\mathbf{r}_b\}$. This means it is parallel to the $\mathbf{e}_b$ since this set and the vector $\mathbf{e}_b$ form an orthogonal frame in $\mathbb{R}^3$. Finally, $(\tilde{\mathbf{R}}^T + \tilde{\mathbf{R}})\mathbf{e}_b$ is parallel to $\mathbf{e}_b$ if and only if: 1) $\tilde{\mathbf{R}} = \mathbf{Id}$, 2) $\tilde{\mathbf{R}}$ is a rotation about $\mathbf{e}_b$, or 3) $\tilde{\mathbf{R}}$ is a rotation about a vector perpendicular to $\mathbf{e}_b$. From (A.22) and using that $\mathbf{R} = \tilde{\mathbf{R}}\mathbf{R}^{\pm}$, the first two cases imply that $(\mathbf{e}_a \times \mathbf{e}_b) = 0$, which contradicts the hypotheses of this case (recall (A.1)). Consequently, $\tilde{\mathbf{R}}$ is a rotation about a vector perpendicular to $\mathbf{e}_b$. In fact, it is actually a rotation about the vector $(\mathbf{e}_a \times \mathbf{e}_b)$. This is because the rotation $\mathbf{R} = \tilde{\mathbf{R}}\mathbf{R}^{\pm}$ takes $\mathbf{e}_a$ to $\mathbf{e}_b$. In summary, we have actually determined the equations (2.45) and (2.46) in the theorem. Moreover, this parameterization solves the first equation in (A.21), and this is the only way to solve this equation given the hypotheses of this case.

(*Step 8: Formula for the parameterized interface* $\mathbf{x}(s)$.) The only equation that remains unsolved for local compatibility is the middle equation in (A.21). This equation determines the parameterized curve $\mathbf{x}(s)$. Indeed, we rewrite this equation in integral

form to obtain

$$\mathbf{e}_a \cdot \mathbf{Q}^b(\mathbf{x}(s)\cdot\mathbf{f}_b)\mathbf{r}_b \pm (1 \pm \mathbf{e}_a\cdot\mathbf{e}_b)(\mathbf{x}(s)\cdot\mathbf{g}_b) = \mathbf{e}_a\cdot\mathbf{r}_b \quad \text{for} \quad \mathbf{x}(s_1)=0,\ \ |\mathbf{x}'(s)|=1. \tag{A.26}$$

Here, we have chosen the initial condition for the curve (to obtain the right-hand side). We are free to do without loss of generality. Now, to derive an explicit formula for the curve, we note that $\mathbf{f}_b$ is not parallel to $\mathbf{g}_b$ by the hypotheses on the groups stated at the start of this section. Thus, there exists a reciprocal basis $\{\mathbf{f}^b, \mathbf{g}^b\}$ which spans $\mathbb{R}^2$ and satisfies $\mathbf{g}^b\cdot\mathbf{g}_b = 1$, $\mathbf{f}^b\cdot\mathbf{f}_b = 1$, $\mathbf{f}^b\cdot\mathbf{g}_b = 0$ and $\mathbf{g}^b\cdot\mathbf{f}_b = 0$. Consequently, we can describe an *arbitrary* curve $\tilde{\mathbf{x}}(t)$ satisfying $\tilde{\mathbf{x}}(t_0)=0$ using this basis as

$$\tilde{\mathbf{x}}(s) = \tilde{u}_1(s)\mathbf{f}^b + \tilde{u}_2(s)\mathbf{g}^b, \quad \tilde{u}_1(t_0) = \tilde{u}_2(t_0) = 0. \tag{A.27}$$

Hence, any curve which satisfies (A.26) absent the normal condition must have the parameterization

$$\tilde{u}_2(t) = \pm\frac{\mathbf{e}_a\cdot\mathbf{r}_b - \mathbf{e}_a\cdot\mathbf{Q}^b(\tilde{u}_1(t))\mathbf{r}_b}{(1\pm\mathbf{e}_a\cdot\mathbf{e}_b)}. \tag{A.28}$$

(Note $(1\pm\mathbf{e}_a\cdot\mathbf{e}_b)\neq 0$ given in (A.1).) This uniquely determines the curve (the range of any function) which can satisfy the conditions in (A.26). Now, we just need to show the existence of an arc-length parameterized version of this curve to complete the proof. For this, we observe that

$$\tilde{\mathbf{x}}'(t) = \tilde{u}_1'(t)\Big(\mathbf{f}^b \mp \frac{\mathbf{e}_a\cdot\mathbf{Q}^b(\tilde{u}_1(t))\mathbf{W}^b\mathbf{r}_b}{(1\pm\mathbf{e}_a\cdot\mathbf{e}_b)}\mathbf{g}^b\Big). \tag{A.29}$$

Further, since $\mathbf{g}^b$ and $\mathbf{f}^b$ are linearly independent, we see that $\tilde{\mathbf{x}}'(t)=0$ if and only if $\tilde{u}_1'(t)=0$. Thus, we obtain a regular parameterization of this curve on any interval by choosing $\tilde{u}_1(t)=t$ (we are free to do this without loss of generality). Hence, we re-parameterize by arc-length, exactly as stated in the theorem, to achieve an $\mathbf{x}(s)$ satisfying (A.26). The proof is now, *finally*, complete! □

A.2 Relationship between Type 1 and Type 2 elliptical interfaces

Here we illustrate the global intersection of elliptical interface as well as the relationship between Type 1 and Type 2 interfaces. Figure A.1 shows three examples of elliptical interfaces. All of them have global self-intersections, but with locally compatible interfaces. The corresponding parameters are given as follows.

(a) (Type 1). $\mathbf{e}_a = \mathbf{e}_3$, $\mathbf{e}_b = \mathbf{Q}_{\mathbf{e}_2}(0.4\pi)\mathbf{e}_a$, $\mathbf{f}_a = (\frac{2}{35}\pi, \frac{4}{35}\pi)$, $\mathbf{g}_a = (-0.24, 0.12)$, $\mathbf{f}_b = \mathbf{f}_a$, $\mathbf{g}_b = -\mathbf{g}_a$.

(b) (Type 2). $\mathbf{e}_a = \mathbf{e}_3$, $\mathbf{e}_b = \mathbf{Q}_{\mathbf{e}_2}(0.4\pi)\mathbf{e}_a$, $\mathbf{f}_a = (\frac{2}{35}\pi, \frac{4}{35}\pi)$, $\mathbf{g}_a = (-0.24, 0.12)$, $\mathbf{f}_b = -\mathbf{f}_a$, $\mathbf{g}_b = \mathbf{g}_a$.

(c) (Type 2). $\mathbf{e}_a = -\mathbf{e}_3$, $\mathbf{e}_b = \mathbf{Q}_{\mathbf{e}_2}(0.4\pi)\mathbf{e}_a$, $\mathbf{f}_a = (\frac{2}{35}\pi, \frac{4}{35}\pi)$, $\mathbf{g}_a = (-0.24, 0.12)$, $\mathbf{f}_b = -\mathbf{f}_a$, $\mathbf{g}_b = \mathbf{g}_a$.

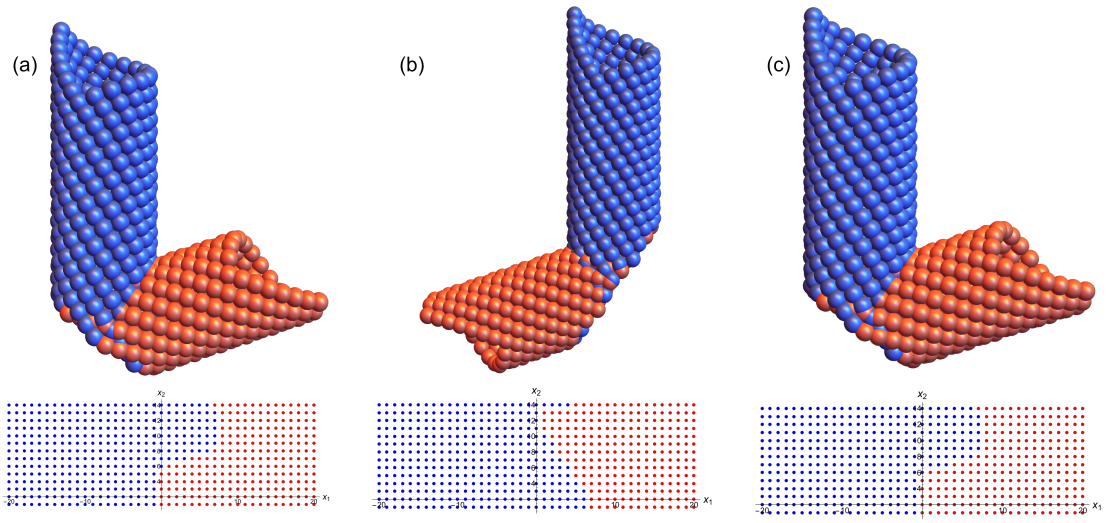

Figure A.1: (a): Type 1 elliptical interface. (b) and (c): Type 2 elliptical interfaces. The bottom figures are corresponding reference domains. Parameters are given in the text.

Here $\mathbf{Q}_{\mathbf{e}_3}(0.4\pi)$ denotes a rotation matrix about $\mathbf{e}_3$ with rotation angle 0.4π. We can easily observe that (a) and (c) have exactly the same interfaces in both the deformed

and reference domains, but they belong to different types of interfaces as defined. (c) is obtained from (b) by changing $\mathbf{e}_a = \mathbf{e}_3$ to $\mathbf{e}_a = -\mathbf{e}_3$, but keeping the other parameters unchanged. This could be explained in the following way.

Recall Theorem 2.5.2. The reference interface curve is given by

$$\mathbf{x}(s) = \big(\tilde{\mathbf{x}}^+ \circ \psi\big)(s - s_1) \tag{A.30}$$

for Type 1 interface and

$$\mathbf{x}(s) = \big(\tilde{\mathbf{x}}^- \circ \psi\big)(s - s_1) \tag{A.31}$$

for Type 2 interface, where

$$\tilde{\mathbf{x}}^{\pm}(t) = t\mathbf{f}^b \pm \Big(\frac{\mathbf{e}_a \cdot \mathbf{r}_b - \mathbf{e}_a \cdot \mathbf{Q}^b(t)\mathbf{r}_b}{(1 \pm \mathbf{e}_a \cdot \mathbf{e}_b)}\Big)\mathbf{g}^b \tag{A.32}$$

and $\psi(s)$ is the inverse of the arc-length function $\varphi(t) = \int_0^t |(\tilde{\mathbf{x}}^{\pm})'(\tilde{t})| d\tilde{t}$. Observe that

$$\begin{aligned} \tilde{\mathbf{x}}^+(t) &= t\mathbf{f}^b + \Big(\frac{\mathbf{e}_a \cdot \mathbf{r}_b - \mathbf{e}_a \cdot \mathbf{Q}^b(t)\mathbf{r}_b}{(1 + \mathbf{e}_a \cdot \mathbf{e}_b)}\Big)\mathbf{g}^b \\ &= t\mathbf{f}^b - \Big(\frac{(-\mathbf{e}_a) \cdot \mathbf{r}_b - (-\mathbf{e}_a) \cdot \mathbf{Q}^b(t)\mathbf{r}_b}{(1 - (-\mathbf{e}_a) \cdot \mathbf{e}_b)}\Big)\mathbf{g}^b. \end{aligned} \tag{A.33}$$

It means that $\tilde{\mathbf{x}}^-(t)$ has the same form as $\tilde{\mathbf{x}}^+(t)$ if you change $\mathbf{e}_a$ to $-\mathbf{e}_a$ (and also $\mathbf{e}_b = -\mathbf{e}_b$ simultaneously by $\mathbf{e}_b = \mathbf{Q}_{\mathbf{e}_2}(0.4\pi)\mathbf{e}_a$). As a result, the reference interface curve have the same form as well (see Figure A.1 (a) (c)), for (a) and (c). Also notice that

$$\mathbf{Q}^b(\mathbf{x}(s) \cdot \mathbf{f}_b)\mathbf{r}_b + (\mathbf{x}(s) \cdot \mathbf{g}_b)\mathbf{e}_b + \mathbf{z}_b = \hat{\mathbf{Q}}^b(-\mathbf{x}(s) \cdot \mathbf{f}_b)\mathbf{r}_b + (-\mathbf{x}(s) \cdot \mathbf{g}_b)(-\mathbf{e}_b) + \mathbf{z}_b, \tag{A.34}$$

where $\mathbf{Q}^b(\cdot)\mathbf{e}_b = \mathbf{e}_b$ and $\hat{\mathbf{Q}}^b(\cdot)(-\mathbf{e}_b) = -\mathbf{e}_b$. By changing $\{\mathbf{e}_b, \mathbf{f}_b, \mathbf{g}_b\}$ to $\{-\mathbf{e}_b, -\mathbf{f}_b, -\mathbf{g}_b\}$, we get the same map (similar for a case). And therefore, the same reference interface curve for (a) and (c) is mapped to the same deformed interface curve in $\mathbb{R}^3$!

Appendix B

Appendix for Chapter 3

B.1 Kinematics of a Miura four-fold intersection

Theorem B.1.1. *The Miura folding deformation* $\mathbf{y}(\mathbf{x})$ *defined in (3.3) is continuous if and only if* η, ξ, ω *satisfy one of the following cases:*

1. $\eta = \omega$ *(plus-phase)*

   (a) $\omega = 0,\ \alpha + \beta = \pi,\ -\pi \le \xi \le \pi$

   (b) $\omega = \pm\pi,\ \alpha = \beta,\ -\pi \le \xi \le \pi$

   (c) *Otherwise,* $\xi = \xi^+(\omega)$ *is uniquely determined and given by*

$$c_{\xi^+(\omega)} = \frac{(1 - c_\alpha c_\beta)c_\omega + s_\alpha s_\beta}{(1 - c_\alpha c_\beta) + s_\alpha s_\beta c_\omega},\ s_{\xi^+(\omega)} = \frac{(c_\beta - c_\alpha)s_\omega}{(1 - c_\alpha c_\beta) + s_\alpha s_\beta c_\eta},\ \textit{if } \omega \in (-\pi, \pi),$$
$$\xi^+(\pi) = -\textit{sign}(c_\beta - c_\alpha)\pi,\ \xi^+(-\pi) = \textit{sign}(c_\beta - c_\alpha)\pi. \tag{B.1}$$

2. $\eta = -\omega$ *(minus-phase)*

   (a) $\omega = 0,\ \alpha + \beta = \pi,\ -\pi \le \xi \le \pi$

   (b) $\omega = \pm\pi,\ \alpha = \beta,\ -\pi \le \xi \le \pi$

(c) Otherwise, $\xi = \xi^-(\omega)$ is uniquely determined and given by

$$c_{\xi^-(\omega)} = \frac{(1 + c_\alpha c_\beta)c_\omega - s_\alpha s_\beta}{(1 + c_\alpha c_\beta) - s_\alpha s_\beta c_\omega},\ s_{\xi^-(\omega)} = \frac{(c_\beta + c_\alpha)s_\omega}{(1 + c_\alpha c_\beta) - s_\alpha s_\beta c_\eta},\ \textit{if } \omega \in (-\pi, \pi),$$
$$\xi^-(\pi) = -\textit{sign}(c_\beta + c_\alpha)\pi,\ \xi^-(-\pi) = \textit{sign}(c_\beta + c_\alpha)\pi. \tag{B.2}$$

Here c_θ, s_θ denote $\cos(\theta)$ *and* $\sin(\theta)$ *respectively.*

Proof. Suppose the reference domain, deformation $\mathbf{y}(\mathbf{x})$, and related notations are the same as Subsection 3.2.1. The deformation $\mathbf{y}(\mathbf{x})$ is continuous at the fold lines $\mathbf{t}_2, \mathbf{t}_3, \mathbf{t}_4$ for all choices of the angles η, ξ, ω in $[-\pi, \pi]$. It remains to impose continuity at $\mathbf{t}_1$.

The deformation $\mathbf{y}$ is continuous at the $\mathbf{t}_1$ fold line if and only if

$$\mathbf{R}_2(\eta)\mathbf{R}_3(\xi)\mathbf{R}_4(\omega)\mathbf{t}_1 = \mathbf{t}_1. \tag{B.3}$$

Multiply (B.3) by $\mathbf{R}_2(\eta)^T$ and dot with $\mathbf{t}_3$, using that $\mathbf{R}_3(\eta)\mathbf{t}_3 = \mathbf{t}_3$. This gives

$$\mathbf{t}_3 \cdot \mathbf{R}_4(\omega)\mathbf{t}_1 = \mathbf{t}_3 \cdot \mathbf{R}_2(\eta)^T\mathbf{t}_1 \tag{B.4}$$

By direct calculation

$$\mathbf{t}_3 \cdot \mathbf{R}_4(\omega)\mathbf{t}_1 - \mathbf{t}_3 \cdot \mathbf{R}_2(\eta)^T\mathbf{t}_1 = (\cos\eta - \cos\omega)\sin\alpha\sin\beta. \tag{B.5}$$

Therefore, under our hypotheses on $\alpha, \beta, \eta, \omega$, we have the necessary condition

$$\eta = \eta^{\pm}(\omega) = \pm\omega. \tag{B.6}$$

Next, we dot (B.3) with $\mathbf{R}_2^T(\eta)$ and then project onto the plane perpendicular to $\mathbf{t}_3$, which is

$$(\mathbf{I} - \mathbf{t}_3 \otimes \mathbf{t}_3)(\mathbf{R}_3(\xi)\mathbf{R}_4(\omega)\mathbf{t}_1 - \mathbf{R}_2^T(\eta^{\pm}(\omega))\mathbf{t}_1) = 0. \tag{B.7}$$

It is necessary that the norms of vector after projection are the same:

$$|(\mathbf{I} - \mathbf{t}_3 \otimes \mathbf{t}_3)(\mathbf{R}_3(\xi)\mathbf{R}_4(\omega)\mathbf{t}_1| = |(\mathbf{I} - \mathbf{t}_3 \otimes \mathbf{t}_3)\mathbf{R}_2^T(\eta^{\pm}(\omega))\mathbf{t}_1|. \tag{B.8}$$

Actually, this is true because the rotations preserve the norm of $\mathbf{t}_1$ and $\omega = \omega^{\pm}(\eta)$ has

ensured that the projections along $\mathbf{t}_3$ are the same. Now we need to consider two cases:

1. $|(\mathbf{I}-\mathbf{t}_3\otimes\mathbf{t}_3)\mathbf{R}_2^T(\eta)\mathbf{t}_1|=0$. In this case, η satisfies $1-(\mathbf{t}_3\cdot\mathbf{R}_2^T(\eta)\mathbf{t}_1)^2=0$ and ξ is the free angle.

2. $|(\mathbf{I}-\mathbf{t}_3\otimes\mathbf{t}_3)\mathbf{R}_2^T(\eta)\mathbf{t}_1|\neq 0$. In this case, $\mathbf{R}_3(\xi)$ is the rotation matrix mapping $(\mathbf{I}-\mathbf{t}_3\otimes\mathbf{t}_3)\mathbf{R}_4(\omega)\mathbf{t}_1$ to $(\mathbf{I}-\mathbf{t}_3\otimes\mathbf{t}_3)\mathbf{R}_2^T(\eta^{\pm}(\omega))\mathbf{t}_1$[1] and η is the free angle.

(Solution to Case 1.) This case is equivalent to $\mathbf{R}_2^T(\eta)\mathbf{t}_1=\pm\mathbf{t}_3$. We firstly notice that $\eta\in\{0,\pm\pi\}$, otherwise, $\mathbf{R}_2^T(\eta)\mathbf{t}_1$ will have $\mathbf{e}_3$ component. Also, $\mathbf{R}_2^T(\pi)\mathbf{t}_1=\mathbf{R}_2^T(-\pi)\mathbf{t}_1$, $\mathbf{t}_1\neq\mathbf{t}_3$. Then we only need to consider two cases $\mathbf{t}_1=-\mathbf{t}_3$ and $\mathbf{R}_2^T(\pm\pi)\mathbf{t}_1=\pm\mathbf{t}_3$. $\mathbf{t}_1=-\mathbf{t}_3$ if and only if $\alpha+\beta=\pi$. This gives the solution:

$$\alpha+\beta=\pi,\ \omega=\eta=0,\ \xi\in[-\pi,\pi]\text{ is the free parameter.} \tag{B.9}$$

$\mathbf{R}_2^T(\pm\pi)\mathbf{t}_1$ is equal to $\mathbf{t}_3$ if and only if $\alpha=\beta$. Furthermore, it never equals $-\mathbf{t}_3$. In this case, $\eta=\pm\pi$, This gives the solution:

$$\alpha=\beta,\ \eta=\pm\omega\in\{\pm\pi\},\ \xi\in[-\pi,\pi]\text{ is the free parameter.} \tag{B.10}$$

These are the 1. (a) (b) and 2. (a) (b) cases of the theorem.

(Solution to Case 2.) We assume $|(\mathbf{I}-\mathbf{t}_3\otimes\mathbf{t}_3)\mathbf{R}_2^T(\eta^{\pm}(\omega))\mathbf{t}_1|\neq 0$. For (B.7) to hold, $\xi=\xi^{\pm}(\eta)$ must satisfy

$$\begin{aligned}\cos(\xi^{\pm}(\omega))&=\frac{\mathbf{P}_{\mathbf{t}_3}\mathbf{R}_4(\omega)\mathbf{t}_1\cdot\mathbf{P}_{\mathbf{t}_3}\mathbf{R}_2^T(\eta^{\pm}(\omega))\mathbf{t}_1}{|\mathbf{P}_{\mathbf{t}_3}\mathbf{R}_4(\omega)\mathbf{t}_1||\mathbf{P}_{\mathbf{t}_3}\mathbf{R}_2^T(\eta^{\pm}(\omega))\mathbf{t}_1|},\\ \sin(\xi^{\pm}(\omega))&=\operatorname{sign}(\mathbf{t}_3\cdot\mathbf{P}_{\mathbf{t}_3}\mathbf{R}_4(\omega)\mathbf{t}_1\times\mathbf{P}_{\mathbf{t}_3}\mathbf{R}_2^T(\eta^{\pm}(\omega))\mathbf{t}_1)\sqrt{1-\cos^2(\xi^{\pm}(\omega))},\end{aligned} \tag{B.11}$$

where $\mathbf{P}_{\mathbf{t}_3}=\mathbf{I}-\mathbf{t}_3\otimes\mathbf{t}_3$. For the open interval $\omega\in(-\pi,\pi)$, we get $c_{\xi^{\pm}}(\omega)$ and $s_{\xi^{\pm}}(\omega)$ by directly calculating B.11. For the case $\omega=\pm\pi$ (folded flat state), we notice that $\mathbf{R}_i(+\pi)=\mathbf{R}_i(-\pi)$, $\cos(\pm\pi)=-1$, $\sin(\pm\pi)=0$, and therefore, the solution to B.11 is not unique. We obtain $\xi^{\pm}(\pm\pi)$ by taking the continuous limits of the function on $(-\pi,\pi)$.

□

[1] Recall $\mathbf{R}_3(\xi)$ is commutative with $(\mathbf{I}-\mathbf{t}_3\otimes\mathbf{t}_3)$.

B.2 Discreteness consideration for the generators of helical groups

Theorem B.2.1. *Suppose* $g_1 = (\mathbf{R}_{\theta_1}|(\mathbf{I}-\mathbf{R}_{\theta_1})\mathbf{z}+\tau_1\mathbf{e})$ *and* $g_2 = (\mathbf{R}_{\theta_2}|(\mathbf{I}-\mathbf{R}_{\theta_2})\mathbf{z}+\tau_2\mathbf{e})$ *are isometries with the same axis and* $\tau_2\theta_1 \neq \tau_1\theta_2$[2]. *Then the group* $G = \{g_1^p g_2^q | (p,q) \in \mathbb{Z}^2\}$ *is discrete if and only if there exists* $(p^\star, q^\star) \in \mathbb{Z}^2 \setminus (0,0)$ *such that* $g_1^{p^\star} g_2^{q^\star} = id$.

Proof. Suppose we have $(p^\star, q^\star) \in \mathbb{Z}^2 \setminus (0,0)$ such that $g_1^{p^\star} g_2^{q^\star} = id$. We prove the group is discrete.

1. Case that $q^\star = 0$. We have $g_1^{p^\star} = id$, then $G \subset \{g_1, g_1^2, \ldots, g_1^{|p^\star|}\}$. $|G|$ is finite, then $G(\mathbf{x})$ has no accumulation point.

2. Case that $q^\star \neq 0$. If $p^\star = 0$, we can prove the result in a similar way to the previous case. Thus, we assume $p^\star \neq 0$. By the multiplication rule, we have that

$$g_1^{p^\star} g_2^{q^\star} = (\mathbf{R}_{p^\star\theta_1+q^\star\theta_2}|(\mathbf{I}-\mathbf{R}_{p^\star\theta_1+q^\star\theta_2})\mathbf{z} + (p^\star\tau_1 + q^\star\tau_2)\mathbf{e}). \tag{B.12}$$

   Therefore, $g_1^{p^\star} g_2^{q^\star} = id$ is equivalent to

$$\begin{cases} p^\star\theta_1 + q^\star\theta_2 = 2k\pi, \quad k \in \mathbb{Z} \\ p^\star\tau_1 + q^\star\tau_2 = 0 \end{cases} \tag{B.13}$$

   Since none of $p^\star$, $q^\star$ vanishes, we have $\tau_1 \neq 0$ and $\tau_2 \neq 0$ by $\tau_2\theta_1 \neq \tau_1\theta_2$. Since $g_1^{-p^\star} g_2^{-q^\star} = g_1^{p^\star} g_2^{q^\star} = id$, we can assume $q^\star > 0$ without loss of generality. For any $(p,q) \in \mathbb{Z}^2$, we have $g_1^p g_2^q = g_1^{p'} g_2^{q'}$, where $q' = q + nq^\star$, $p' = p + np^\star$, $n \in \mathbb{Z}$, $q' \in \{1, \ldots, q^\star\}$, $p' \in \mathbb{Z}$. Then we can assume the power (p,q) is on the subdomain $\mathbb{Z} \times \{1, 2, \ldots, q^\star\}$. We claim that for any $\mathbf{x} \in \mathbb{R}^3$, given any $d > 0$, there exists $m \in \mathbb{Z}^+$ and domain $\mathcal{U} = ([p - m|p^\star|, p + m|p^\star|] \times [1, q^\star]) \cap \mathbb{Z}^2$, such that $||g_1^p g_2^q(\mathbf{x}) - g_1^{\hat{p}} g_1^{\hat{q}}(\mathbf{x})|| > d$ for any $(\hat{p}, \hat{q}) \in (\mathbb{Z} \times \{1, 2, \ldots, q^\star\}) \setminus \mathcal{U}$. To prove this, we realize that the Euclidean distance between $g_1^p g_2^q(\mathbf{x})$ and $g_1^{\hat{p}} g_2^{\hat{q}}$ satisfies

$$\begin{aligned} ||g_1^p g_2^q(\mathbf{x}) - g_1^{\hat{p}} g_1^{\hat{q}}(\mathbf{x})|| &\geq |\hat{p}\tau_1 + \hat{q}\tau_2 - p\tau_1 - q\tau_2| \\ &\geq |mp^\star\tau_1| - |q^\star\tau_2|. \end{aligned} \tag{B.14}$$

[2] This is the non-degenerate condition and ensures that $g_1^p g_2^q(\mathbf{x})$ is not a single helix.

Then we can choose m to be the smallest integer greater than $\frac{d+|q^\star\tau_2|}{|p^\star\tau_1|}$. Since $\mathcal{U}$ contains only finite number of points, and the distance between $g_1^p g_2^q(\mathbf{x})$ and any other point with powers outside $\mathcal{U}$ is greater than d. Thus, $g_1^p g_2^q(\mathbf{x})$ is not an accumulation point. Due to the arbitrarity of (p, q) and $\mathbf{x}$, we conclude that there is no accumulation point and the group is discrete.

Conversely, we assume the group is discrete and prove the existence of $(p^\star, q^\star) \in \mathbb{Z}^2 \setminus (0, 0)$. For the sake of contradiction, we assume there is no $(p^\star, q^\star) \in \mathbb{Z}^2 \setminus (0, 0)$ such that $g_1^{p^\star} g_2^{q^\star} = id$. Notice that we can always have $(\tilde{p}, \tilde{q}) \in \mathbb{R}^2 \setminus (0, 0)$ such that $g_1^{\tilde{p}} g_2^{\tilde{q}} = id$, i.e.,

$$\begin{cases} \tilde{p}\theta_1 + \tilde{q}\theta_2 = 2k\pi, \quad k \in \mathbb{Z} \\ \tilde{p}\tau_1 + \tilde{q}\tau_2 = 0 \end{cases} \tag{B.15}$$

because of the fact that $\tau_2\theta_1 \neq \tau_1\theta_2$. Then at least one of $\tilde{p}, \tilde{q}$ is irrational (If not, we can multiply $(\tilde{p}, \tilde{q})$ by some integer M to get the integer pair $(M\tilde{p}, M\tilde{q})$ making $g_1^{M\tilde{p}} g_2^{M\tilde{q}} = id$.). We claim that, if at least one of $\tilde{p}$ and $\tilde{q}$ is irrational, $\mathbf{x}$ is one accumulating point of the structure $g_1^p g_2^q(\mathbf{x}), (p, q) \in \mathbb{Z}^2$. It is equivalent to prove that,

$$\forall\ \epsilon > 0, \exists\ m, n, k \in \mathbb{Z},\ s.t.\ ||(k\tilde{p}, k\tilde{q}) - (m, n)|| < \epsilon, \tag{B.16}$$

since

$$||g_1^p g_2^q(\mathbf{x}) - \mathbf{x}|| = 0 \iff (p, q) = (k\tilde{p}, k\tilde{q}), \text{for some } k \in \mathbb{Z}. \tag{B.17}$$

We discuss $(\tilde{p}, \tilde{q})$ in the following three situations.

1. One of $\tilde{p}$ and $\tilde{q}$ is irrational. Without loss of generality, we assume $\tilde{p}$ is irrational and $\tilde{q} = m_1/n_1$. Since $(kn_1\tilde{p} \mod 1, kn_1\tilde{q} \mod 1)$ is dense in $[0, 1] \times \{0\}$, (B.16) holds naturally.

2. Both of $\tilde{p}$ and $\tilde{q}$ are irrational. Also, $\tilde{p}, \tilde{q}, 1$ are linearly dependent. In this case, there exist $m, n, r \in \mathbb{Z}$ such that $m\tilde{p} + n\tilde{q} + r = 0$. Then we have

$$(kn\tilde{p} \mod 1, kn\tilde{q} \mod 1) = (kn\tilde{p} \mod 1, km\tilde{p} \mod 1) \tag{B.18}$$

Since $k\tilde{p} \mod 1$ is dense in $[0,\ 1]$ and m, n are finite, then we can always find

$k \in \mathbb{Z}$ such that $||(kn\tilde{p} \mod 1, km\tilde{p} \mod 1)|| < \epsilon$ for any $\epsilon > 0$. Therefore, (B.16) holds.

3. Both of $\tilde{p}$ and $\tilde{q}$ are irrational. Also, $\tilde{p}, \tilde{q}, 1$ are linearly independent. Using *Kronecker's Approximation Theorem*, $(k\tilde{p} \mod 1, k\tilde{q} \mod 1), k \in \mathbb{Z}$ makes a dense set in the unit square [95]. Thus (B.16) follows.

Therefore $\mathbf{x}$ is an accumulation point which is a contradiction. Finally, the proof is done! □